

Immobilization of Antibodies and Enzymes on 3-Aminopropyltriethoxysilane-Functionalized Bioanalytical Platforms for Biosensors and Diagnostics

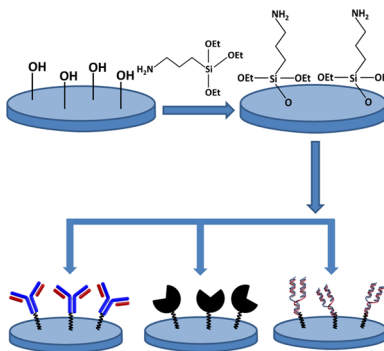
Sandeep Kumar Vashist,^{*,†,‡} Edmond Lam,[§] Sabahudin Hrapovic,[§] Keith B. Male,[§] and John H. T. Luong^{||}

[†]HSG-IMIT - Institut für Mikro- und Informationstechnik, Georges-Koehler-Allee 103, 79110 Freiburg, Germany

[‡]Laboratory for MEMS Applications, Department of Microsystems Engineering - IMTEK, University of Freiburg, Georges-Koehler-Allee 103, 79110 Freiburg, Germany

[§]National Research Council Canada, Montreal, Quebec H4P 2R2, Canada

^{||}Innovative Chromatography Group, Irish Separation Science Cluster (ISSC), Department of Chemistry and Analytical, Biological Chemistry Research Facility (ABCRF), University College Cork, Cork, Ireland



CONTENTS

1. Introduction	11083
2. Preparation of APTES-Functionalized Bioanalytical Platforms	11084
2.1. General Aspects of Silanization	11084
2.2. Wet Chemistry	11085
2.2.1. Organic Silanization	11085
2.2.2. Aqueous Silanization	11087
2.3. Chemical Vapor Deposition	11087
2.4. Characterization of APTES-Functionalized Surface	11087
3. Antibody–Enzyme Immobilization	11089
3.1. Covalent	11089
3.2. Oriented	11101
3.3. Site-Specific	11101
3.4. PNA and DNA-Directed	11102
3.5. Noncovalent Attachment	11102
3.6. Affinity	11102
3.7. Entrapment	11104
4. Applications in Biosensors and Diagnostics	11104
4.1. Microtiter Plate Formats	11104
4.2. Optical Biosensors	11104
4.3. Microfluidic/Lab-on-a-Chip Applications	11108
4.4. Microgravimetric Biosensors	11109
4.5. Electrochemical Biosensors	11110
4.5.1. Modification of Pristine Electrodes	11110
4.5.2. Film-Modified Electrodes	11111
4.5.3. Graphene and CNT Modification	11112
4.6. Nanotechnology-Based Applications	11112
4.6.1. Gold	11112
4.6.2. Iron	11113
4.6.3. Silicon	11117
4.6.4. Quantum Dots	11118
4.7. Other Detection Methods and Biomolecule Patterning	11118
5. Critiques and Outlook	11119
6. Conclusions	11120
Author Information	11121
Corresponding Author	11121
Notes	11121
Biographies	11121
Acknowledgments	11122
Abbreviations	11122
References	11123

1. INTRODUCTION

Biosensing and diagnostic platforms with high sensitivity, specificity, and fast response time are based on immobilized biomolecules such as antibodies (Abs), aptamers, enzymes, nucleic acids, receptors, and whole cells for the detection of target analytes. Such sensing biomolecules should be bound to the surface of a signal transducer with a required specific chemical, electrical, or optical property. The biological recognition event generates a quantifiable signal, which is equated to the amount or concentration of the analyte. Thus, the biomolecule immobilization plays a crucial role in achieving high sensitivity and selectivity with prolonged device lifetime. The substrate materials such as electrodes, microtiter plates (MTPs), nanoparticles (NPs), nanotubes, graphene, etc., for biomolecule immobilization must be modified to introduce functional groups that bind to biomolecules with high bonding strength, high activity, good orientation, and excellent long-term stability.

Chemisorbed monolayers of silane compounds, a class of self-assembled monolayers (SAM), on glass or oxidized silicon surfaces with active silanol (Si—OH) groups were first reported by Sagiv.¹ For biosensing applications, silane SAMs with terminal

Received: February 18, 2014

Published: October 9, 2014



amino, epoxy, or chloro groups are necessary for attaching biomolecules. Such silane derivatives also provide a means to tailor adhesion, biocompatibility, charge, hydrophilicity, and hydrophobicity of a surface. 3-Aminopropyltriethoxysilane (APTES) has been used extensively for the functionalization of bioanalytical platforms as its role in surface modification has been intensively investigated and well understood.² Table 1 shows

Table 1. Properties of APTES

IUPAC name	1-propanamine, 3-(triethoxysilyl)-
synonyms	(γ -aminopropyl)triethoxysilane, (3-aminopropyl) triethoxysilane, 1-propanamine, 3-(triethoxysilyl)-; 3-(triethoxysilyl)-1-propanamine; 3-(triethoxysilyl) propylamine; triethoxy(3-aminopropyl)silane; A-1100; A-1112; AGM 9 (VAN); NUCA 1100; Silane 1100; Silicone A-1100 and UC-A 1100
molecular formula	C ₉ H ₂₃ NO ₃ Si
appearance	colorless liquid
molar mass	221.37 g mol ⁻¹
density	0.946 g mL ⁻¹ at 25 °C
melting point	-70 °C
boiling point	217 °C
vapor pressure	0.02 hPa @ 20 °C
water solubility	7.6 × 10 ⁵ mg L ⁻¹ @ 25 °C
hazard	toxic; the target organs of APTES are nerves, liver, and kidney

some general properties of APTES. The APTES-amino groups also facilitate the formation of siloxane bonds with surface Si-OH,^{3,4} which obviates the need of a curing step after surface modification. One of the classical examples is the reaction of the Si-OH on a glass/silica surface using APTES. Silicon and silicon derivatives, metals, and polymers are commonly used to serve as a solid support in bioanalytical platforms. In some cases, they are modified with NPs, nanotubes, graphene, quantum dots (QDs), etc., to form nanocomposites. The amino-functionalized silane then forms covalent bonds with the amino (glutaraldehyde (GLD)-mediated reaction) or carboxyl groups (1-ethyl-3-[3-(dimethylamino)propyl]-carbodiimide (EDC)-mediated cross-linking) of biomolecules. However, it is somewhat difficult to control this immobilization step as the protein's surface is rich in hydrophilic amino acids, that is, Lys, Glu, and Asp. The use of thiol-based immobilization strategies enables the site-specific binding of biomolecules. Yet it is not efficient as biomolecules have a limited number of cysteine residues on their surface. Hence, these immobilization strategies offer more site-specific reactions, but the protein density is low and a thiol silane, for example, 3-mercaptopropyltrimethoxysilane, should be used to enable the formation of a disulfide bond between the biomolecule and thiol silane.

Nevertheless, silanized platforms with APTES offer biomolecule stability, high immobilization density, reduced biofouling, leach-proof biomolecule binding, and enhanced analytical performance. APTES serves as superglue to anchor the target biomolecule on a solid surface and also acts as a spacer, allowing more steric freedom to the biomolecule during the immobilization step for higher specific activity. These platforms are advocated for the fabrication of commercial glucose biosensors and other biosensors for detecting important molecules, biomarkers, pathogens, and environmental contaminants. APTES has also been widely used in different assay platforms:

enzyme-linked immunosorbent assays (ELISA), biosensors and immunosensors (IMS) based on surface plasmon resonance (SPR)-based assays, microgravimetric assays using microcantilevers and piezoelectric quartz crystals, surface acoustic wave-based assays, and nanomaterial-based assays. During the last two decades, different strategies have been developed for the immobilization of Abs and enzymes, involving covalent, oriented, covalent-oriented, site-specific, affinity tags, and the peptide nucleic acids (PNA)- and deoxyribonucleic acid (DNA)-directed ones for grafting organosilanes on silica and metal oxides.⁵ In biosensor technology, a direct electron transfer between the enzyme and its underlying electrode is of considerable interest toward the development of simple "reagentless" biosensors or biodevices with remarkably improved detection sensitivity and selectivity.

This work provides a critical review of the immobilization of Abs and enzymes on APTES-functionalized bioanalytical platforms. The important role of immobilization strategies will be discussed along with their impact on sensitivity, detection limit, operational and storage stability, and reusability toward the development of potential and commercial biosensing devices.

2. PREPARATION OF APTES-FUNCTIONALIZED BIOANALYTICAL PLATFORMS

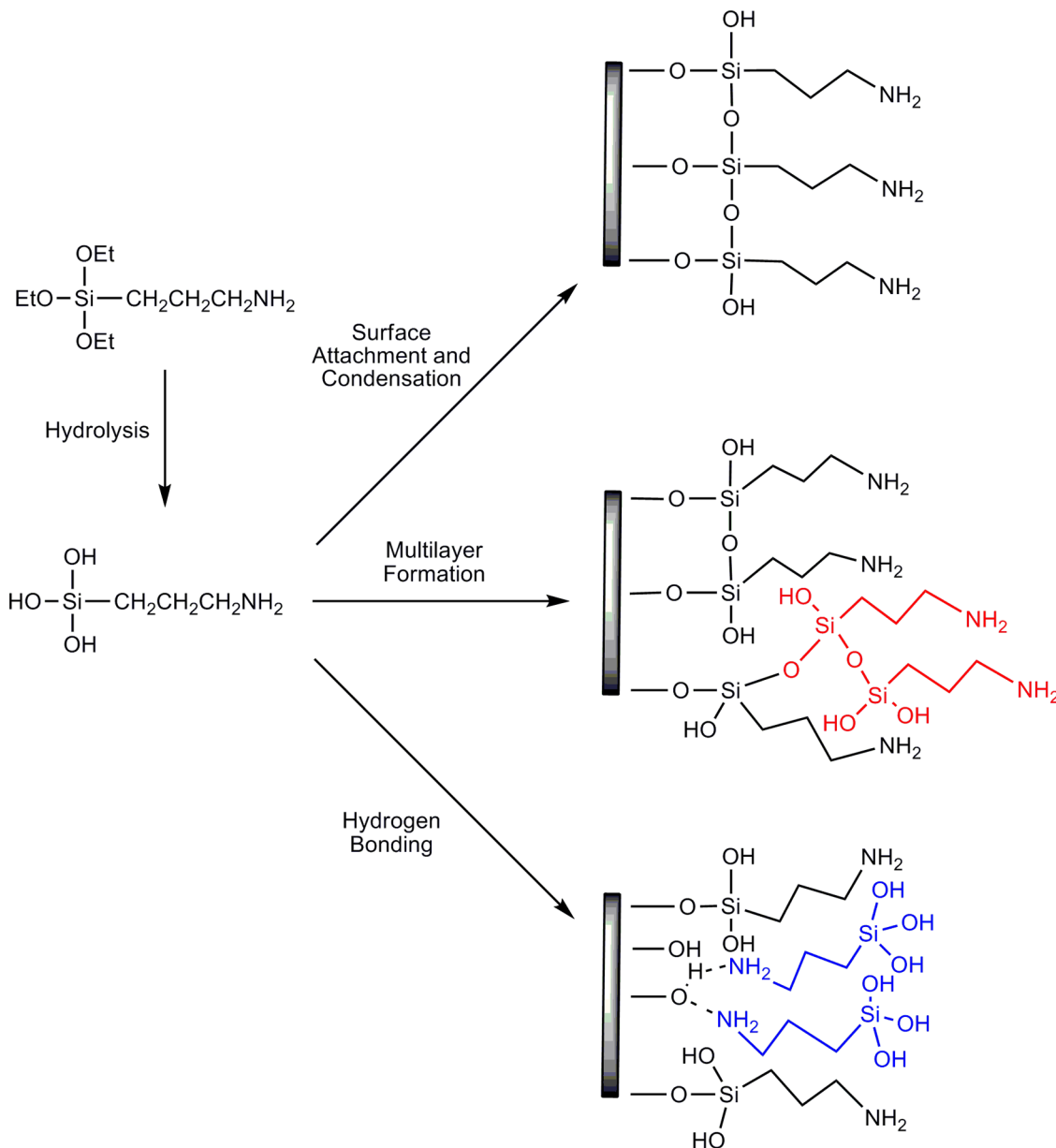
2.1. General Aspects of Silanization

APTES can be deposited on solid materials, electrode materials, nanomaterials, and nanocomposites under variable conditions of concentration, solvent, temperature, and time. In addition, curing conditions such as air/heat drying might be necessary depending upon the intended application. Pertinent information on the thickness, morphology, and conformation of the APTES layer reported in the literature is often different and conflicting.

Silanization occurs on any substrate, normally with chemically active hydroxyl groups for silane grafting.⁶ Some substrates (e.g., silica, agarose, etc.) already have hydroxyl groups, while others require a pretreatment step using KOH/NaOH, acid, piranha solution, or plasma treatment to introduce hydroxyl groups. For instance, silanization with APTES for controlling the interactions between inert stainless steel for the preparation of working or counter electrodes and biocomponents generally involves a pretreatment step that may involve heat, acid etching, and/or chemical treatment.⁷ Phosphoric acid chemisorption has been demonstrated for silanization of TiO₂ films.⁸ APTES assembling is enhanced via phosphoric acid preadsorption on the anatase TiO₂ film as compared to pristine TiO₂ with no phosphoric acid treatment.

In general, APTES reacts with the free hydroxyls of an oxidized substrate by S_N2 exchange with loss of ethanol. APTES bonds to a substrate in three different ways (Scheme 1). Surface attachment and condensation lead to horizontal polymerization when a surface-bound APTES molecule forms siloxane with its neighboring surface-bound APTES.^{6,9} In vertical polymerization, the surface-bound APTES reacts with a nearby APTES in solution.¹⁰ In the third scenario, where the substrate possesses surface hydroxyl groups, the amine of APTES forms a hydrogen bond with the metal surface or becomes protonated by abstracting protons from the surface.¹¹ Therefore, a mixture of neutral amine and protonated and hydrogen-bonded amines coexists on the solid surface; the former orients away from the surface for biomolecule immobilization, whereas the latter is close to the surface. The amine group is transformed with various curing conditions and substrate-dependent. For the substrate

Scheme 1. Different Bonding Modes for APTES on a Substrate Surface



without oxide groups, amines react quickly with carbon dioxide of the atmosphere to form bicarbonates and then imines in the presence of heating.

The silanization mechanism is complex with adsorption and chemical sorption contributing to the rate-determining steps. Initially, silanization is fast and governed by the Langmuir model leading to a SAM followed by a slow kinetic saturation process.^{12,13} Silanization is classified as wet chemistry or chemical vapor deposition (CVD). The former is performed in liquid medium and classified as organic, aqueous, or evaporation-based, depending upon the choice of solvents. Silanization is initiated via the hydrolysis of ethoxy terminal groups of APTES by the moisture (organic phase and evaporation-based approaches) or by water (aqueous phase). The CVD approach is based upon the deposition of silane vapor on a substrate surface.

Another popular and commercially available silane, (3-glycidoxypropyl)-trimethoxysilane (GOPS), is also frequently used for covalent bonding of biomolecules. Epoxy groups are very stable in neutral pH, and under aqueous reaction conditions,

are reactive toward nucleophiles such as amines, thiols, or acids. Immobilization of biomolecules to an epoxy-modified substrate occurs via a two-step procedure: adsorption followed by covalent reaction between amino acid side groups (amino, thiol, or hydroxyl) and epoxy groups. However, high ionic strength is necessary to promote biomolecule adsorption using GOPS, which could denature proteins/fragile enzymes,¹⁴ limiting its widespread applications.

2.2. Wet Chemistry

2.2.1. Organic Silanization. An anhydrous solvent with a negligible trace amount of water is required in the preparation for controlling the degree of polymerization of APTES at the surface and in solution. APTES concentrations above 10% result in the formation of oligomers and polymers, whereas 0.4% APTES allows for monolayer coverage.¹⁵ Silanization at 60–90 °C disrupts noncovalent interactions including hydrogen bonding to minimize the density of silane molecules that are weakly adhered to the surface. Extensive rinsing after silanization with toluene,

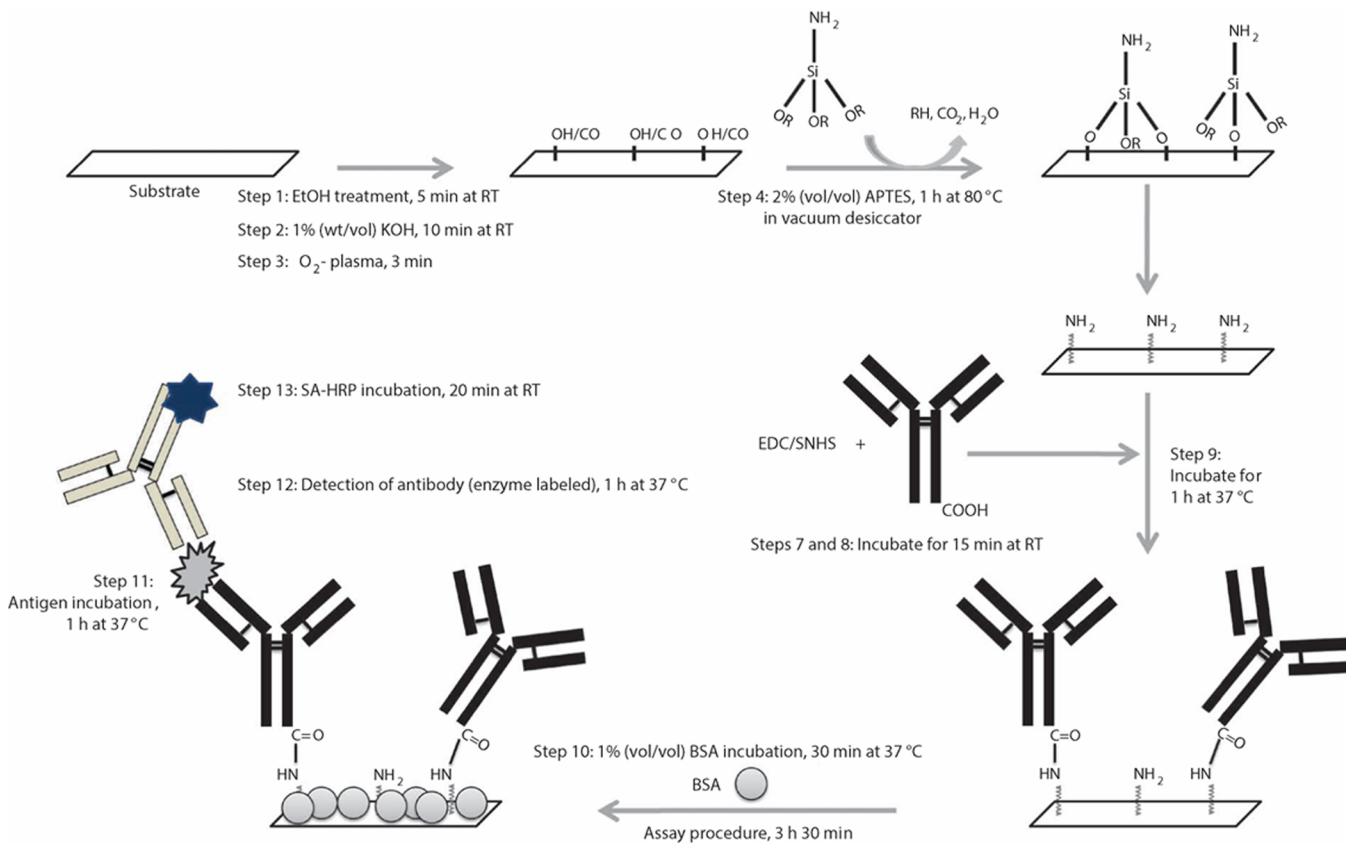


Figure 1. Treatment of a substrate with KOH and O_2^- plasma prior to APTES functionalization as part of an APTES-based sandwich ELISA procedure. Reproduced with permission from ref 60. Copyright 2011 Nature America Inc.

ethanol, or even water removes such weakly bonded silane molecules and hydrolyzes residual alkoxy linkages in the silanized layer. The drying—curing step, if performed at 110 °C, promotes the formation of siloxane linkages and converts ammonium ions to more reactive, neutral amines. However, the amine groups are dissociated at higher temperature and are completely eliminated at 150 °C.

To date, toluene-diluted APTES is widely used for the silanization (25 and 75 °C) of different materials ranging from plastics to metals.^{16–19} The grafting efficiency of different APTES concentrations, prepared in anhydrous toluene under nitrogen atmosphere on plasma-activated glass slides, has been demonstrated for the enhancement of cellular-adhesion.⁶ A monolayer of APTES is expected at room temperature with toluene as the reaction solvent (15 min at room temperature followed by air curing or 15 min at 200 °C). The more forcing conditions, such as increasing reaction and curing time, end up with the formation of multilayers.¹⁵

The ultraviolet/zone-activated glass is silanized by incubating with 1% APTES in anhydrous toluene at 60 °C.²⁰ Metallic NPs, however, require an additional step to generate an oxide layer on the particle surface. For example, Pb–Sn hybrid nanostructures are heated to generate an oxide layer for subsequent salinization with APTES (10% in toluene for 1 h).²¹ Similarly, TiO₂ surfaces are silanized using APTES reconstituted in toluene.²² Fe₃O₄ NPs are silanized by treatment with APTES reconstituted in toluene and DMF followed by incubation for 24 h with continuous stirring.²³ The silanization procedure has been extended to flat silicon surfaces,²⁴ mesoporous silica nanofibers,²⁵ monodispersed silica nanospheres,^{26,27} Ag nanotriangles,²⁸ attapulgite,²⁹

agarose,³⁰ zirconium,³¹ multiwalled carbon nanotubes (MWCNTs),³² and quartz fibers.³³

Acetone is another popular solvent to silanize carbon nanotubes (CNT, 30 min followed by drying at 60 °C),³⁴ silicon dioxide (5% APTES in acetone),³⁵ Pt electrodes (0.2% APTES in acetone, 12 h at 120 °C),³⁶ glassy carbon electrodes (GCE, 10% APTES in acetone for 5 h),³⁷ and optical grating coupler sensor chips.³⁸ Benzene,³⁹ anhydrous hexane,^{40,41} dimethyl sulfoxide (DMSO)/ethanol,⁴² ethanol (under reflux),^{43–48} chloroform,^{49,50} methanol,⁵¹ and glacial acetic acid/methanol⁵² are also useful for silanization. The APTES surface density is governed by solvent viscosity, which in turn affects the number of siloxane bridges formed. Hydrocarbons like isoctane and pentane are better solvents as they result in significantly higher APTES surface density. Pentane allows for greater mobility of the surface-bound silane due to its low viscosity, enabling the formation of more siloxane bonds. In contrast, the surface density of APTES molecules is not optimal when aromatic solvents such as toluene are used.⁵³ Therefore, the choice of organic solvent plays a critical step in silanization that can significantly affect a specific bioanalytical application.

APTES monolayer films prepared in a dry organic solvent must be cured under mild conditions and incubated in water before use. In contrast, thick films need to be treated in an oven or incubated in ambient conditions for a few days. APTES silanization of iron oxide NPs using 0.2% APTES in a mixture of methanol/toluene is not suitable at 30 °C. The highest APTES functionalization density is achieved at 70 °C using 2% of APTES.⁵⁴ If silanization is conducted at a lower reaction temperature and a lower silane concentration, it takes more than a day to get a silanized surface with a lower APTES

functionalization density. Only a minute amount of polymerized APTES is formed if silanization with APTES (10 mM) is conducted in dry toluene under reflux at 70 °C for 24 h.⁵⁵

2.2.2. Aqueous Silanization. Water plays a dual role as a solvent and catalyst for the hydrolysis of silane, a prerequisite for silane grafting. In aqueous solution, APTES is hydrolytically unstable as the ethoxy groups are easily hydrolyzed to produce ethanol and trisilanol groups. At neutral pH, the half-life of APTES is 56 h (at 10 °C) and 8.4 h (at 24 °C), respectively.⁵⁶ However, the Si–C bond will not further hydrolyze, and the aminopropyl group remains intact. The transient Si–OH groups also condense with other available Si–OH groups. In aqueous solution, the amine groups of APTES are positively charged.⁵⁷ Yet if the substrate is negatively charged, for example, silicon oxide,⁵⁸ APTES will electrostatically bind to the substrate surface. For silanization in water or ethanol, the APTES molecules are in the form of a monolayer even after a day. Thick APTES layers can be obtained after deposition from water using high APTES concentrations that could be attributed to different orientations of APTES at the surface.⁵⁹

Different polymeric substrates can be pretreated with 1% (w/v) KOH and oxygen plasma (e.g., using a reactive ion etcher) to generate the desired hydroxyl groups for silanization. Subsequently, these resulting polymers are incubated with 2% (v/v) APTES in deionized water for 1 h (Figure 1).⁶⁰ This simple treatment obviates the use of complicated oxygen plasma for silanization.⁶¹ Recently, this procedure has been proven in SPR-based immunoassays (IAs) using Au-coated SPR chips.^{62,63} The Au SPR chip is simply treated with a piranha solution for 2 min to generate the desired surface hydroxyl groups and incubated in 2% (v/v) APTES in water for 1 h. A typical mixture of the piranha solution is 3:1 (v/v) concentrated sulfuric acid to 30% H₂O₂ solution.

Of interest is aqueous silanization of an aluminized plastic surface by dip-coating with APTES:water (1:5) at pH 7 for 30 min, followed by incubation at 100 °C,⁶⁴ whereas polydimethylsiloxane (PDMS) and plastic are salinized with 5% (v/v) APTES.⁶⁵ SnO₂ surfaces can also be activated and coated with silanes prepared in deionized water.⁶⁶ For a diblock copolymer functionalized surface, an M5 4-(2-hydroxyethyl)-1-piperazineethanesulfonic acid (HEPES)-based buffer solution serves as the solvent with APTES simply drop-coated on the surface.⁶⁷ The effect of silanization on poly(methyl methacrylate) (PMMA)–alumina bonding of 3-methacryloxypropyl-trimethoxysilane, APTES, and *N*-(2-aminoethyl)-APTES, reconstituted in water, has been discussed elsewhere.⁶⁸

Aqueous silanization has also been advocated for various nanoparticulate surfaces due to its simplicity. Magnetic NPs are silanized using a water-doped organic solvent (~2% water)⁶⁹ or 10% (v/v) APTES in water.⁷⁰ Similarly, Si⁷¹ and Au⁷² NPs are incubated using various concentrations of APTES in ethanol:water (95:5) or only in deionized water.

The kinetics of silanization is described as a function of time and solvent. APTES (26.5 mM aqueous solution) is ideal for homogeneous coating.⁷³ The APTES adsorption and desorption kinetics for Si can be observed by solid/liquid ellipsometry. At 0.4% APTES, APTES first adsorbs to the silicon¹⁵ by noncovalent means and then reacts covalently with the surface.⁷⁴ Under mild curing, only the close one or two APTES monolayers on the silicon are stable, whereas the remaining APTES layers are weakly bound and thus removed. For APTES silanization of Fe₃O₄ NPs, the initial binding depends on reaction temperature and APTES concentration.⁷⁴ However, the former is more

important than the latter for silanization. For instance, the initial grafting density (within 1 h at 30 °C) is 64 mg g⁻¹ at 0.2% of APTES loading as compared to 224 mg g⁻¹ at 2% APTES loading. At 70 °C with 0.2% APTES loading, the APTES functionalization density is 236 mg g⁻¹. The overall reaction kinetics is complex involving both adsorption and chemical sorption.

2.3. Chemical Vapor Deposition

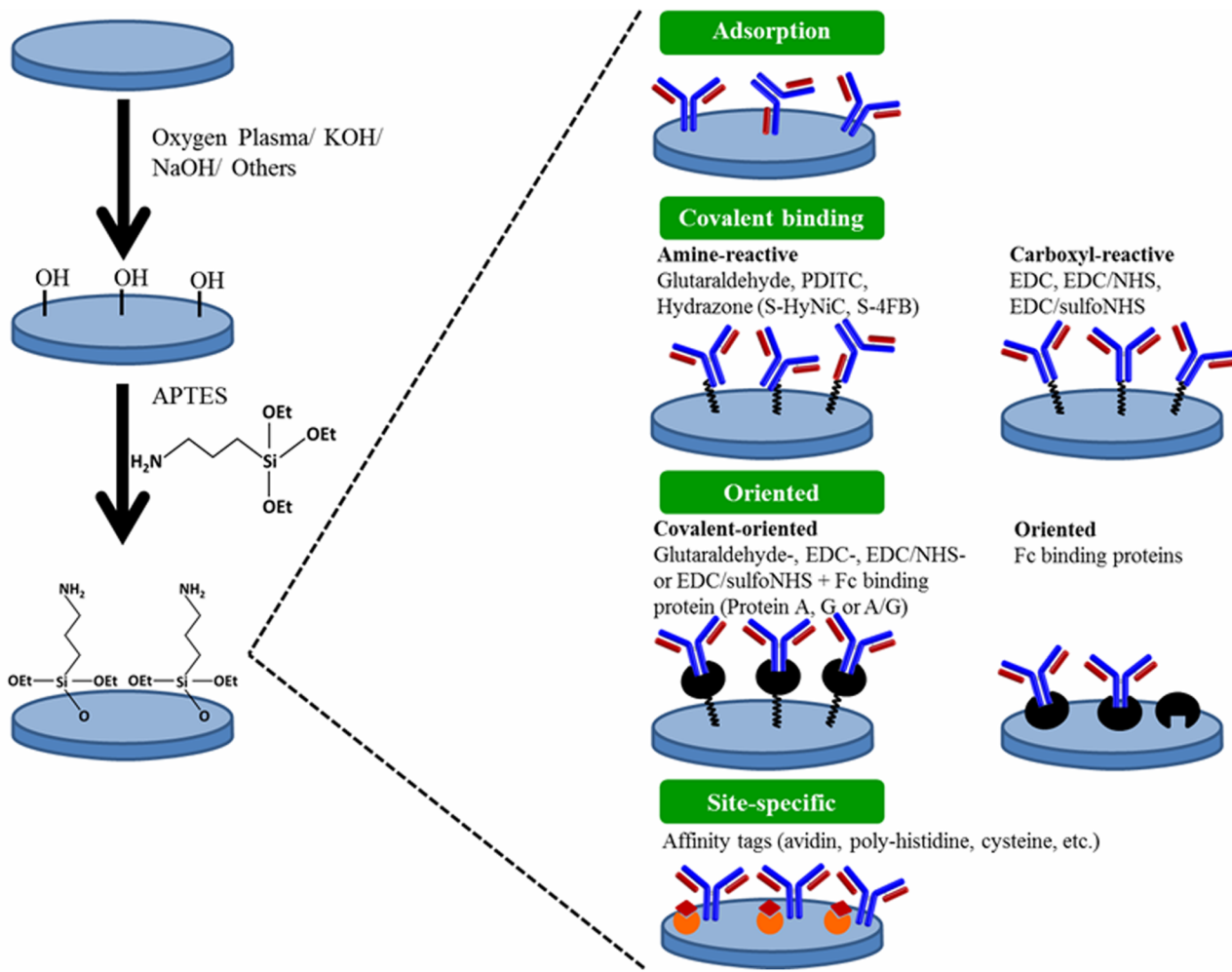
CVD is applicable for mass production of silanized substrates. It obviates the limitations of other approaches such as the presence of trace water in solution and the purity of silane. An activated substrate is simply placed in an environment saturated with silane vapor, leading to substrate silanization. As the silane polymers have negligible vapor pressure at the reaction temperatures, they do not get deposited on the target, thereby resulting in smooth monolayers. However, the attachment mechanism of silane molecules to the substrate is uncertain. The APTES layer thickness on silica is 5 and 6 Å at the deposition temperature of 70 and 90 °C, respectively, corresponding to the length of an APTES molecule, illustrating the formation of a monolayer on the substrate.⁷⁵

There are two types of CVD procedures, concentrated and dilute, which are dependent upon the APTES vapor density. As an example, the APTES film thickness on a piranha-activated and oven-dried glass surface is directly correlated to the vapor density.⁷⁶ Silanization in the vapor phase using a vacuum plasma deposition epitaxial system is pioneered by Jonsson and Olofsson.⁷⁷ There is higher heterogeneity in the APTES film formed at high-density vapor, leading to the development of several CVD procedures. Nevertheless, a simplified CVD setup is more practical where APTES is incubated along with the substrate at high temperatures inside vacuum desiccators, resulting in a cheaper alternative known as low vapor density CVD.^{78–80} The vapor deposition system offers stringent control over the vapor density, thickness, and homogeneity of the silane layer. Krumdieck and Raj⁸¹ described one of the first mechanical low-pressure metalorganic CVD (MOCVD) systems for surface functionalization,^{82,83} enabling the use of MOCVD for silanization.⁸⁴ Olofsson's mechanical CVD can be improved further by using novel mechanical components.⁸⁵ Consequently, plasma enhanced-CVD (PECVD) has been adopted as a potential CVD technique for surface functionalization of point-of-care (POC) diagnostic platforms.⁸⁶

2.4. Characterization of APTES-Functionalized Surface

The morphology and thickness of APTES layers are dependent on the conditions of deposition and curing, and it is of great interest to characterize the structure and chemistry of APTES at interfaces. For APTES freshly deposited on an unreactive, Fourier transform infrared (FTIR)-featureless Au surface, the FTIR signature of APTES has been well described in the literature.¹⁵ In brief, the peaks at 1132 and 1194 cm⁻¹ are characteristics of Si–OCH₂CH₃ groups, while a low frequency shoulder on the peak at 1132 cm⁻¹ indicates partial polymerization or Si–O–Si bond formation. Curing conditions after deposition also affect the FTIR signature, as exemplified by a new peak at 1034 cm⁻¹ that shows the formation of siloxane bonds when APTES on Au is exposed to air for 24 h.⁸⁷ However, a strong peak at 1126 cm⁻¹ indicates the presence of an enormous Si–OCH₂CH₃ on the Au surface. Three prominent peaks (1475, 1578, and 3300 cm⁻¹) reveal the existence of an amine bicarbonate salt formed by interaction with carbon dioxide and water vapor in the atmosphere.⁸⁸ The APTES adsorption on

Scheme 2. Schematic of Most Commonly Used Ab Immobilization Strategies on APTES-Functionalized Bioanalytical Platforms



silicon dioxide with some covalent attachment or cross-linking has been reported for the deposition of APTES on silicon dioxide in dry solvents.¹⁵

A mixture of protonated and neutral amine groups coexists on silicon dioxide or aluminum oxide when APTES is freshly deposited.⁸⁹ Protonated and hydrogen-bonded APTES amines are close to the silicon dioxide surface and interact with it via electrostatic and hydrogen bonds, while free amines and carbon are away from the surface. Longer reaction times result in multilayers followed by the formation of macroscopic aggregates of APTES. Irregular shapes of APTES samples with a dense, web-like structure should be expected from toluene deposition under reflux conditions.

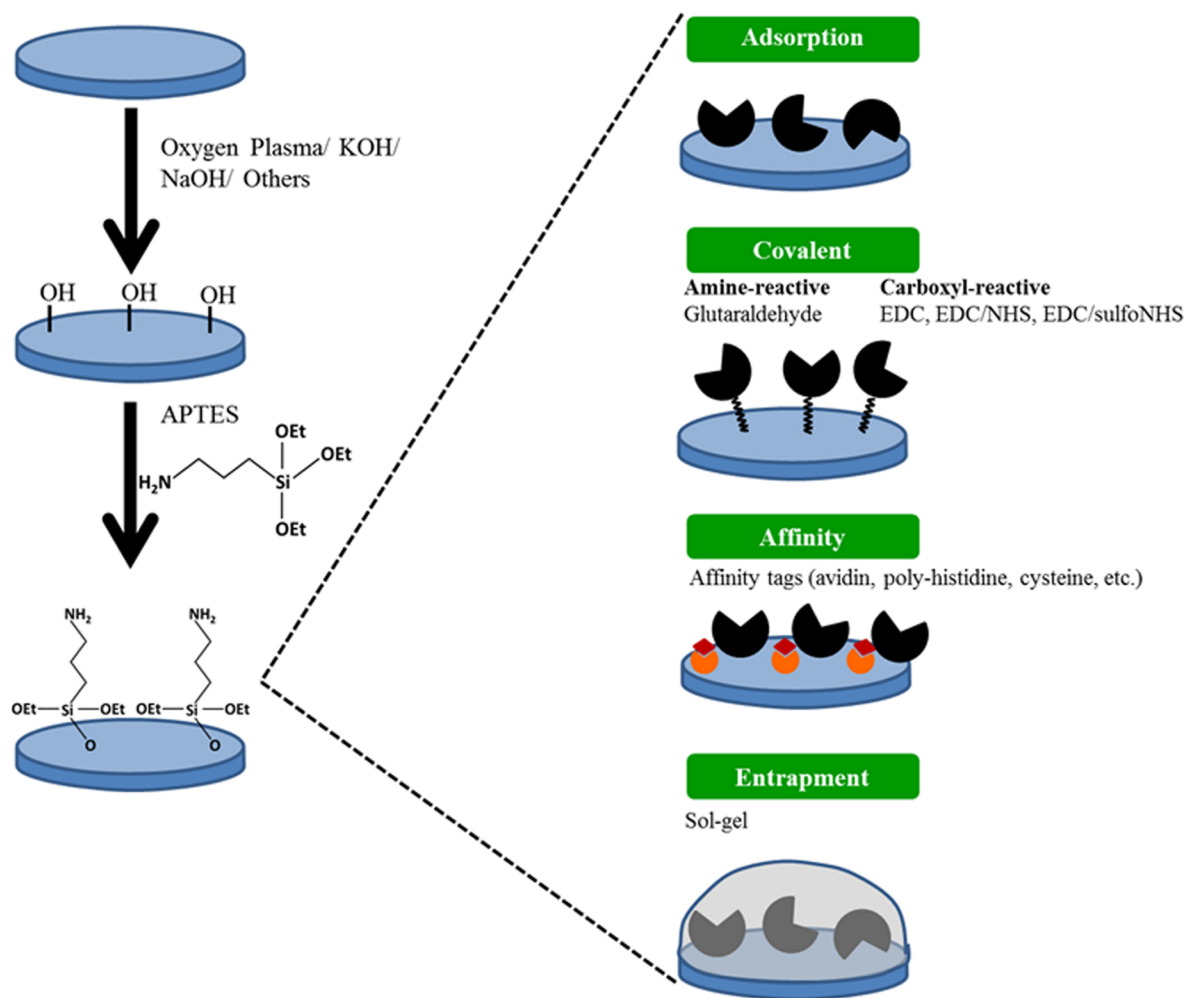
Several different techniques can be used for probing the surface roughness before and after silanization and bioconjugation. Such techniques also enable the estimation of protein immobilization density and morphology. The analysis of atomic force microscopy (AFM) height histograms provides useful information about average height and roughness of an organic layer.⁹⁰ The average height of an APTES layer on Si₃N₄ is 0.80 ± 0.02 nm, in agreement with Kim et al. (0.8–1.3 nm)⁹¹ with a surface roughness of 0.23 ± 0.01 nm. Noncontact AFM is often used for probing the 3-D structure of bound biomolecules. Although the specific biomolecular binding can be quantified, AFM does not provide pertinent information related to biomolecule surface density. Such information can be obtained

by other techniques such as SPR, ellipsometry, or isotopic labeling.^{92–95}

The protein/amino-organosilane/interface structure can be confirmed by X-ray photoelectron spectroscopy (XPS), whereas homogeneous protein binding is probed by a near-field scanning optical microscope in reflection and fluorescence mode. A surface analytical method such as XPS can be used to identify and quantify the presence of an immobilized biomolecule film from the increase of the signals in the N 1s, C 1s, and O 1s regions. The thickness of protein coatings is measured by angle-resolved XPS (ARXPS) and evaluated according to Paynter et al.⁹⁶ The photoelectrons from amine (NH₂, 399.8 eV) are taken as characteristic for the APTES film, while protonated amino groups (NH₃⁺, 401.4 eV) of the N 1s core-level show the protein layer. Surface coverage with proteins can be determined with ARXPS^{97,98} or microgravimetry.⁹⁸ Time-of-flight secondary ion mass spectrometry (ToF-SIMS) is another technique to analyze immobilized biomolecules.^{99,100} The disulfide bond signal in ToF-SIMS is directly related to the activity of adsorbed protein coatings. A pertinent model with combined information from AFM, ARXPS, and ToF-SIMS can provide insight into the vertical structure with respect to the surface density of biomolecules.

Contact angle measurement is extremely sensitive to contamination; therefore, purified liquids and very clean solid surfaces are required to attain good reliability and reproducibility

Scheme 3. Schematic of Most Commonly Used Enzyme Immobilization Strategies on APTES-Functionalized Bioanalytical Platforms



to within a few degrees. With a contact angle of less than 90° , the solid surface is considered hydrophilic, and, beyond this value, the solid surface is considered hydrophobic. In general, the silicon surface modified with APTES is hydrophobic as exemplified by a contact angle of $\sim 50^\circ$ obtained for silicon modified with APTES-GLD.¹⁰¹

There is considerable use of APTES and related organosilanes in the synthesis of bonded silica chromatographic stationary phases,¹⁰² a subject that is beyond the scope of this Review. FTIR and solid-state NMR spectroscopy are useful for probing bonding methodology, surface coverage, and silanol conversion efficiencies with supercritical-CO₂ as reaction solvent.¹⁰³

3. ANTIBODY–ENZYME IMMobilization

Various enzyme/Ab immobilization strategies, based on physical adsorption, covalent binding, affinity, entrapment, and other chemistries, will be described along with their advantages and limitations (Schemes 2 and 3).

Tables 2 and 3 summarize pertinent applications that use APTES for the immobilization of Abs and enzymes, respectively.

3.1. Covalent

The amine group of APTES enables the covalent bonding of biomolecules based on the use of a functional linker. GLD, a homobifunctional agent, cross-links the amino groups of APTES-functionalized surfaces to the biomolecule amino groups.³⁶

Aldehyde groups form imine bonds with amine groups of lysine common to almost every protein or enzyme to form reversible Schiff bases. If necessary, the carbon–nitrogen double bond can be reduced by a reducing agent to produce stable secondary amine linkages. In aqueous solution, GLD might possess different structures, which in turn affect immobilization reactivity. A dimer GLD form enables fast protein immobilization as compared to its monomer counterpart.¹⁰⁴ In a low ionic medium, immobilization proceeds via ionic exchange with the amino groups on the support followed by the covalent attachment. In a high ionic medium, the biomolecule is directly immobilized by covalent bonding with slower immobilization kinetics.

The binding of Abs by their amino groups might lead to improper orientation of Abs by masking antigen-binding sites at the amino terminal. This shortcoming can be circumvented by using heterobifunctional cross-linkers and fragment crystallizable (F_c)-binding proteins (FBP). The most widely used heterobifunctional cross-linker combination is EDC and *N*-hydroxysuccinimide (NHS)/*N*-hydroxysulfosuccinimide (SNHS), where EDC of the EDC-NHS/SNHS complex first binds to the carboxyl-terminal of the Abs (see Figure 1).⁶⁰ The zero-length cross-linker EDC-NHS/SNHS leaves the activated surface after an amide bond between NH₂-APTES and the COOH-Ab is formed. Commercial manufacturers often

Table 2. APTES-Based Antibody Immobilization Strategies and Their Applications in Biosensors and Diagnostics

ref	description of APTES-based antibody immobilization strategy	biochip substrate	application
16	glass – APTES – GLD – coating Abs (anti-MYO, anti-CK-MB, anti-Trl, anti-FABP)	glass capillaries	detection of human myocardial proteins by chemiluminescence IA
17	SU-8 photoresist – cerium ammonium nitrate treatment – APTES – GLD – anti-CRP Ab	SU-8 photoresist	immobilization of IgGs on SU-8 photoresist surfaces
18	silicon nitride – APTES – GLD – Abs against bovine PrP field effect transistors (FET) – APTES – GLD – antialpha fetoprotein	resonator (silicon nitride deposited on silicon wafer)	detection of PrP using nanomechanical resonator arrays and secondary mass labeling
19	glass – APTES – Au NPs – Ag – IgG	FET	detection of tumor marker antialpha fetoprotein using stable Ab-modified FET
20	quartz optical fibers – APTES – carbonyldimidazole–polyclonal Ab against Newcastle disease virus (NDV) – NDV	microscope glass slide	Au NP-based silver-enhanced IAs
33	Pt – APTES – GLD – anti-MA Ab	quartz optical fibers	detection of NDV
36	GCF – APTES – Au NPs – <i>Staphylococcal Protein A</i> – anti-GA IgG	Pt	development of IMS to determined MA
37	OGC sensor chip – APTES – GLD – anti- <i>Salmonella</i> Ab	GCF	detection of GA in the rice grain using SWASV technique-based IMS
38	IrO _x electrodes – APTES – GLD – anti-CEA/anti-AFP	OGC sensor chip	detection of <i>Salmonella</i> with a direct-binding OGC IMS
41	microchips on glass slides – APTES – GLD – goat IgG	IrO _x electrodes	simultaneous electrochemical immunosensing of CEA and AFP
43		microchips (with dual-ring working and counter electrodes, and a sensing cavity chamber) on glass slides	development of electrochemical enzyme IA microdevice using dual ring electrodes with a sensing cavity chamber
44	LiTaO ₂ – SiO ₂ – APTES – GLD – HBsAg	LiTaO ₂	a Love-mode SAW IMS was employed for the real-time detection of HBsAbs in whole blood samples
45	silicon – APTES – GLD – avidin – Ab GP3 (mouse monoclonal biotin-labeled anti-MI3)	Si wafer	detection of phage M13K07 using optical protein-chip
46	silicon – APTES – GLD – anti-human cTnT Ab	SiNW	detection of cTnT using complementary metal–oxide semiconductor (CMOS) SiNW sensor arrays
243	nanoporous Al – APTES – GLD – anti-SEB Ab	nano porous Al	detection of SEB by time-resolved EIS
47	silica – APTES – GLD – goat antihuman IgG Ab	silica monolithic capillary	detection of human IgG in human serum using immunoadsorption monolithic capillary microextraction coupled MCN-ICP-MS
48	interdigitated electrodes precoated with sol–gel derived BST film – preactivated dengue virus – APTES – GLD – antidengue virus Ab	BST-coated interdigitated electrodes	detection of dengue infection using sol–gel derived BST thin film and interdigitated electrodes
50	Nb/NbOx/Hf – APTES – GLD – k47 Ab	Nb/NbOx/Hf	detection of atrazine
51	COC – APTES – PDITC – goat antihuman IgG	COC (Zeonor and Zeonex)	Ab immobilization on COC for sandwich IA
52	COC – APTES – toluene-2,4-diisocyanate – goat antihuman IgG		detection of trace levels of TNT in seawater using microcapillary reversed-displacement IMS
71	COC – APTES – succinimidyl-[4-(N-maleimidomethyl)cyclohexane-1-carboxylate – goat antihuman IgG		elucidation of the surface amine-silanization reaction profile on fluorescent Si NPs
101	Cy5-labeled anti-TNT Ab	boronoflate glass microcapillary	covalent immobilization of proteins for imaging ellipsometry-based biosensor
105	Si NPs – APTES – EDC-sulfonNHS activated mouse IgG	dye-doped Si NPs	comparison of various EDC-based Ab immobilization strategies on APTES-functionalized immunodiagnostic platforms
107	Si – APTES – GLD – human IgG	Si slides	attachment of Abs to biosensor surfaces for label-free IA
108	PS and Au – APTES – EDC, EDC/SNHS and EDC/NHS – Ab	PS	preparation of IMS bioselective matrix
109	polystyrene – APTES – cross-linker – (N-(γ -maleimidobutyryloxy) succinimide ester – IgG	monocrystalline silicon wafer	preparation of uniform Ab-bound glass
176		PS	development of graphene-based IA for LCN2
177		polystyrene	development of modified polystyrene surface for ELISA development

Table 2. continued

ref	description of APTES-based antibody immobilization strategy	biochip substrate	application
180	mesoporous Si NPs – APTES – GLD – anti-CEA Ab	Si NPs	development of ultrasensitive chemoluminescence IMS using HRP-labeled mesoporous Si NPs
181	polystyrene – APTES – 4,4-bis(4-hydroxyphenyl) valeric acid-BSA conjugate	polystyrene	development of IA for hapten–protein conjugates on modified polystyrene surface of microtiter plate
186	glass – Au – Si NPs/APTES/EDC/NHS – Protein A – antifibrinogen Ab	glass	detection of fibrinogen by LSPR
187	Au SPR chip – KOH – APTES – anti-HFA	Au SPR chip	SPR-based IA biosensor was designed for the detection of HFA
188	glass – APTES – GLD – goat antihuman IgG/goat antirabbit IgG	glass slides	development of an optical IMS based on SELS
190	silicon microring – 2% APTES – GLD – anti-IgE or antithrombin aptamers	Si microring	SOI format to detect human IgE and human thrombin
191	Si microring – APTES – succinimidyl hydrazinonicotinamide – succimidyl 4-formylbenzoate – anti-CEA	Si microring	development of a Si microring resonator for label-free detection of antigens
192	glass – APTES – photoresist – biomolecule	glass	development of APTES-functionalized nanoporous polymer gratings
193	guided-mode resonance filter (silicon nitride deposited on adhesive polymer resin functionalized glass) – APTES – GLD – Abs against cardiac markers	guided-mode resonance filter biosensor chips	detection of cardiac markers in human serum using a GMR biosensor
194	fiber optics – APTES – GLD – BPA-BSA	fiber optics	an AFQOB for the detection of BPA leaching risk using fluorescent-labeled anti-BPA monoclonal Abs
195	silica capillary – APTES – GLD Abs for <i>E. coli</i> O157:H7	silica capillary	the detection of <i>E. coli</i> O157:H7 by monitoring the side reaction of <i>p</i> -nitrophenol an optical biosensor based on FTIR spectroscopy for the detection of pathogenic
197	titania sol–gel films – APTES – GLD – Abs against <i>E. coli</i> O157:H7	titania	<i>E. coli</i>
38	OGC sensor chip – APTES – GLD anti- <i>Salmonella</i> Abs	OGC sensor chip	the detection of <i>Salmonella</i> using a direct binding OGC IMS based on optical waveguide light mode spectroscopy
198	glass – APTES – streptavidin – biotinylated antimouse IgG-Fc specific/biotinylated mono- or poly clonal anti-PSA Abs	glass	development of an integrated microfluidic processor for automated microfluidic IAs based on solid phase capture of Abs
201	glass – APTES – EDC/NHS – IgG	glass	development of multiplexed protein microarrays in a single microfluidic channel
209	glass – APTES – streptavidin-coated beads – biotinylated capture Ab	glass substrate	development of on-chip IA using electrostatic self-assembly of streptavidin-coated beads on silanized glass substrates
215	PZT glass cantilever – APTES – EDC – sulfoNHS activated anti- <i>E. coli</i> O157:H7 Ab	PZT cantilever	detection of <i>E. coli</i> O157:H7 using PZT cantilever sensor
216	PZT cantilever – APTES – EDC-sulfoNHS – Ab	PZT cantilever	the label-free detection of fentogram levels of <i>E. coli</i> and other microbes was demonstrated in flowing liquid samples using PZT microcantilever-based IMS detection of BA spores
217	Pt electrode – APTES – Nafion – BSA solution containing GLD and GOx – Perfluorocarbon Polymer	PZT cantilever	development of long-term lifetime amperometric glucose sensor
221	ITO – APTES – GLD – Ab	ITO	development of a disposable IMS for the detection of HER-3 cancer biomarker
231	ITO electrode – APTES – Au NPs – VEGF Ab fragment	ITO electrode	electrochemical detection of VEGFs using VEGF Ab fragments modified Au NPs/ITO electrode
232	Au PCB – APTES – 1,4-penylene diisothiocyanate – antiaflatoxin M1 Ab	Au	development of electrochemical immunochip sensor for aflatoxin detection
242	sol–gel derived BST thin film – APTES – GLD – antihuman IgG	BST thin film	detection of human IgG using sol–gel derived BST thin film
247	CdS-G-agarose hybrid – APTES – GLD – AFP	CdS-G-agarose hybrid	electroluminescence IMS for ultrasensitive detection of AFP
253	MEG – APTES – EDC/NHS-activated Ab	MEG grown on silicon carbide	development of a MEG-based IMS for hCG
254	GCE – Nafion-cysteine-graphene sheets – Au NPs – anti-GRP	GCE	detection of ProGRP using glucose oxidation as a means to detect other biomolecules
260	stainless steel – APTES – Au NPs – monoclonal Ab	stainless steel	development of impedimetric IMS for doxorubicin
262	Fe ₃ O ₄ NPs – APTES – GLD – IgG	Fe ₃ O ₄ NPs	immobilization of Abs on Fe ₃ O ₄ NPs
263	Fe ₃ O ₄ NPs – APTES – GLD – fluorescein-labeled antimouse IgG	Fe ₃ O ₄ NPs	development of Fe ₃ O ₄ NPs for biorecognition
264	Au – Fe ₃ O ₄ /CdSe–Cds NP/polyelectrolyte nanocomposite – Au NPs – anti-CEA Ab	Au	ECL detection of CEA using Fe ₃ O ₄ /QDs
268	Fe ₃ O ₄ NPs	Fe ₃ O ₄ NPs	detection of <i>Salmonella</i> using personal glucose meters
270	Fe ₃ O ₄ NPs – APTES – GLD – monoclonal Abs	Fe ₃ O ₄ NPs	

Table 2. continued

description of APTES-based antibody immobilization strategy	biochip substrate	application	ref
Fe ₃ O ₄ NPs – APTES – GLD – Ab	Fe ₃ O ₄ NPs	development of Fe ₃ O ₄ NPs-based ELISA to detect multiresidue organophosphorous pesticides	271
polycarbonate	polycarbonate	development of self-assembled nanoparticulate film for covalent attachment of Abs to plastic	272
Si NPs – APTES – carboxyl-functionalized Au-coated glass	Si NPs	development of a local SPR-based nanochip	273
SiNWs/NPs – APTES – EDC – monoclonal Ab CD54	SiNWs and NPs	comparison of Ab-functionalized SiNWs and Si NPs by measuring their specific binding with THP-1 monocyte cells using flow cytometry	275
silicon – APTES – GLD – goat antihuman IgG	Si	detection of proteins by heterostructured ZnO/Au NPs-based resonant Raman scattering	283
glass – APTES – anti-HSA Ab	glass	detection of HSA using biotinylated polyclonal anti-HSA Ab bound to streptavidin-conjugated CdSe/ZnS QD	284
Fe ₃ O ₄ NPs – APTES – Au – Ab of CA125	Fe ₃ O ₄ NPs	ECL sensor using QDs for the detection of carbohydrate antigen 125	285
ITO – graphene – Fe ₃ O ₄ NPs – Ab for PSA	ITO	ECL sensor using QDs for the detection of PSA	286
Si – APTES – anti-CEA monoclonal Ab/anti-CEA labeled with Alexa 647	Si	patterning of biomolecules on silicon-based analytical devices	288
epoxy-functionalized mPDGs – APTES/octadecyltrichlorosilane – monoclonal Ab	mPDGs	development of mPDGs for the fluorescent detection of human IL-10	289
quartz – APTES (10%) – GLD – Ab	quartz fibers	detection of T2 mycotoxin	295
silicon – APTES (CVD) – GLD – Ab	silicon	characterization of the biosensor surface	296
N-vinyl-2-pyrrolidone/allyl alcohol modified polyethylene – APTES – high affinity heparin oligosaccharides	N-vinyl-2-pyrrolidone/allyl alcohol modified polyethylene	immobilization of heparin oligosaccharides and determining its anticoagulant activity	297
Au – APTES – (GLD – albumin/hexamethylenediamine) – 2,4-dichlorophenoxyacetic acid	Au	characterization of monoclonal Abs to 2,4-dichlorophenoxyacetic acid	298
piezoelectric quartz crystal – APTES – GLD – protamine	piezoelectric quartz crystal AT-cut	determination of IgM	299
piezoelectric quartz crystal – APTES – tressyl chloride – protamine	piezoelectric quartz crystal	functionalization of piezoelectric crystal with APTES for immunobiosensing	300
Piezoelectric quartz crystal – APTES – teraphthalidcarboxaldehyde – Protein G – IgG	Piezoelectric quartz crystal	fabrication of APTES-functionalized SPR chip for immunobiosensing	301
Au-coated glass chip – APTES – GLD – anti-HSA/anti-atrazine Ab – HSA/ atrazine	Au-coated glass chip	AFM studies of immobilized Abs	302
silicon – APTES – oxidized anti-HBsAg IgG – HBsAg	silicon wafer	site-directed immobilization of IgG on APTES-functionalized silicon	303
silicon – APTES – oxidized rabbit anti-HBsAg IgG (aldehydes generated on the carbohydrate side chains at the C-terminal of IgG using sodium periodate-oxidized reactions) – HBsAg	silicon wafer	detection of staphylococcal enterotoxin C ₂	304
Au-coated piezoelectric quartz crystal – APTES – GLD – antistaphylococcal enterotoxin C ₂ Ab – staphylococal enterotoxin C ₂	Au-coated piezoelectric quartz crystal	development of more efficient and effective glass-base immunosupports	305
glass wool fibers – APTES – NaIO ₄ oxidized goat antibody Ab – biotinylated ALP	glass wool fibers	development of immunoaffinity solid-phase microextraction coating for biological sample analysis	306
fused silica fiber – APTES – GLD – theophylline Ab – theophylline	fused silica fiber	comparing various antigen coupling methods for optical fiber-based IMMs	307
optical silica fiber	optical silica fiber	immobilization of Ab on silicon membranes containing arrays of micro pores	308
microporous silicon membranes – APTES – PDITC – Cy5-labeled goat antihuman IgG	microporous Si membranes	detection of cynidium mosaic protivirus and odontoglossum ringspot tobamovirus	309
quartz crystals – APTES – GLD – cynidium mosaic protivirus/odontoglossum ringspot tobamovirus Ab	circular AT-cut 10 MHz Quartz crystal microbalances with Au electrodes	investigation of blood protein adsorption onto chitosan	310
polished Si wafer – APTES – GLD-linked chitosan – polyclonal Ab	polished Si wafer	development of microfluidic enzyme IA	311
Si microchip – APTES – GLD – antiatrazine Ab	Si microchip	development of Ab microarrays	312
glass – APTES – NaIO ₄ oxidized Abs	glass slides	immobilization of proteins on silicon surface modified with mixed silanes layer for imaging ellipsometry-based biosensor	313
Si – mixed silanes (APTES and methyltriethoxysilane) – GLD – human IgG	Si wafer		

Table 2. continued

ref	description of APTES-based antibody immobilization strategy	biochip substrate	application
314	glass – APTES – GLD – antimouse IgG peroxidase conjugates	glass	polymer grafting on glass for protein chip applications
315	glass – APTES – agarose gel – NaIO ₄ – GLD – IgG	agarose gel on glass slides	enzyme IA on microarray that was prepared on the basis of the oxidation of agarose gel
316	silicon nitride – APTES – aldehyde – human transferrin/6x His-HrpW – Primary Ab – secondary Ab	glass beads	regeneration of Abs for repeated use in IMA
317	silica – APTES – FITC – anti-HBsAg (mouse monoclonal IgG1)	silicon nitride	development of silicon nitride surface modification strategy for developing biosensors
318	Au-coated Si – APTES – EDC-Neutravidin – biotinylated human IgG	silica sphere	preparation of amine-functionalized FITC-doped Si NPs
319	glass – APTES – GLD – goat antihuman IgG	Au-coated Si chip	quantification of human IgG immobilized on Au-coated Si chip
320	silicon – APTES – NaIO ₄ oxidized IgG	glass slide	development of signal enhanced QCM-based IA using colloidal Au immunocomplex
321	glass – APTES – chicken IgG	Si wafer	immobilization of IgG on APTES-functionalized Si wafer surfaces
322	glass – APTES – GLD – rabbit IgG	glass cover slides	immobilization of proteins on the modified glass surfaces
323	silicon – APTES – GLD – human IgG	glass slides	optimization of printing buffer for protein microarrays
324	piezoelectric cantilever – APTES – EDC-sulfoNHS-Ab complex	silicon wafer	detection of ultrathin biological films by ellipsometry
216	silica – APTES – GLD – streptavidin – biotinylated anti-IgG	piezoelectric cantilever (PZT layer bonded to borosilicate glass or fused silica layer)	detection of biologics in flowing liquid samples
325	silicon – APTES – GLD – antihuman IgG	silica	monitoring of siloxane monolayer formation on silica using a fiber Bragg grating
326	silica – APTES	Si wafer	reduction of morphological anomalies in protein arrays using non-nucleophilic additives
327	glass – APTES – GLD – antimouse IgG-FITC labeled	glass slide	development of protein chips using APTES
328	SiO ₂ – APTES – GLD – anti-turbo GFP Ab	SiO ₂ substrates	precise micro-/nanoscale patterning of functional biomolecules
329	glass – APTES – rabbit γ-globulins	glass capillaries	development of capillary waveguide fluoroIMs
330	SiO ₂ – APTES – anti-M13KO7 IgG1 FITC-labeled	SiO ₂ surface of differential capacitive biosensor	Ab immobilization on SiO ₂ and polyester surfaces for biomedical applications by light-guided surface engineering
331	PDMS – APTES – GLD – antiglutathione S-transferase Ab	PDMS column	development of a miniaturized, polymer-supported immunoprecipitation method for the on-chip purification of proteins from complex mixtures
332	SiO ₂ – APTES – biotin-NHS – streptavidin – biotinylated antirabbit IgG	Au/SiO ₂ template substrates	creation of patterned biofunctional surfaces using chemically modified Au/SiO ₂ template substrates
333	waveguide glass – APTES – cholic acid/cysteine/cyanuric chloride complex – hapten – 6HEX labeled anticholic acid Ab	waveguide glass	detection of protease activity using the Ab-hapten complexes attached to waveguide glass
334	porous silica – APTES – GLD – FITC-labeled rabbit IgG	porous silica	microcontact printing of proteins on nanoporous silica for POC immunoassays
335	interdigitated microelectrode SiO ₂ sensor chip – APTES – GLD – anti-Japanese encephalitis virus (JEV) Abs	interdigitated microelectrode sensor chip	comparison of different methods to immobilize anti-JEV Abs on interdigitated microelectrode sensor for electrochemical detection
336	sensor chip – APTES – anti-JEV Abs		photoinduced protein immobilization on quartz glass slides using benzophenone
337	quartz glass – APTES – benzophenone – UV light – protein (IgG and BSA) – silicon nanofiber – APTES – GLD – Protein A – anti-JEV Abs	Si	Debye screening manipulation for quantitative spatial analysis of induced charge on a nanosensor surface
338	Cr – APTES – GLD – Ab/Ag	Cr	reusable chromium-coated QCM for immunosensing
339	TiO ₂ – APTES – GLD – protein	TiO ₂	development of highly sensitive microarray
340	silicon nitride – APTES – bis(sulfosuccinimidyl)suberate – antigutathione-S-transferase Ab	silicon nitride	biofunctionalization of cantilever for adhesion studies
341	glass – APTES – GLD – antiglyphosate Ab	glass	detection of glyphosate by UV spectroscopy and fluorescence
342	Fe ₃ O ₄ NPs – poly(allylamine hydrochloride) – CdSe-Cds QD – APTES – Au – Au NPs – Ab	Fe ₃ O ₄ NPs	magnetic electroluminescence using magnetic NPs for efficient immunosensing of a cancer biomarker
343	interdigitated sensor – APTES – GLD – Protein A – anti-JEV		label-free detection of viral antigens
344			interdigitated sensor

Table 2. continued

description of APTES-based antibody immobilization strategy	biochip substrate	application
SiNW – APTES – GLD – anti-CRP Ab	SiNW	development of SiNW array for CRP detection in serum
Au printed circuit board – APTES – GLD – anti-CRP Ab	Au printed circuit board	detection of CRP using glucosamine-Cu cubes
SiNW – APTES – poly(sodium 4-styrenesulfonate) – poly(allylamine hydrochloride) – antiavian influenza Ab	SiNW	development of a dual-gate FET
titania – APTES – GLD – anti-PSA Ab	titania	to improve the protein immobilization efficiency of titania
Zeonor – APTES – dextran – NaIO ₄ – anti-CRP Ab	Zeonor	development of a polymer chip with silane-dextran chemistry for POC diagnostics
Polymer – APTES – EDC/SNHS – Ab	polymeric solid supports (PS), polycarbonate, poly(methyl methacrylate), cyclic olefin polymers (i.e., Zeonor and Zeonex)	development of rapid and highly sensitive chemiluminescent IA for human fetuin A
Zeonor – APTES – Ab fused silica capillary – hexadecyltrimethylammonium bromide, water, and TEOS and APTES mixed with ethanol – GLD – monoclonal Ab	Zeonor fused silica capillary	characterizing the biomolecular adsorption in polymeric microfluidic channels
silicon surfaces – APTES – GLD – Ab	Si surfaces	characterization of a highly selective immunosorbent that is coupled online to nanol C UV was presented and used for the selective extraction of microystin LR from blue-green algae extracts
photonic crystal – APTES – PDITC – Protein A – IgG Ab		evaluation of surface free energies of Ab-bound surfaces, where Abs were bound to APTES-functionalized Si surfaces
PDMS – APTES – GLD – Ab		development of a prospective label-free detection system for IgG Ab
TiO ₂ nanotube arrays-based electrodes – APTES – EDC/NHS – Ab	PDMS chip	comparison of two acoustic wave biosensors for IA applications
CMOS chip – APTES – GLD – Ab	TiO ₂ nanotube arrays-based electrodes CMOS chips	development of a signal-amplified electrochemical IMS
		development of a capacitive biosensor array on a CMOS chip using magnetic microbeads and on-chip electromagnetic manipulation
		development of optofluidics-based IMS for BPA
		development of a label-free photonic crystal biosensor for the detection of cTnI
		liquid crystal-based biosensor for BSA
		development of very highly sensitive sandwich ELISA procedure for IVD
		development of rapid sandwich ELISA procedure to detect HFA in 30 min
		development of a disposable biosensor for the very highly sensitive detection of RBP with attogram sensitivity
11094	ITO-coated glass plate – 3-mercaptopropionic acid capped Au NP – BSA PS MTP – Ab diluted in 1% APTES (1:1, v/v) Polystyrene MTP – KOH – EDC-activated Ab diluted in 1% APTES (1:1, v/v)	ITO
		ITO-coated glass plate
		PS
		PS
		PS
		ITO

Table 3. APTES-Based Enzyme Immobilization Strategies and Their Applications in Biosensors and Diagnostics

	APTES-based enzyme immobilization strategy employed	biochip substrate	application	ref
	glass microchannel – APTES – poly(maleic anhydride- <i>alt</i> - α -olefin)/GLD – FITC-labeled HRP	glass microchannel	development of a method to incorporate enzymes into microfluidic system channels	35
GCE – GLD-cross-linked GOx – APTES	GCE		development of a rapid and highly simplified procedure for reagentless glucose electrochemical biosensor	111
GCE – graphene/MWCNTs (in APTES) – EDC-activated GOx	GCE		comparison of graphene versus MWCNTs for electrochemical glucose bioensing	112
composite sol–gel glass – APTES + 2-(3,4-epoxycyclohexyl)-ethyltrimethoxysilane – GOx Pt electrode–permselective hybrid sol–gel film (APTES + TEOS + triethoxy- H_3 I H_2 H_2 H -tridecafluoro- α -octylsilane + BSA + chitosan) – GLD + GOx	composite sol–gel glass Pt		detection of glucose using encapsulated GOx within sol–gel glass development of amperometric glucose biosensor using permselective hybrid sol–gel film	173
GCE – graphene (in APTES) – EDC-activated GOx	GCE		development of GOx-bound graphene-functionalized GCE for mediatorless amperometric glucose sensing	175
GCE – APTES – GLD-cross-linked GOx	GCE		demonstrating the effect of APTES concentration on the MWCNTs-based reagentless glucose bioensing	218
GCE – APTES – MWCNTs (in dimethylformamide) – GLD-cross-linked GOx	GCE		development of GOx-bound APTES-functionalized MWCNTs for amperometric glucose bioensing	220
GCE – APTES – MWCNTs (in APTES) – GLD-cross-linked GOx	GCE		development of long-term analyte sensor	221
GCE – MWCNTs in APTES – GLD – GOx			development of silica nanowires-based electrochemical glucose biosensor	223
Au electrode/polymer-coated electrode – APTES – GLD/EDC – GOx			development of a novel one-pot electrodeposition strategy of using APTES-chitosan hybrid gel film to immobilize GOx for electrochemical glucose detection	224
Au electrode–vapor–liquid–solid grown silica nanowires – APTES – EDC/NHS – GOx			detection of putrescine	226
Au/platinized Au electrode – APTES + <i>p</i> -benzoquinone + chitosan + GOx	Au/platinized Au		improved detection of putrescine using PDDA to aid in dispersion of film materials	227
GCE – MWCNTs – Nafion – APTES – POx	GCE		disposable Au screen-printed electrodes for the detection of xanthine	228
GCE – MWCNTs – PDDA – Nafion – APTES – POx	CGE		detection of uric acid	229
Au – APTES/CNTs – Fe ₃ O ₄ NPs – xanthine oxidase	Au		increased anti-inflammatory effect of carageenan-induced paw edema in rats with immobilized enzymes	265
ITO – APTES – bis(sulfosuccinimidyl)subrate – uricase	ITO		development of trypsin bound hairy polymer chains hybrid Fe ₃ O ₄ NPs	269
Fe ₃ O ₄ NPs – serratipeptidase	Fe ₃ O ₄ NPs		investigating the effects of ZnO morphology on HRP immobilization and its catalytic activity	282
silica-coated Fe ₃ O ₄ NPs – APTES – GLD – trypsin	silica-coated Fe ₃ O ₄ NPs		enhanced DNA sensor with a QD/ZnO composite	287
ZnO nanocrystals – APTES + TEOS – GLD – HRP	ZnO nanocrystals		preparation of AuAg bimetallic NPs and their use for glucose sensing	359
ITO – ZnO – QDs – DNA/biotin – HRP/streptavidin	ITO		development of covalent strategy for the coimmobilization of cholesterol oxidase and HRP	360
quartz slide – APTES – AuAg bimetallic NPs – GOx	quartz slide		development of α -amylase-bound zirconium dynamic membranes	361
perlite – APTES – GLD – coimmobilization of cholesterol oxidase and HRP	perlite		development of bovine carbonic anhydrase-bound mesoporous silica for hydration and sequestration of CO ₂	362
zirconium – APTES – GLD – α -amylase	zirconium		development of catalase-bound CPG and its use in batch and plug-flow reactors	363
mesoporous silica – APTES – GLD – bovine carbonic anhydrase	SBA-15		mesoporous silica platform for cellulose-immobilized systems	364
controlled pore glass (CPG) – APTES – GLD – catalases	CPG		development of carbonic anhydrase-bound platform and its use to accelerate the hydration of CO ₂ for biomimetic CO ₂ sequestration in an aqueous solution	365
organo-functionalized mesoporous silica (FDU-12) – APTES – cellulase chitosan–acetic acid – APTES – hexadecyltrimethylammonium bromide – GLD – carbonic anhydrase	FDU-12		development of glucose- <i>α</i> -amylase-bound porous silica	366
CPG – APTES – GLD – cellulose/d-xylanase	CPG		macroporous silica gels	367

Table 3. continued

ref	APTES-based enzyme immobilization strategy employed	biochip substrate	application
368	porous glass beads – APTES – GLD – protocatechuate 3,4-dioxygenase soil – HNO ₃ – acetone – APTES – GLD – enzymes (laccase, GOx, tyrosinase, protease, β -D-glucosidase, acid phosphatase)	porous glass beads soil and clay	immobilization of protocatechuate 3,4-dioxygenase on CPG development of immobilization strategy for binding enzymes to soils and days
369	porous glass – APTES – GLD – glucoamylase	porous glass	preparation of APTES-treated porous glass and its use for glucoamylase immobilization
370	solid support – HNO ₃ (except hydroxyapatite) – APTES – GLD – amyloglucosidase/ α -amylase	CPG (many types)/Micropil (various types)/Unisphere uncoated alumina/Lichrospher/Kromasil/hydroxyapatite (various types)	comparison of enzyme immobilization on various inorganic supports
371	CPG – APTES – GLD – β -glucuronidase	CPG	immobilization of enzyme onto silica beads for the hydrolysis of urinary phenol prior to reversed-phase liquid chromatographic analysis
372	CPG – APTES – GLD – laccase	CPG	immobilization of laccase on CPG
373	CPG – APTES – GLD/EDC – Dextranase fused-silica capillary – 6 M HCl – APTES – GLD – trypsin	CPG fused-silica capillary	immobilization of dextranase on CPG and study of kinetics characterization of reaction dynamics in a trypsin-modified capillary microreactor
374	CPG – APTES – GLD – laccase Al ₂ O ₃ – APTES – GLD – enzyme (urease, GOx, acetylcholine esterase, and α -chymotrypsin)	CPG Al ₂ O ₃	immobilization of laccase on CPG development of enzyme monolayer functionalized FET for biosensing
375	ceramic membrane – APTES – GLD – glucoamylase	ceramic membrane	development of surface-modified ceramic membrane for enzyme immobilization
376	silica support – APTES/2-hydroxyethylmethacrylate – GLD – alcalase 2T mesoporous silica – APTES/ethanolamine – glyoxal – enzyme (lysozyme and catalase) nanoporous silica (SBA-15) – APTES – penicillin G acylase	silica derivatives mesoporous silica SBA-15	studying the effect of various silica derivatives on the immobilization and stabilization of the enzyme continuous surface modification for enzyme immobilization immobilization of penicillin G acylase on functionalized nanoporous silica
377	nanostructured silica – APTES – GLD – penicillins G acylase high-porosity mullite advanced ceramic material monolith – carbon nanofiber coating – APTES – GLD – polyethyleneimine – enzyme (β -galactosidase and lipase)	mesoporous silica high-porosity mullite advanced ceramic material monolith Florisil	design of mesoporous materials for immobilizing penicillin G acylase development of structured reactors for enzyme immobilization immobilization of catalase and study of its kinetics onto magnesium silicate
378	magnesium silicate (Florisil) – APTES – GLD – bovine liver catalase Na-Y zeolite – APTES – Au NPs	zeolite	immobilization of fungal protease on Au NP-loaded zeolite microspheres and study of its biocatalytic activity
379	stainless steel – APTES – GLD – lysozyme SiO ₂ – APTES – GLD – glutamate DHD mesoporous silica (pretreated with methanesulfonic acid) – APTES – acrolein glycol acetal + pyridine – triacylglycerillipase activated carbon – APTES – GLD – laccase nano-SiO ₂ – APTES – novel carriers with reactive aldehyde groups – porcine pancreatic lipase silicic acid + APTES – amino-chemically surface modified gel – GLD – invertase nanoporous silica – APTES – GLD – enzyme porous glass – APTES – GLD – enzyme (soybean peroxidase/HRP) TiO ₂ surfaces – APTES – ascorbic acid – enzyme (HRP and GOx) porous silicon dioxide – APTES – GLD – GOx	stainless steel SiO ₂ mesoporous silica activated carbon nano-SiO ₂ porous silica matrix nanoporous silica porous glass TiO ₂ porous silicon dioxide	covalent immobilization of tritylglycerol lipase onto functionalized mesoporous silica supports advantages of laccase immobilization covalent immobilization of tritylglycerol lipase onto functionalized nanoscale SiO ₂ spheres preparation of chemically surface modified gel for enzyme immobilization preparation of single enzyme NPs in nanoporous silica development of peroxidase-bound glass beads for phenol removal characterization of enzyme immobilization on TiO ₂ surfaces characterization of enzyme immobilization on silicon-based materials
380	mesoporous silica monolith – tetramethoxysilane:APTES (5:6 v/v) – GLD – penicillin acylase glass beads – APTES – triethylamine + dry cyclohexane + phthaloyl chloride – α -amylase SBA-15 mesoporous molecular sieve – APTES – penicillin acylase	mesoporous silica monolith glass beads SBA-15 mesoporous molecular sieve	covalent binding of penicillin acylase in mesoporous silica covalent binding of α -amylase on functionalized glass beads immobilization of penicillin acylase on SBA-15
391			
392			
393			
394			
395			
396			
397			
398			
399			

Table 3. continued

ref	APTES-based enzyme immobilization strategy employed	biochip substrate	application
400	ceramic monoliths – APTES – GLD – β -galactosidase	ceramic monoliths	immobilization of β -galactosidase on ceramic monoliths
401	SBA-15 – APTES – GLD – enzyme (α -chymotrypsin and lipase)	SBA-15	development of cross-linked enzyme aggregates in SBA-15
402	Si substrates (crystalline Si, porous Si, silicon nitride) – APTES – GLD – β -lipase	silicon substrates	covalent binding of lipase on semiconducting materials
403	organic–inorganic hybrid silica monoliths – TEOS + APTES + ethanol + cetyltrimethyl ammonium bromide + H ₂ O – GLD – trypsin	organic–inorganic hybrid silica monoliths	development of immobilized trypsin reactor based on hybrid silica monoliths
404	SBA-15 – APTES – pepsin	SBA-15	preparation of active biocatalysts by immobilizing pepsin in mesoporous SBA-15 and investigating the reusability of the bioreactor
405	silicone nanoflament coated-glass slides – O ₂ plasma – [2-(carbomethoxy)-ethyl]trichlorosilane – APTES – DY-647-NHS labeled α -chymotrypsin and lysozyme	silicone nanoflament coated-glass slides	use of superhydrophobic silicone nanoflaments for selective protein enrichment and purification applications
406	SiO ₂ – NH ₃ and H ₂ O ₂ water solution – APTES – GLD – GOx	SiO ₂	characterization of GOx immobilization on SiO ₂ surfaces
407	Si NPs – APTES – GLD – enzyme (GOx, invertase, esterase, and urease)	silica nanoparticles	determination of optoelectronic properties of a nanostructure system composed of enzyme-functionalized silica microparticles
408	silicon – APTES – dendrimer porphyrin – EDC/NHS – GOx	Si	development of a dendrimer-coated surface for GOx binding and analysis of protein activity
409	mesoporous silica SBA-15 and MCF – APTES – succinic anhydride – EDC – alkaline serine endopeptidase	SBA-15 and MCF	covalent binding of alkaline serine endopeptidase on SBA-15 and MCF
410	porous alumina membranes – H ₂ O ₂ – APTES – GLD – glucose-6-phosphate DHD	porous alumina membranes	development of a method for the covalent binding of human CYP2E1 and glucose-6-Phosphate DHD in porous alumina membranes for xenobiotic metabolic studies
411	porous alumina membranes – H ₂ O ₂ – APTES – N,N-dimethyl-formamide + N-succinimidyl 3-maleimidopropionate – human CYP2E1	mesoporous silica foams	improvement of microwave-assisted covalent binding of penicillin acylase using macromolecular crowding with glycine quenching
412	mesoporous silica foams – APTES – irradiation in microwave reactor – penicillin acylase carbon felt – APTES – various coupling agents (GLD; ascorbic acid; 1,4-benzoquinone; terephthaloyl succinimide ester + disuccinimidyl suberate) – tyrosinase	carbon felt	covalent binding of tyrosinase onto carbon felt using various coupling agents
413	GCE – APTES – GLD – acetylcholineesterase – choline oxidase	GCE	amperometric detection of paraoxon ethyl, aldicarb, and sarin using acetylcholinesterase-choline oxidase bound to Au–Pt bimetallic NP modified GCE
414	silica – TEOS and APTES in water/oil microemulsion – GLD – penicillin G acylase	silica	synthesis of aminopropyl-functionalized silicas by water/oil microemulsion and their use for immobilizing penicillin G acylase
415	Si wafer – APTES – sulfosuccinimidyl 4-(N-maleimidomethyl)-cyclohexane-1-carboxylate – rat phenol sulfotransferase	Si wafer	analysis of immobilized enzyme on planar surfaces in a microflow reactor
416	SiO ₂ – APTES – GLD – GOx	SiO ₂	development of molecular-thin functional microarrays of GOx
417	Ta ₂ O ₃ – APTES – GLD – acetylcholine esterase	Ta ₂ O ₃	investigation of the feasibility of transducing molecular-recognition into a measurable potentiometric signal
418	silica gel – APTES – GLD – β -galactosidase	silica gel	investigating the pretreatment of β -galactosidase with lactose to prevent the formation of covalent bonds near the active site during immobilization
419	silica gel – APTES – GLD – GL-7-ACA acylase	silica gel	covalent binding of GL-7-ACA acylase on silica gel
420	ZrO ₂ microtubes – APTES – EDC-activated lysozyme	ZrO ₂ microtubes	fabrication of ZrO ₂ microtubes with specific surface functionalization for bacteria filtration and digestion
421	SBA-15 – APTES – GLD – laccase	SBA-15	development of laccase-bound mesostructure silica material and its use for the degradation of naphthalene
422	MWCNTs – APTES – GLD – organophosphate hydrolase	CNTs	development of organophosphate hydrolase-bound CNTs with enhanced stability for the amperometric detection of paraoxon
423	macroporous silica gel – APTES – GLD – papain	macroporous silica gel	development of highly stable papain-bound macroporous silica gel for industrial application
424	silica-coated superparamagnetic Fe ₃ O ₄ microspheres – TEOS + APTES – GLD – penicillin G acylase	silica-coated superparamagnetic Fe ₃ O ₄ microspheres	development of penicillin G acylase-bound silica-coated superparamagnetic Fe ₃ O ₄ microspheres

Table 3. continued

	APTES-based enzyme immobilization strategy employed	biochip substrate	development of a nanosensor to evaluate the effect of metabolic agents on cancer metabolism and survival	ref 425
aluminum-coated optical fiber nanoprobes – APTES – GLD – lactate dehydrogenase monolithic hybrid silica – TEOS + APTES – GLD – trypsin	aluminum-coated optical fiber nanoprobes monolithic hybrid silica	development of device to enrich and digest proteins apart from performing online sample buffer exchange	development of contactless, low-cost, and rapid drug screening methodology by inkjet printing	ref 426
SiO ₂ surfaces – plasma oxide activation – APTES – GLD – GOx	SiO ₂	demonstrating the potential of immobilized laccase to polymerize technical lignosulfonates	demonstrating the potential of immobilized laccase to polymerize technical lignosulfonates	ref 427
aluminum oxide spherical beads – APTES – GLD – laccase	aluminum oxide spherical beads	covalent binding of catalase onto fluorasil using a spacer-arm and its application to batch and plug-flow type reactor systems	development of a stable and efficient aldolase immobilization technique using consecutive microwave irradiation at low temperature	ref 428
fluorisil – APTES – GLD – 6-amino hexanoic acid – 1-cyclohexyl-3-(2-norpholinoethyl) carbodiimide metho- <i>p</i> -toluen sulfonate – catalase	fluorisil	development of effective lipase-bound glass beads for hydrolysis of Naproxen methyl ester	development of effective lipase-bound glass beads for hydrolysis of Naproxen methyl ester	ref 429
mesocellular siliceous foam – <i>p</i> -benzoquinone – 2-deoxy-D-ribose-5-phosphate aldolase – microwave reactor (output power 30 W) coupled with a cooling module	mesocellular siliceous foam	synthesis and characterization of enzyme–magnetic NP complexes	synthesis and characterization of enzyme–magnetic NP complexes	ref 430
glass beads – APTES – GLD – lipase	glass beads	development of a novel glass-based support incorporating TiO ₂ and its use for immobilizing HRP to treat aqueous halogenated phenolic waste	development of a novel glass-based support incorporating TiO ₂ and its use for immobilizing HRP to treat aqueous halogenated phenolic waste	ref 431
glass beads – APTES – GLD – sol–gel encapsulation (using aqueous polyvinyl alcohol, aqueous sodium fluoride, and isopropyl alcohol, APTES + TEOS) – lipase	Fe ₃ O ₄ NPs	development of lipase-bound silica NPs for the enzyme-catalyzed resolution of racemic naproxen 2,2-trifluoroethyl thioester	development of lipase-bound silica NPs for the enzyme-catalyzed resolution of racemic naproxen 2,2-trifluoroethyl thioester	ref 432
Fe ₃ O ₄ NPs – APTES – GLD – GOx	porous glass	development of lipase-bound ordered mesoporous SBA-15 with improved adsorption	development of lipase-bound ordered mesoporous SBA-15 with improved adsorption	ref 433
porous glass – APTES – sodium borate buffer + HRP + sodium periodate	silica NPs	development of tyrosinase-bound carbon felt-based working electrode for the amperometric detection of phenolic compounds on Au NPs assembled onto mesoporous SBA-15 and its use for industrial-scale CO ₂ sequestration	development of tyrosinase-bound carbon felt-based working electrode for the amperometric detection of phenolic compounds on Au NPs assembled onto mesoporous SBA-15 and its use for industrial-scale CO ₂ sequestration	ref 434
silica NPs – APTES – GLD – lipase	SBA-15	development of porcine pancreatic lipase immobilization strategy for binding to the synthesized amino-functionalized short rod-shaped mesoporous silica	development of porcine pancreatic lipase immobilization strategy for binding to the synthesized amino-functionalized short rod-shaped mesoporous silica	ref 435
ordered mesoporous SBA-15 – APTES – porcine pancreatic lipase	carbon felt	development of a versatile and easy-to-use site-selective surface modification strategy using microcontact printing and the selectivity of enzymatic degradation	development of a versatile and easy-to-use site-selective surface modification strategy using microcontact printing and the selectivity of enzymatic degradation	ref 436
carbon felt – APTES – GLD – tyrosinase (under ultrasonic treatment)	SBA-15	development of reversible glucose immobilization onto Cu(II) metal–ligand functionalized magnetic SBA-15	development of reversible glucose immobilization onto Cu(II) metal–ligand functionalized magnetic SBA-15	ref 437
mesoporous SBA-15 – APTES – HAuCl ₄ (lead to the formation of Au NPs) – human carbonic anhydrase	short rod-shaped mesoporous silica	development of immobilization strategy for binding GOx onto cobalt-based silica core/shell NPs	development of immobilization strategy for binding GOx onto cobalt-based silica core/shell NPs	ref 438
short rod-shaped mesoporous silica – APTES – porcine pancreatic lipase	PDMS	development of invertase-bound glass-ceramic support and analyzing its performance in batch bioreceptor	development of invertase-bound glass-ceramic support and analyzing its performance in batch bioreceptor	ref 439
PDMS – O ₂ plasma – APTES – GLD – trypsin	magnetic SBA-15	detection of glucose using GOx-bound long period grating fibers	detection of glucose using GOx-bound long period grating fibers	ref 440
magnetic SBA-15 – APTES – 2-bromoisoobutyryl bromide – GMA/CuBr ₂ /Bpy/DMF/H ₂ O – glucoamylase	Co-based silica core/shell NPs	development of invertase-bound glass-ceramic support and analyzing its performance in batch bioreceptor	development of invertase-bound glass-ceramic support and analyzing its performance in batch bioreceptor	ref 441
magnetic SBA-15 – APTES – 2-bromoisoobutyryl bromide – GMA/CuBr ₂ /Bpy/DMF/H ₂ O – imidazole – glucoamylase	glass-ceramic support	development and characterization of glucoseylase-bound graphite nanosheets–Fe ₃ O ₄ NPs hybrid	development and characterization of glucoseylase-bound graphite nanosheets–Fe ₃ O ₄ NPs hybrid	ref 442
magnetic SBA-15 – APTES – 2-bromoisoobutyryl bromide – GMA/CuBr ₂ /Bpy/DMF/H ₂ O – iminodiacetic acid – glucoamylase	Co-based silica core/shell NPs – EDC – GOx	development of a β -galactosidase immobilized microreactor and its use for the continuous synthesis of lactose	development of a β -galactosidase immobilized microreactor and its use for the continuous synthesis of lactose	ref 443
Co-based silica core/shell NPs – EDC – GOx	long period grating fibers	ref 444	ref 444	
glass-ceramic support – APTES – GLD – invertase	graphite nanosheets – Fe ₃ O ₄ NPs – APTES – GLD – glucoamylase	ref 445	ref 445	
long period grating fibers – H ₂ SO ₄ – APTES – GOx	MWCNTs – APTES – MWCNTs – MWCNTs – APTES – EDC·HCl + β -galactosidase	ref 446	ref 446	
graphite nanosheets – Fe ₃ O ₄ NPs hybrid	PDMS-coated glass microchannel	ref 447	ref 447	
PDMS-coated glass microchannel	PDMS-coated glass microchannel	ref 448	ref 448	

Table 3. continued

ref	APTES-based enzyme immobilization strategy employed	biochip substrate	application
PDMS-coated glass microchannel – APTES – GLD – SWCNTs-DNA + β -galactosidase ceramic membrane surface – APTES – surface corona discharge induced plasma chemical process – CVD – glucamylase	TiO ₂ NPs – APTES – Au NPs – ferrocene-labeled secondary Ab – GOx	TiO ₂ ceramic membrane surface	development of glucoamylase-bound ceramic membrane surfaces
palygorskite (also called attapulgite) – APTES – GLD – linoleic acid isomerase TiO ₂ nanofiber membrane – APTES – GLD – ProteX 6L (an alkaline protease)	TiO ₂ nanofiber membrane	TiO ₂ development of GL-bound electropun TiO ₂ nanofiber for the synthesis of sucrose monolaurate	
SiO ₂ deposited Au electrodes – APTES – GLD – GOx silicon capillary – APTES – GLD – GOx	SiO ₂ deposited Au silicon capillary	development of amperometric glucose sensor	
microporous silica support – APTES – GLD – GOx Fe ₃ O ₄ /SiO ₂ NPs – APTES – GLD – GOx Pt disk electrode – chitosan/silica sol–gel hybrid membranes (prepared by mixing chitosan with APTES) + Au NPs + K ₃ Fe(CN) ₆ + HRP	microporous silica support Fe ₃ O ₄ /Si NPs Pt	development of a micromachined enzyme reactor for a flow injection analysis system for glucose detection	
glass microbeads – APTES – GLD – GOx	glass microbeads	development of GOx bound microporous silica support	
porous Celite beads – APTES – GLD – HRP	porous Celite beads	preparation of GOx bound Fe ₃ O ₄ /Si NPs	
diatomaceous earth support Celite R-633 – APTES – GLD or glyoxal–laccase silica-gel carrier – APTES – laccase	diatomaceous earth support Celite R-633	development of H ₂ O ₂ biosensor by entrapping HRP in membranes doped with K ₃ Fe(CN) ₆ and Au NPs	
dendritic composite magnetic particles (Fe ₃ O ₄ + APTES + TEOS) – GLD – porcine pancreatic lipase (PPL) modified palygorskite supports – APTES – lipase mesoporous silica SBA-15 – APTES – lipase	dendritic composite magnetic particles modified palygorskite supports SBA-15	development of microfluidic device involving heterogeneous microbeads and microarray-based detection	
palygorskite support – APTES – GLD – lipase magnetic sol–gel composite supports – APTES + TEOS – GLD – lipase Fe ₃ O ₄ NPs – APTES – GLD – lipase	palygorskite support magnetic sol–gel composite supports Fe ₃ O ₄ NPs	investigation of enzyme-catalyzed conversion of phenol in a HRP-bound membraneless electrochemical reactor	
mesoporous ZSM-5 zeolites silica-coated Fe ₃ O ₄ NPs	mesoporous ZSM-5 zeolites silica-coated Fe ₃ O ₄ NPs	covalent immobilization of laccase on Celite R-633 and its use to eliminate nonylphenol, BPA, and triclosan	
AlGaN/GaN solution gate FETs – APTES – laccase tetramethoxysilane + APTES + pepsin	silicone elastomer AlGaN/GaN solution gate FETs	development of highly stable silicagel bound laccase for continuous analysis	
Fe ₃ O ₄ NPs – APTES – GLD – peroxidase – entrapment in PEG hydrogel microparticles by photopatterning	sol–gel Fe ₃ O ₄ NPs	preparation of PPL-bound dendritic composite magnetic particles	
3-D poly(ethylene- <i>alt</i> -maleic anhydride) copolymer film – APTES – α -amylase Poly(octadecene- <i>alt</i> -maleic anhydride) copolymer film – APTES – α -amylase silica capillary – APTES + methyltriethoxysilane – 1 M DMF solution of succinic anhydride – EDC/ NHS – cucumicin	maleic anhydride copolymers	development of sol–gel immobilized pepsin-based strategy for the assay development strategy based on the entrapment of enzyme-linked Fe ₃ O ₄ NPs within PEG hydrogel microparticles prepared by photopatterning	
Co–Cr–Mo surface – APTES – GLD – trypsin	silica capillary	development of an immobilization strategy for binding α -amylase onto reactive copolymer films	
		immobilization of cucumicin in nanostructured silica capillary	
		immobilization of trypsin to silanized Co–Cr–Mo surface	

Table 3. continued

	APTES-based enzyme immobilization strategy employed	biochip substrate	application	ref
magnetic silica microspheres – TEOS + APTES – GLD – trypsin		magnetic silica microspheres	preparation of magnetic silica microspheres and their use for on-chip proteolysis systems	472
BDD thin film substrate – ZnO nanorod microarray – APTES + TEOS – GLD – tyrosinase		BDD thin film substrate	development of tyrosinase-bound ZnO nanorod microarrays on boron-doped nanocrystalline diamond to detect phenolic compounds	473
silica-coated fiberglass core in microchip – APTES + TEOS – GLD – trypsin		silica-coated fiberglass core in microchip	preparation of trypsin-bound silica-coated microchip for effective proteolysis	474
GCE – APTES – EDC-activated GOx		GCE	development of mediatorless electrochemical glucose sensing procedures based on the leach-proof covalent binding of GOx to GCE	475
GCE – graphene/poly-L-lysine (in APTES) – EDC-activated GOx				
GCE – (GOx + HRP) GLD-cross-linked – APTES				
GCE – (GOx + HRP) GLD-cross-linked-graphene/MWCNTs/chitosan (in APTES)				
nano porous alumina membranes – APTES + triethylamine – N,N'-carbonyldiimidazole + triethylamine – glutathione transferase		nano porous alumina membranes	characterization of glutathione transferase immobilized on nanoporous alumina membrane	476
Fe ₃ O ₄ /Si NPs – APTES – GMA – phospholipase A ₁		Fe ₃ O ₄ /Si NPs	development of phospholipase A ₁ on Fe ₃ O ₄ /SiO _x -g-P(GMA) NPs	477
superparamagnetic Fe ₃ O ₄ NPs – APTES – penicillin G acylase + GLD		superparamagnetic Fe ₃ O ₄ NPs	development of penicillin G acylase magnetic cross-linked enzyme aggregates	478
Si (GLD/terephthalaldehyde/1,4-phenylene diisothiocyanate/1,3-phenylene diisothiocyanate) – glucose-6-phosphate DHD		Si	determining the effect of cross-linking agent on the activity and thermostability of glucose-6-phosphate DHD	479
silica monolith capillary – prepolymer sol-gel (polyethylene glycol + TEOS + acetic acid) – APTES – GLD – lipase		silica monolith	preparation of lipase-bound silica monolith in a fused silica capillary to develop a microreactor for performing lipid transformations	480
diatom-biosilica particles – plasma – APTES – GLD – tyrosinase		diatom-biosilica particles	development of tyrosinase-bound diatom biosilica for the biodegradation of phenolic compounds	481
Au electrode – electrodeposition of Au NPs-Pt NPs – APTES – GLD – lysine oxidase		Au	detection of lysine using lysine oxidase-bound Au NPs-Pt NPs modified Au electrode	482
Fe ₃ O ₄ NPs – APTES – GLD – amyloglucosidase		Fe ₃ O ₄ NPs	preparation of amyloglucosidase-bound Fe ₃ O ₄ NPs	483
Fe ₃ O ₄ NPs – APTES – GLD – serratiopeptidase		Fe ₃ O ₄ NPs	preparation and characterization of serratiopeptidase-bound Fe ₃ O ₄ NPs	265
Fe ₃ O ₄ NPs – APTES – GLD – lipase		Fe ₃ O ₄ NPs	preparation of lipase-bound Fe ₃ O ₄ NPs and their use for the enrichment of polyunsaturated fatty acids	484
capillary – APTES – GLD – trypsin		capillary	screening of trypsin inhibitors by capillary electrophoresis using a trypsin-bound microreactor	485
MWCNTs-conc H ₂ SO ₄ + HNO ₃ (3:1 v/v) – APTES – succinic acid anhydride – lipase B		MWCNTs	development of MWCNTs-lipase B nanoconjugates for multiple usages in nonaqueous biocatalysis	486
mesoporous SBA-15 – APTES – GLD – hydrolase		SBA-15	development of hydrolase-bound mesoporous SBA-15 for coprecipitation of cholesterol	487
TiO ₂ NPs/TiO ₂ -functionalized membranes – APTES – GLD – laccase		TiO ₂ NPs and TiO ₂ -functionalized membranes	immobilization of laccase on TiO ₂ NPs and TiO ₂ -functionalized membranes	488
TiO ₂ NPs/TiO ₂ -functionalized membranes – APTES – laccase				
BDD electrode – KOH – APTES – GLD – GOx			demonstration of direct electron transfer between GOx and BDD, and detection of glucose	246

recommend the use of EDC-SNHS/EDC-NHS in their immobilization protocols; however, EDC alone still yields positive results.¹⁰⁵ Notice also that the NHS ester readily reacts with the amine group of lysine to form stable amide bonds, NHS ester is unstable in aqueous conditions, and ester hydrolysis competes with biomolecule attachments. NHS derivatives in solution at pH 8.0 have a half-life of only 1 h.¹⁰⁶ Nevertheless, heterobifunctional cross-linking is applicable for a variety of IAs, using ELISA, SPR, microarrays, advanced optical platforms, microfluidics, micro-, and nanomaterials.

The covalent binding of Abs on APTES-functionalized platforms has also been performed using 1,4-phenylene diisothiocyanate (PDITC).⁵¹ This homobifunctional cross-linker has on its on a phenyl ring two isothiocyanate groups that can bind to amines. The former reacts with the free amine groups on the APTES-functionalized platform to form a thiourea linkage, while the other binds to the Ab amine groups. The hydrazone bond has also been used for covalent binding of Abs.¹⁰⁷ The Abs are bound to succinimidyl 4-formylbenzoate (S-4FB) via the aldehyde moiety of S-4FB. Thereafter, S-4FB-bound Abs are covalently attached to APTES-functionalized surfaces via a hydrazone bond by the activation of succinimidyl 6-hydrazinonicotinamide acetone hydrazine (S-HyNic).

The covalent attachment of Abs is widely performed on surfaces rich in silicon, for example, silicates. The Abs covalently bound on monocrystalline silicon are highly stable and retain functional activity for over 2 months.¹⁰⁸ Similarly, highly uniform Ab immobilization has been achieved on APTES-functionalized glass.¹⁰⁹ This procedure involves the reduction of an imine bond formed between aldehyde and amine at reaction sites to aziridine, which stabilizes the complex and prevents protein leaching.

The leach-proof covalent binding of enzyme to electrodes with a prolonged shelf life is highly critical for the development of commercially viable POC glucose biosensors. The aldehyde groups of biomolecules bind covalently with the amine groups of APTES on the substrate via the formation of Schiff base.¹¹⁰ The GLD coupling procedure can be performed under ambient conditions, which are ideal for developing biosensors with high activity and stability. The water-soluble EDC-mediated reactions convert the carboxyl group into unstable O-acylisourea, which forms an amide bond with the amine group of APTES. As a few examples, the preparation of a glucose oxidase (GOx)-bound GCE involves the drop-casting of 10 mg mL⁻¹ GOx cross-linked via GLD on 1% (w/v) KOH-pretreated GCE, followed by the immediate drop-casting of 4% APTES to form a highly stable GOx-bound GCE.¹¹¹ This strategy is also applicable for covalent immobilization of GOx on a graphene-functionalized GCE.¹¹² The GCE pretreated with 1% KOH is allowed to react with graphene (1 mg mL⁻¹ dispersed in 0.125% APTES). APTES plays a dual role in this procedure, acting as a surface modification agent that introduces amino groups on the GCE and graphene, besides its role as a dispersion agent. Thereafter, EDC-activated GOx is bound covalently to the graphene-modified GCE by heterobifunctional cross-linking. The incorporation of graphene on GCE significantly increases the active surface area for enzyme immobilization, resulting in enhanced response signal. Similarly, the same GOx immobilization strategy can be extended to the MWCNT-functionalized GCE.

3.2. Oriented

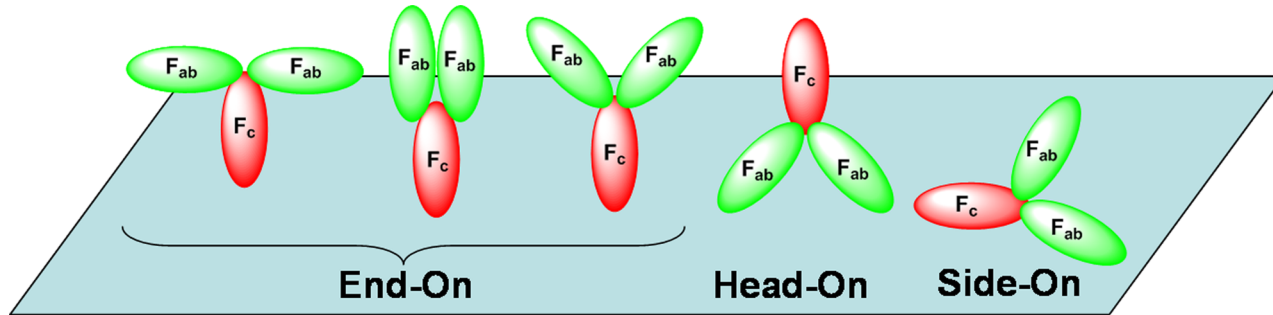
Most of the oriented Ab immobilization strategies employ FBP, such as Protein A,^{113,114} Protein G,^{115,116} and Protein A/G¹¹⁷ that bind Abs through the F_c region, leaving the antigen-binding

sites at the fragment antigen-binding (F_{ab}) region free for antigen binding. The native Protein A is a cell wall component produced by several strains of *Streptococcus aureus*, but the recombinant Protein A is produced in *E. coli*. With a MW of ~46 kDa and isoelectric point (pI) of 5.16, it contains five high affinity ($K_a = 10^8$ mol⁻¹) binding sites, which are capable of binding to the F_c region of immunoglobulin G (IgG) from several species such as rabbit and human. A Protein A molecule can bind to a maximum of two Abs due to spatial constraints.¹¹⁸ However, Protein A and IgG binding is not equivalent for all species and even for the subclasses of a particular IgG. As an example, Protein A covalently bound on a silanized Au-coated SPR chip by EDC-SNHS can be useful for the oriented immobilization of antihuman fetuin A (anti-HFA) Ab.⁶³ This orientation strategy results in a superior analytical performance as compared to covalent, noncovalent, Protein A noncovalently bound, and commercial CMS (carboxymethyl dextran) SPR chip-based Ab immobilization strategies. Although these intermediate proteins have been widely used for direct binding assays, such as those based on SPR, microcantilevers, and quartz crystal microbalance (QCM), they are not widely employed for sandwich IAs. This could be rationalized that the secondary Abs can bind to the vacant binding sites on these intermediate proteins, which leads to a higher background signal and nonspecific binding. The blocking of these vacant sites further adds to the assay cost. To date, the oriented immobilization strategies are not widely used for enzyme immobilization in biosensor construction.

Similarly, Protein G is another FBP, which is a bacterial cell wall protein from group G *Streptococci*. The native Protein G has two IgG binding domains apart from sites for albumin and cell surface binding, but these nonspecific binding sites have been eliminated from recombinant Protein G (MW = ~22 kDa and pI = 4.5) produced commercially from *E. coli*. Protein G has higher affinity than Protein A for most mammalian IgGs, but it does not show any binding to human IgM, IgA, and IgD. Despite having tremendous similarity in the tertiary structures, Protein A and G have different amino acid compositions. The optimal binding of Protein A and G occurs at pH of 8.2 and 5, respectively, but is still sufficient at pH 7.0–7.6. Because of the inherent differences in the binding properties of these FBPs, assessment of their binding to specific capture Abs is a prerequisite for a particular bioanalytical application. Indeed, this problem has been solved by the production of Protein A/G, which results from the gene fusion of the F_c-binding domains of Protein A and G. It binds to all human IgG subclasses with the exception of IgA, IgE, IgM, and to a lesser extent IgD. Besides its stronger affinity, the binding is less pH-dependent with optimum Ab binding at pH 5–8. Apart from the FBPs, Protein L (MW = ~36 kDa and pI = 4.5) isolated from *Peptostreptococcus magnus* has been employed as an intermediate protein.^{119,120} Protein L binds to the kappa light chains of a wider range of IgG classes and subclasses without interfering with the antigen-binding sites of the Ab. Furthermore, it binds to the F_{ab} fragments and single chain variable fragments.

3.3. Site-Specific

The ability to introduce desired amino acids and functional groups at a specific position in Abs and their derivatives enables the development of site-specific immobilization strategies.^{121,122} It involves the insertion or chemical binding of an amino acid, an oligopeptide, or an affinity tag at the specific site of an Ab or its derivatives that binds to the complementary affinity molecule immobilized on a matrix surface. Commercially available tags include polyhistidine,¹²³ avidin–biotin,¹²⁴ and FLAG

Scheme 4. Different Possible Orientations of IgG on a Substrate

tags.^{125–127} Free amino acids containing the sulfhydryl group (such as cysteine) can also be used for Ab immobilization on Au surfaces via self-assembly.^{128,129} The incorporation of cysteine on the Ab fragment apart from the antigen recognition site enables the use of sulfhydryl linkers that leads to more efficient solid-phase immobilization.^{130,131} The cysteine tag also broadens the choice of solid supports as Abs can be immobilized on various substrates including cyanogen bromide (CNBr)-activated surfaces.¹³² It provides the robustness to the tagged Ab required for leach-proof immobilization.¹³³ The tagging-based strategies are highly efficient. However, tagging of Abs adversely affects their functional activity due to the conformational change, thereby resulting in reduced binding efficiency.¹³⁴

3.4. PNA and DNA-Directed

Complementary PNAs are chemically synthesized single-stranded nucleic acids that feature an amino acid derivative of alkylamide instead of the normal phosphodiester backbone.^{135,136} PNAs can form nonionic and achiral PNA–PNA, PNA–RNA, and PNA–DNA constructs that are resistant to enzymatic hydrolysis and temperature, attractive properties that may allow for the use of PNA in immobilization strategies. PNA-conjugated Ab has been immobilized on surfaces grafted with the antisense oligonucleotide or PNA by hybridization.^{137,138} The ability to control surface-Ab distance through PNA monomers provides strong site specificity and orientation for Ab capturing.^{139–141} Hybridized oligonucleotide tags are also attractive as they can be separated from their complementary strands by changing the pH or divalent ion strength.¹⁴²

3.5. Noncovalent Attachment

Protein/enzyme molecules can be attached to different interfaces with various mechanisms and forces acting between protein and surface, including hydrophobic, electrostatic, and van der Waals forces.^{143–145} Generally proteins tend to adhere onto hydrophobic surfaces due to the release of water dipoles from the hydrophobic surface to the bulk solution during protein adsorption. In addition, the protein concentration plays an important role in the steady-state adsorption of proteins only on hydrophilic surfaces,¹⁴⁶ not hydrophobic ones.¹⁴⁷ Proteins can undergo conformational changes and unfold due to different forces acting during the adsorption process, affecting their biological activity. “Hard” proteins (lysozyme, β -lactoglobulin, α -chymotrypsin, etc.) upon adsorption retain their dissolved state without spreading. In contrast, “soft” proteins (bovine serum albumin (BSA), IgG, fibrinogen, or α -lactoglobulin) can spread on the surface upon adsorption. “Soft” proteins tend to adsorb onto various surfaces as compared to “hard” proteins that adsorb onto hydrophilic surfaces only when there is electrostatic attraction between protein molecules and the surface.¹⁴⁸ Surface

roughness also affects adsorption and the morphology of adsorbed protein. For example, larger amounts are adsorbed to the hydrophobic surfaces as compared to the hydrophilic ones. Only on smooth hydrophilic or hydrophobic surfaces does collagen form elongated assemblages with small or high surface features, respectively.¹⁴⁹ Random orientation is often encountered with protein adsorption; that is, there are a few different possible orientations of IgG on the surface (Scheme 4).

Amine groups on APTES-functionalized surfaces with positive charge at neutral pH can interact with negatively charged enzymes via electrostatic interaction. This is the simplest approach to immobilize enzymes onto solid surfaces for applications that require no directional orientation of the immobile biomolecules. The mechanisms involved in adsorption include ion exchange, ion pairing, hydrophobic bonding, and polarization of π -electrons. As an example, the negatively charged DNA backbone binds strongly to the positively charged APTES-coated mica.¹⁵⁰ Resulting structures are stable enough for AFM imaging in air or buffer. Of notice is an important medical application using amine-terminated silicon surfaces, that is, hydrogen-terminated silicon surface, as an immobilization carrier for bone morphogenetic protein 2 (BMP2).¹⁵¹ However, immobilized enzymes can be often desorbed by simple change of pH or ionic strength.

Hydrophobic interaction is simple and useful for the binding of lipophilic biomolecules, for example, membrane-bound dehydrogenase enzymes. The main driving force for adsorption can be attributed to the hydrophobic interaction between such lipophilic membrane-bound enzymes and the alkane moiety of silanes.¹⁵² This is a fast, direct, and simple procedure for lipophilic biomolecules; however, denaturation of adsorbed biomolecules with random orientation is often encountered.

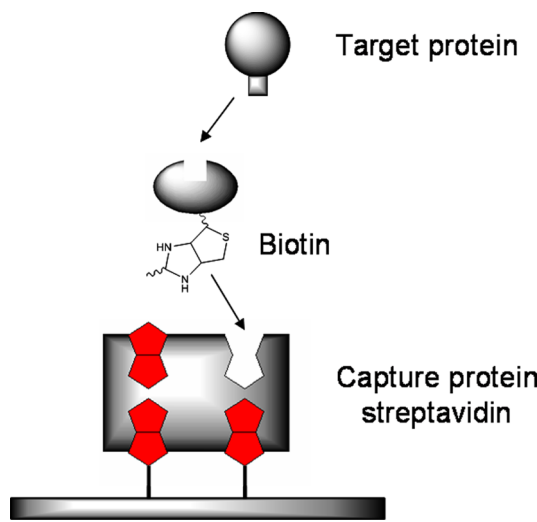
Protein surface density is higher for adsorbed proteins than for covalently bound ones. Considering IgG molecule (156 kDa) with nominal dimensions of $14.5 \times 8.5 \times 4$ nm, the area covered by singular IgG molecule with side-on orientation is minimal and about 2.6 mg m^{-2} .¹⁵³ With adsorption on the GOPS and APTES modified surface, respectively, the protein surface density is 1.55 ± 0.05 to $2.00 \pm 0.04 \text{ mg m}^{-2}$ as compared to 0.20 ± 0.02 to $0.55 \pm 0.05 \text{ mg m}^{-2}$ for covalently bound ones.¹⁵⁴ The protein structure is unaffected by the duration of incubation of the silanized substrate with the IgG solution.

3.6. Affinity

The specific molecular interaction between the avidin and biotin pair ($K_d \sim 10^{-15} \text{ M}$) is a well-known phenomenon and has been extensively advocated for biomolecule immobilization as the cubic shape avidin possesses four biotin binding sites. Conceptually, avidin is covalently attached to APTES-surfaces by either GLD-mediated or EDC-mediated reactions as previously

described. Avidin then acts as a biocompatible linker between APTES-surfaces and biotinylated biomolecules. Although avidin/streptavidin is randomly attached to the APTES-modified surface, the interaction between biotinylated biomolecules and avidin/streptavidin is more specific to effect oriented immobilization of the target biomolecule as shown in Scheme 5. Vice

Scheme 5. Immobilization of a Protein by Affinity through a Streptavidin/Biotin Interaction



versa, the APTES-functionalized surface can be biotinylated and binds to avidin. Several biotinylated biomolecules are commercially available, and various protocols have been established for biotinylation of biomolecules.^{155–160} Biotin is a small compound (244.3 Da); therefore, biotinylation does not affect biomolecule

conformation and biological activity. This procedure is more popular for the immobilization of Abs as compared to enzymes. Besides avidin–biotin, recombinant proteins can be selectively attached to an artificial polypeptide scaffold system via heterodimeric association of a separate leucine zipper pair consisting of 43 amino acids with an affinity constant of 10^{-15} M.¹⁶¹

The capture ligand approach involving the use of protein trans-splicing mechanism deserves a brief comment here because this approach can offer some potential in biomolecule immobilization. Intein fragments exhibits protein splicing activity, and the intein self-processing domain can split into two fragments: the former is incorporated to the target biomolecule, whereas the latter is attached to the APTES-modified surface. The process is lengthy (16 h), which is similar to other intein-mediated approaches.¹⁶² Nevertheless, this approach has been employed for the immobilization of proteins onto cysteine-functionalized substrates.^{163,164} The main drawback of this procedure is the requirement of a relatively high proteins concentration (100 mM) to effect direct ligation to cysteine-modified biosensor surfaces.

The hexahistidine tag is most commonly used in high throughput protein purification^{165,166} as well as for the immobilization of histidine-tagged proteins on electrode surfaces.^{167–169} However, specificity and stability of this tag are lower as compared to other affinity methods, and the preparation involves many reagents and steps.¹⁷⁰ Recently, Sanz et al.¹⁷¹ described an elegant immobilization procedure for proteins tagged to the affinity polypeptide C-LytA, a choline-binding protein (CBP) of the pneumococcal cell wall,¹⁷² on functionalized graphite electrodes. In brief, a SAM of choline-functionalized thiol chains is synthesized over thiocarboxylic acid-treated Au, which displays selective affinity for β -galactosidase tagged to

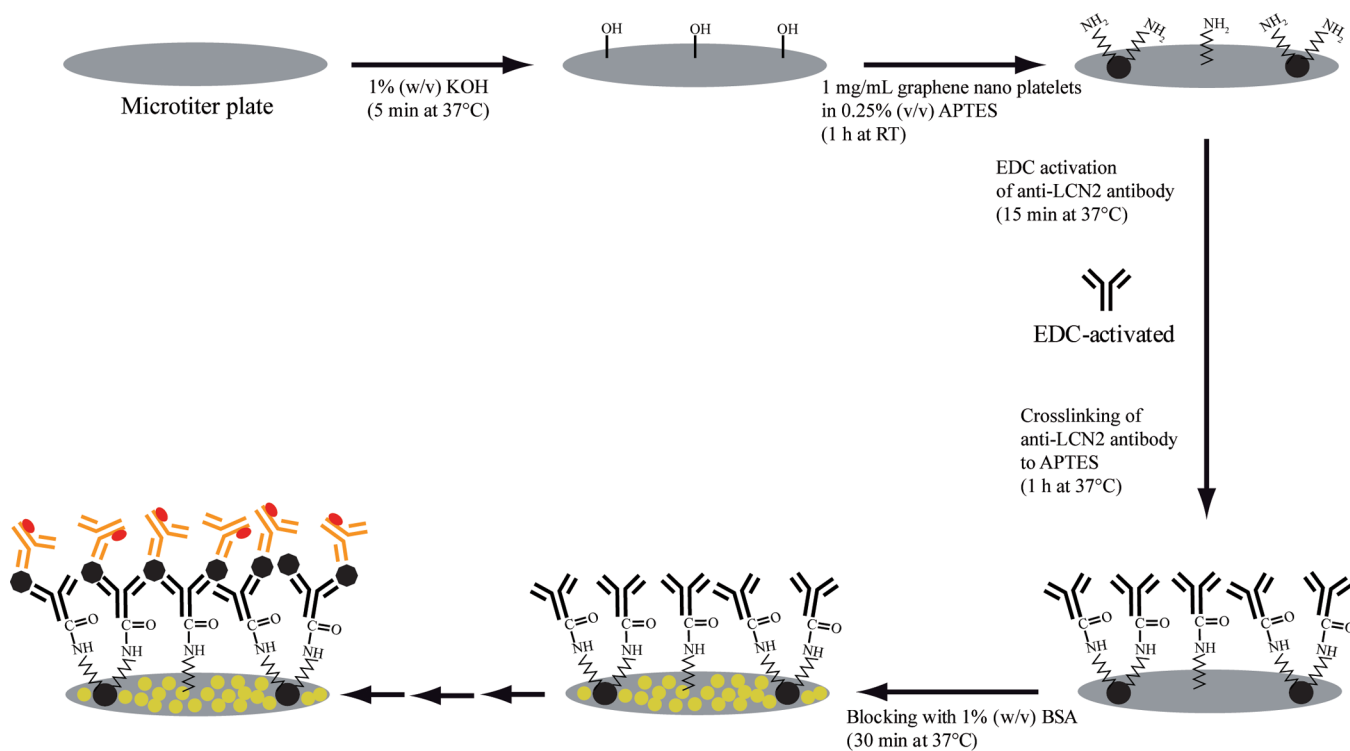


Figure 2. APTES-based sandwich ELISA procedures using graphene nano platelets-based Ab immobilization for the detection of human lipocalin-2 (LCN2). Reproduced with permission from ref 176. Copyright 2014 Elsevier B.V.

C-LytA (CLyt-bGal protein). The C-LytA system exhibits higher buffer compatibility and is not subject to interference with other metalloproteins. The binding is also completely reversible, which enables the reuse of the electrode and opens the possibility of developing other tailor-made supports.

3.7. Entrapment

Silica sol–gel films have been used to encapsulate enzyme and redox mediators. A porous, silane surface using APTES, GOx, and [2-(3,4-epoxycyclohexyl)ethyl]trimethoxysilane was deposited on Pt for glucose detection.¹⁷³ The thick sol–gel film adversely affected detection time. The Pt electrode required high detection potentials (+0.7 V vs Ag/AgCl), which compromises detection linearity at higher glucose concentrations. Methyl-trimethoxysilane (MTMOS), tetraethoxysilane (TEOS), APTES, and GOPS can be assembled onto highly oriented pyrolytic graphite (HOPG) for glucose detection.¹⁷⁴ The best matrix for GOx immobilization is GOPS, followed by APTES, MTMOS, and TEOS. The chemical structure and composition of the sol–gel mixture changes the roughness, size, and distribution of pores in the film, which affect the response time, sensitivity, and detection limit of glucose.

A sol–gel approach has been attempted for making permselective organic–inorganic hybrid films consisting of three organosilanes (APTES, TEOS, triethoxy-1H,1H,2H,2H-tridecafluoro-*n*-octylsilane) and two biomacromolecules, BSA and chitosan, deposited on Pt.¹⁷⁵ 3D sol–gel Si–OH condensation networks cross-linked by APTES and coupled with molecular interactions between different components of the films are a suitable environment for H₂O₂ permeation. This biosensing scheme offers a detection limit of 32 μM and a response time of only 3 s. However, the long-term stability of the biosensor is questionable as the glucose signal decreases to 76%, while the ascorbic acid interference signal increases to 126% of initial responses after only 5 days of storage.

4. APPLICATIONS IN BIOSENSORS AND DIAGNOSTICS

4.1. Microtiter Plate Formats

The immobilization of biomolecules on MTPs is generally achieved by silanization on pretreated plates with available surface hydroxyl groups. Highly sensitive and rapid sandwich ELISA procedures have been developed for the detection of disease biomarkers, such as HFA, human albumin (HA), and human lipocalin-2 (LCN2). The resulting microtiter plate format is capable of detecting HFA with linearity of 9 pg mL⁻¹ to 20 ng mL⁻¹ and sensitivity of 39 pg mL⁻¹, that is, ~16-fold more sensitive and 3-fold faster than the established commercial ELISA (Figure 2).¹⁷⁶ HFA is a specific biomarker for hepatocellular carcinoma and atherosclerosis. Doubtlessly, this generic Ab immobilization procedure can be extended to other commercially available substrates such as polystyrene, poly(methyl methacrylate), cellulose acetate, polycarbonate, and cyclic olefin polymers (Zeonex). Adapting the same silanization protocol, improvements in other IA formats for chemiluminescent enzyme IA and SPR IA could also be anticipated.

Further improvement and simplification of this immobilization procedure is feasible by using only EDC as the heterobifunctional cross-linker for HFA, HA, and LCN2.¹⁰⁵ The analytical sensitivity of the IA increases by 80-fold with the addition of graphene nanoplatelets (GNPs) by virtue of higher Ab immobilization density associated with the increased surface area. The use of GNPs does not lead to any additional processing steps or increase in IA time or complexity. The assay can detect

LCN2 in plasma, serum, and whole blood without any interference from endogenous physiological substances. Argon plasma is an alternative for generating reactive hydroxyl moieties on the MTPs for APTES-functionalization and subsequent binding of rabbit IgG via cross-linkers.¹⁷⁷ After immobilization, about 95% of covalently bound IgGs are retained after extensive washing on the plasma-treated polystyrene MTP in comparison to an untreated MTP. The resulting plasma-treated MTPs exhibit similar or even better analytical performance as compared to commercially available preactivated MTPs.

Recently, a simple immobilization procedure involving the dilution of a capture Ab in the ratio of 1:1 (v/v) in 1% (v/v) APTES to form a stable complex via ionic and hydrophobic interactions was demonstrated.¹⁷⁸ The complex is covalently bonded to a polystyrene-based MTP, pretreated with KOH. This IA platform shows 51-fold increased sensitivity than the commercial IVD kits for HFA, C-reactive protein (CRP), HA, and LCN2. Moreover, the Ab-bound MTPs, stored at 4 °C in 0.1 M PBS, are stable for 2 months, attesting the leach-proof and functionally stable binding of capture Abs.

The Ab can also be preactivated with EDC and admixed with 1% (v/v) APTES in the ratio of 1:1 (v/v) to form a stable complex. Similarly, the complex is covalently bonded to a polystyrene-based MTP, pretreated with KOH toward the development of a prospective rapid IVD procedure for detecting HFA in just 30 min.¹⁷⁹ Both of the aforementioned procedures exhibit high precision equivalent to that of the commercial sandwich ELISA in the real sample matrices.

Sensitive detection of carcinoembryonic antigen (CEA) is feasible using horse radish peroxidase (HRP)-functionalized mesoporous silica NPs (MSN) as labels.¹⁸⁰ The HRP-functionalized MSN is prepared by simultaneous coimmobilization of HRP and anti-CEA Ab onto the APTES/GLD-functionalized MSN. The maximum chemiluminescent intensity is obtained at the HRP–CEA mass ratio of 10:1. The use of HRP-functionalized MSN enhances chemiluminescent signal and sensitivity, 10-fold higher than the conventional IA with the anti-CEA monoclonal Ab simply bound to the 96-well MTP by passive adsorption.

The highly sensitive detection of bisphenol A (BPA) was demonstrated using direct hapten-coated polystyrene MTP-based competitive indirect ELISA (ciELISA).¹⁸¹ The H₂SO₄/HNO₃ pretreated polystyrene MTP is functionalized with APTES and subsequently bound to the carboxyl group of 4,4-bis(4-hydroxyphenyl) valeric acid (BVA), an analogue of BPA, by the *N,N'*-dicyclohexylcarbodiimide (DCC) method. This is followed by the addition of BPA, anti-BPA Ab, and goat antimouse IgG-HRP conjugate, and the 3,3',5,5'-tetramethylbenzidine (TMB) reaction substrate for HRP. The direct hapten-coated ciELISA detects BPA with a limit of detection of 0.27 ng mL⁻¹ as compared to 15.90 ng mL⁻¹ for the hapten-protein coated format. The assay is capable of detecting BPA in tap water and seawater samples with recoveries between 70% and 142%.

4.2. Optical Biosensors

Optical-based biosensors have been designed for the monitoring of biomolecular interactions in real-time because they are usually label-free (not requiring enzymes or fluorescent dyes), easy to fabricate, and easily multiplexed to enable an array-based format for high throughput efficiency. SPR, FTIR, and refractive index (RI) are the most common techniques used in conjunction with optical biosensors. However, immobilization of the biomolecules to obtain biosensors with high sensitivity remains problematic.

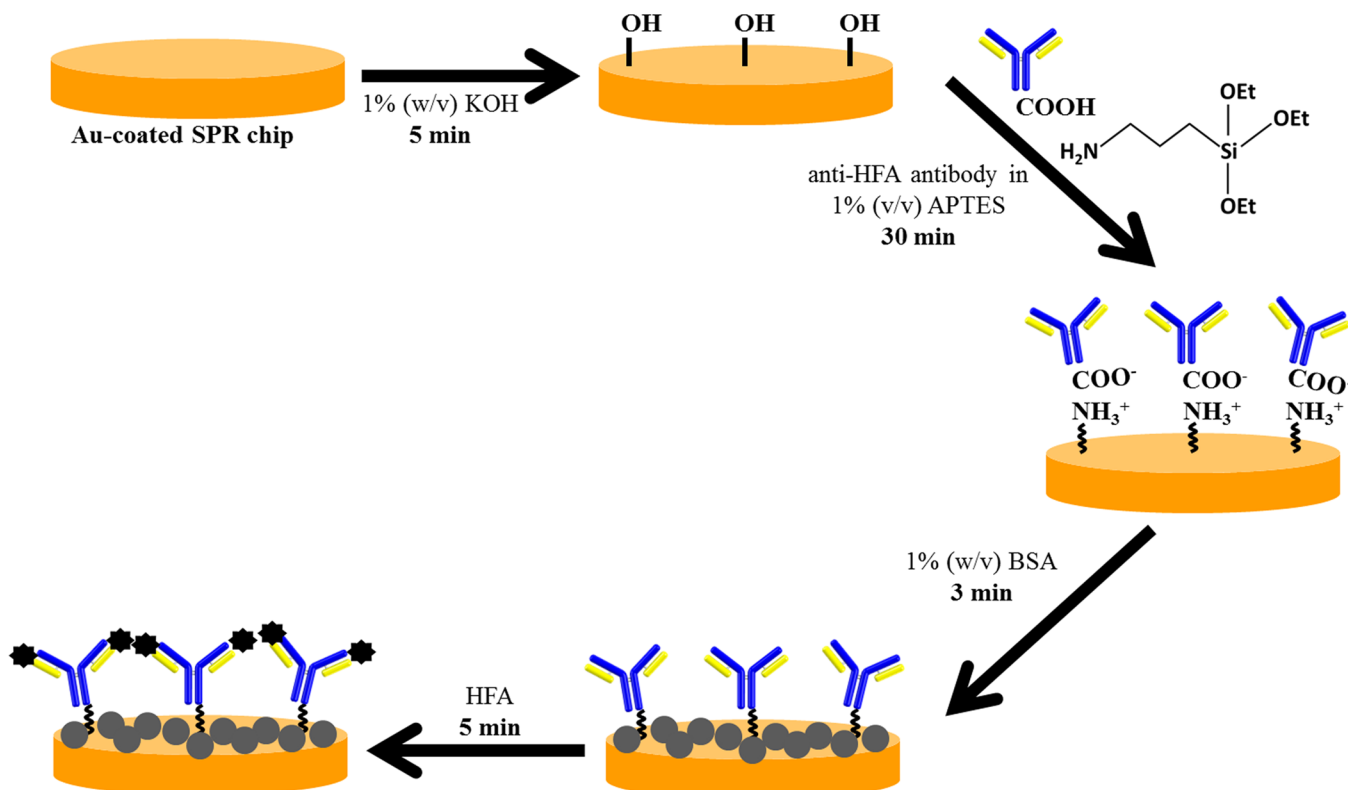


Figure 3. Schematic of the developed SPR-based IA procedure for human fetuin A (HFA). Reproduced with permission from ref 187. Copyright 2014 Royal Society of Chemistry.

These problems have been addressed in many examples by the use of APTES to minimize the sensor preparation time, reagents, and required steps.

In SPR, p-polarized laser light reflects at the interface of an optically dense and less dense medium to generate an evanescent field at a specific angle, which is apparent by collective motions of conducting electrons (plasmons) in a thin metal layer (30 nm). Au films are commonly used due to their lower dielectric constant, biocompatibility, and inertness. Again, SAM has been shown to be immensely useful for this sensor type.¹⁸² The SPR Au chip can be cleaned with piranha treatment for a few minutes, which oxidizes the Au surface, as shown by the contact angle of about 9.3°. The further washing of chips with deionized water leads to the adsorption of water molecules and generates the desired hydroxyl groups,^{183,184} as apparent from an increase in contact angle to 28–32°. After silanization, the contact angle of water for the SAM of APTES on Au surface is $59 \pm 1^\circ$.¹⁸⁵

Conventional SPR biosensors are difficult to realize in a large-scale array format because they operate in total internal reflection mode. However, localized SPR (LSPR) using surface modified silica NPs on an Au layer can overcome some of these issues as it operates using the transmission mode. An optical sensor was developed for the detection of fibrinogen in the range of 10 ng mL⁻¹ to 10 μg mL⁻¹. In this configuration, APTES modified silica NPs are attached through EDC to form a dense monolayer (100 nm) on an Au-coated glass substrate.¹⁸⁶ The silica NP layer is then capped with another layer of Au before the attachment of Protein A through EDC and NHS. Antifibrinogen Ab is then attached to the Protein A to detect fibrinogen. The Ab–antigen interaction is monitored by following the absorbance increase at 550 nm after 30 min (BSA as a control shows no absorption increase).

Recently, an SPR-based IA biosensor was designed for the detection of HFA using a simplified Ab immobilization procedure.¹⁸⁷ In this system, the anti-HFA capture Ab is simply added to 1% APTES and deposited for 30 min on a KOH-treated Au-coated SPR chip (Figure 3). The Ab bound chip is first blocked with BSA before interacting with HFA for 5 min. The IA detects HFA in the range of 0.3–20 ng mL⁻¹, and the chip could be regenerated with glycine-HCl for at least 35 repeated HFA analyses, indicating the leach-proof capture Ab binding to the chip. The detection of HFA spiked into real sample matrixes with this system compares well with commercial HFA sandwich ELISA. The chips are very stable after 2 months of storage without biological activity loss. Considering the simplicity and rapidity of this procedure, the chip can be easily prepared 30 min before the intended use.

A cost-effective, label-free, and simple optical immunosensing system is desired for the measurement of surface enhanced light scattering (SELS) signals of solid supports, by simultaneous scanning the excitation and the emission of the response signal.¹⁸⁸ The goat antihuman IgG, goat antirabbit IgG, and rabbit antihuman IgG, respectively, are bound to the APTES-GLD functionalized glass slides, which detect human IgG, rabbit IgG, and human IgG in the linear ranges of 0.1–100 μg mL⁻¹ (limit of detection (LOD) 10 ng mL⁻¹), 0.1–100 μg mL⁻¹ (LOD 50 ng mL⁻¹), and 0.1–10 μg mL⁻¹ (LOD 10 ng mL⁻¹), respectively. The Ab-bound sensor is highly specific and not subject to any interference from other proteins. It can be effectively regenerated for repeated use by treatment with carbamide solution.

Of notice is the use of a silicon-on-insulator (SOI) optical biosensor based on a microring resonator (cavity radius of 5 μm) for specific protein binding detection. This format exhibits

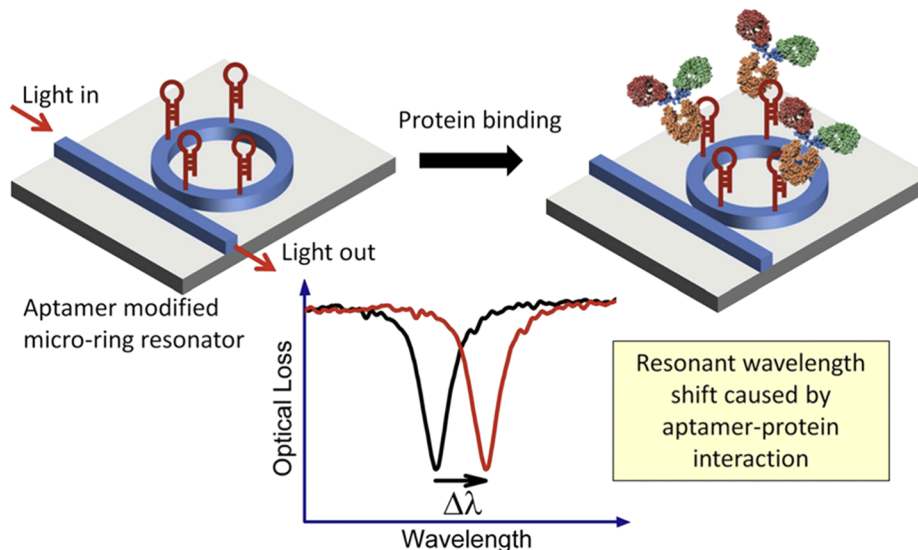


Figure 4. Schematic of an aptamer modified microring resonator and the resultant resonant shift caused by an aptamer–protein interaction. Reproduced with permission from ref 190. Copyright 2013 Elsevier B.V.

advantages as compared to the system using traditional passive photonic components because its dimensions are reduced drastically. Silicon surfaces are silanized using 1% APTES followed by the coupling of biotin using EZ link-NHS-LC-biotin for the detection of avidin in the range of 50 ng mL^{-1} to $5 \mu\text{g mL}^{-1}$. The measurement is based on the shift in resonance wavelength (as low as 7.5 pm) due to changes in the dielectric surroundings of the cavity. This SOI format when coupled with complementary metal–oxide semiconductor fabrication offers the high throughput and resolution required for practical and routine applications.¹⁸⁹ This similar SOI format is extended to detect human IgE and human thrombin with a detection limit of 33 pM and 1.4 nM, respectively. The system consists of an array of three sensor microrings and one reference microring. The silicon microring (cavity radius of $5 \mu\text{m}$) device is treated with 2% APTES followed by GLD activation for immobilization of anti-IgE and antithrombin aptamers, respectively. This sensing approach is advantageous in the development of POC diagnostic devices due to its stability and specificity.

Resonant wavelength red-shifts (increase in the effective RI) are used to determine the IgE and thrombin concentrations after 30 min of binding (Figure 4). The detection of IgE is more sensitive than human thrombin due to the significantly higher affinity of binding between IgE and its aptamer. The system, when designed by using the two different aptamers attached to the individually addressable microrings, is very successful in terms of selectivity when challenged with a mixture of IgE and thrombin.¹⁹⁰ Another application of the SOI microring optical resonator arrays is the label-free detection of CEA in undiluted fetal bovine serum in less than 30 min.¹⁹¹ The anti-CEA Abs are bound to the substrate by hydrazone bond formation chemistry. It detects CEA in the range of 0 – 121 ng mL^{-1} with LODs of 2 and 25 ng mL^{-1} in buffer and serum, respectively. Therefore, it can monitor the entire clinically relevant range of 5 – 100 ng mL^{-1} . The anti-CEA Ab-bound surface is regenerated effectively with glycine for repeated use and provides high accuracy as verified by standard ELISA.

Ultrasensitive, label-free detection of human cardiac troponin-T (cTnT) is feasible by using complementary metal–oxide semiconductor-compatible silicon nanowire (SiNW) sensor

arrays.⁴⁶ The SiNW-sensor arrays are fabricated on an N-doped silicon-SOI substrate with a 145 nm buried oxide layer. The SiNW device has 36 clusters of five individually addressable nanowires each. The SiNW array chips functionalized with APTES-GLD and anti-cTnT Abs enable cTnT detection in assay buffer and undiluted human serum down to 1 and 30 fg mL^{-1} , respectively. This remarkable LOD is 3 orders of magnitude lower than the available ELISA-based assay formats.

Label-free biosensors containing APTES functionalized nanoporous (20 – 100 nm) polymeric gratings have also been designed to detect biomolecules. Application of gratings for biosensing has been hindered because the as-prepared polymers with optical properties encounter problems immobilizing biomolecules. Modifying the traditional holographic polymer-dispersed liquid crystal (H-PDLC) system by adding APTES directly to the photopolymer suspension enabled the gratings to capture biomolecules. The concentration of APTES chosen (10%) was critical in maintaining a high index modulation (0.07), which enhanced the signal-to-noise ratio. Changes in the RI before and after the additions of the target analytes resulted in the sensor's capability of detecting biomolecules such as biotin in the range of 0.05 – 0.5 mg mL^{-1} . The optical biosensor is also capable of detecting sequential biomolecular interactions as demonstrated by a series of additions of biotin, streptavidin, biotinylated antirabbit IgG, and finally rabbit IgG, whereas goat IgG as a control for the last step shows no response.¹⁹²

A guided-mode resonance (GMR) biosensor was developed for the rapid detection of cardiac biomarkers, that is, cardiac troponin I (cTnI), creatine kinase MB (CK-MB), and myoglobin (MYO), in human serum in 30 min.¹⁹³ The dose–response ranges and LODs for cTnI, CK-MB, and MYO were 0.05 – 10 ng mL^{-1} and 0.05 ng mL^{-1} , 0.1 – 10 ng mL^{-1} and 0.1 ng mL^{-1} , and 0.03 – $1.7 \mu\text{g mL}^{-1}$ and 35 ng mL^{-1} , respectively. The capture Abs are bound to GLD by cross-linking. The immobilization of Abs is evaluated by sandwich APTES-functionalized Si_3N_4 surface ELISA and sandwich immunogold assays. The developed technology holds great promise to develop low-cost and portable biosensors.

An all-fiber optofluidics-based bioassay platform (AFOB) has been attempted for the highly sensitive, selective, and rapid

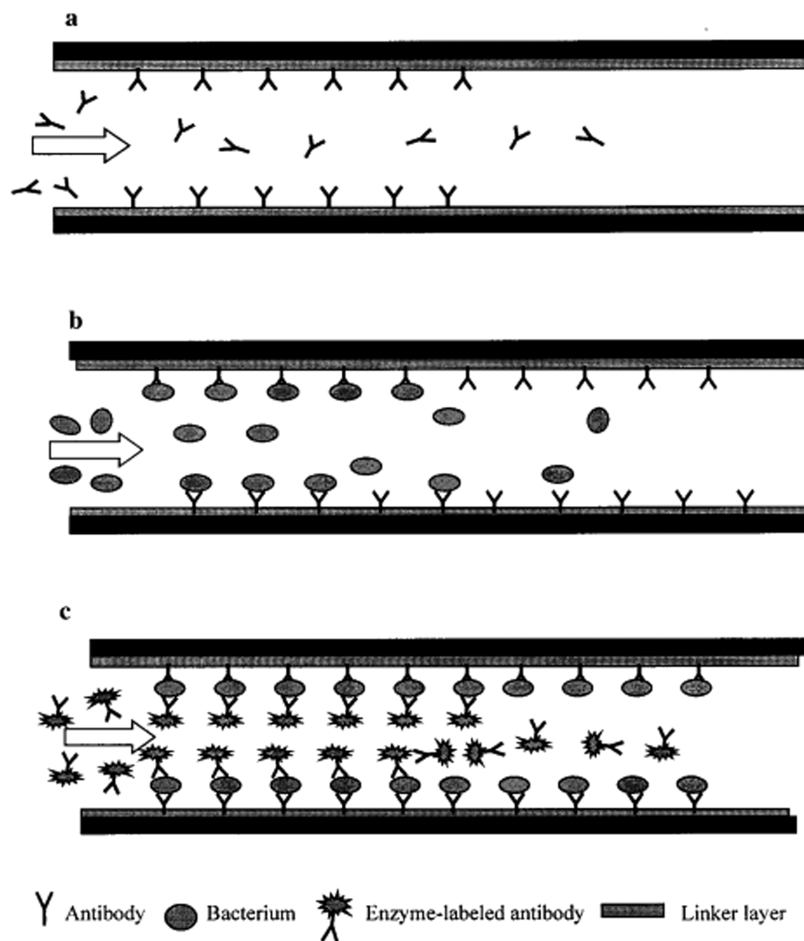


Figure 5. Schematic diagram of a fused-silica capillary column for the detection of *E. coli* O157:H7: (a) immobilization of Abs via APTES and GLD, (b) *E. coli* capture, and (c) formation of immunocomplex by the addition of alkaline phosphatase-labeled anti-*E. coli* O157:H7 Ab. Reprinted with permission from ref 195. Copyright 2001 American Chemical Society.

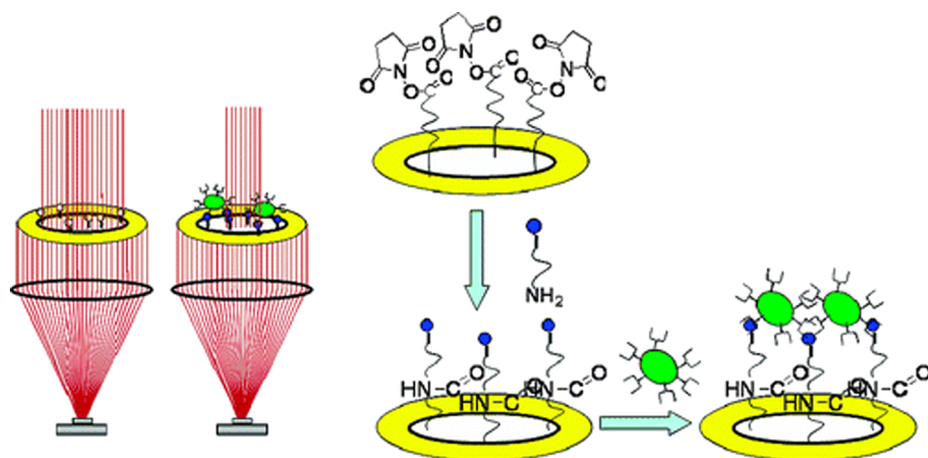


Figure 6. An optical biosensor was designed for the label-free detection of *E. coli* O7:K1. (left) Difference in transmission of laser beam between a reference well with only immobilized Abs and a well containing both Abs and *E. coli* cells blocking a part of the laser beam. (right) Schematic of the coupling of Abs to the activated glass slide followed by immobilization of *E. coli*. Reprinted with permission from ref 196. Copyright 2006 American Chemical Society.

assessment of BPA leaching risk.¹⁹⁴ It involves the covalent binding of BPA-BSA on the APTES and GLD-functionalized fiber optic sensor and the detection of BPA using fluorescent-labeled anti-BPA monoclonal Abs. With linearity of 0.5–100 $\mu\text{g L}^{-1}$ and LOD of 0.06 $\mu\text{g L}^{-1}$, the sensor is proven for the

detection of BPA in a spiked environmental sample matrix with recoveries in the range of 90–120%.

Optical biosensors have also been designed to detect whole microorganisms rather than just small molecules such as proteins. The detection of pathogenic microorganisms is critical

for controlling foodborne illnesses. Conventional methods based on culture and colony counting are time-consuming, expensive, complicated, and may require signal amplification or labeling. Detection by fluorescence or SPR has led to rapid analysis using a variety of optical biosensors. In one example, a fused-silica capillary column is treated with APTES, and then Abs to virulent *E. coli* O157:H7 are attached through GLD coupling. *E. coli* in a sample is then bound to the Abs on the column (Figure 5). A "sandwich" immunocomplex is formed by the addition of alkaline phosphatase-labeled anti-*E. coli* O157:H7 Ab, which binds to the *E. coli* bound in the previous step. The absorbance of *p*-nitrophenol, the product of the enzyme and *p*-nitrophenyl phosphate reaction, can be monitored at 400 nm. The biosensing approach is capable of detecting *E. coli* in the range of 10^2 – 10^6 cfu mL $^{-1}$ with the total assay being completed within 1.5 h. Its selectivity was confirmed by testing with other microorganisms such as *S. typhimurium*, *L. monocytogenes*, and *C. jejuni*.¹⁹⁵

An optical biosensor was designed for the label-free detection of *E. coli* O7:K1 cells using laser transmission intensity measurements. In brief, specific Abs for *E. coli* are coupled to the wells of a CodeLink activated glass slide, followed by binding of the *E. coli* cells (Figure 6). Detection is accomplished using a laser diode (635 nm), and the transmission intensity difference between the reference (only Ab) and the sample is calculated. The assay system detects as few as 45 cells within 1 h.¹⁹⁶

In another label-free system, an optical biosensor based on FTIR spectroscopy is useful for the detection of pathogenic *E. coli*. Titania thin films prepared by the sol–gel method are treated with 0.2 M APTES and GLD for the attachment of Abs against *E. coli* O157:H7. FTIR spectroscopy provides mid-IR fingerprints of the *E. coli* pathogen in a sample, which could be detected at concentrations as low as 1×10^2 CFU mL $^{-1}$ within 30 min. Specificity of the optical biosensor was validated by using *E. coli* K12 as a control, which did not give a response.¹⁹⁷ For the label-free detection of phage M13K07,⁴⁵ a silicon wafer is sequentially functionalized with APTES, activated with GLD, and coupled to avidin. Thereafter, mouse monoclonal biotin-anti-M13 Ab is immobilized, which detects phage M13K07 based on the increase in thickness of the phage M13K07 layer corresponding to the increase in its concentration from 0.1×10^{10} to 2.5×10^{10} pfu mL $^{-1}$. The developed optical chip exhibits a sensitivity of 10^9 pfu mL $^{-1}$.

Another successful application is the detection of *Salmonella* using a direct binding optical grating coupler (OGC) IMS based on optical waveguide light mode spectroscopy.³⁸ The procedure involves the rotation of an OGC sensor chip placed in a flow-through cell in a defined angle by a goniometer and the measurement of the photon signals diffracted and propagated inside the waveguide film using two photodiode detectors. The anti-*Salmonella* Ab is bound to the APTES-functionalized sensor chip by GLD. With a LOD of 1.3×10^3 CFU mL $^{-1}$ for *Salmonella*, the sensor also displays high selectivity for *Salmonella* and can be reused for 10 repeated runs with a coefficient of variability of 2.87% after regenerating the Ab-bound chip with 10 mM HCl.

4.3. Microfluidic/Lab-on-a-Chip Applications

Manipulation of liquid inside a microscale fluidic network reduces consumption of reagents and allows facile reactions between analyte and biomolecule, resulting in reduced assay times. Therefore, IAs using a microfluidic format are designed for rapid and sensitive detection of important antigens in clinical diagnostics. Glass and silicon-based microfluidic devices

equipped with SPR, Raman spectroscopy, and electrochemical analysis have been developed extensively. For microfluidic IAs, Ab or antigen is immobilized inside microchannels. Silicon and glass share similar surface chemistry; thus the route to biomolecule immobilization is similar and APTES has been widely used for surface coatings. For example, a chemiluminescence IA in glass capillaries was developed for the detection of MYO, CK-MB, troponin I (TnI), and fatty acid binding protein (FABP) in human plasma.¹⁶ The capillaries were functionalized with APTES and subsequently bound to capture Abs using ultrasound waves to promote diffusion of materials. This significantly improved the silanization and Ab immobilization leading to increased detection response and sensitivity. The LODs for MYO, CK-MB, TnI, and FABP in human plasma are 1.2, 0.6, 5.6, and 4 ng mL $^{-1}$, respectively. The IA is much better than the sandwich ELISA performed on Maxisorb MTP.

An integrated microfluidic device was developed for solid-phase sandwich IA, based on microparticle labeling (Figure 7).¹⁹⁸

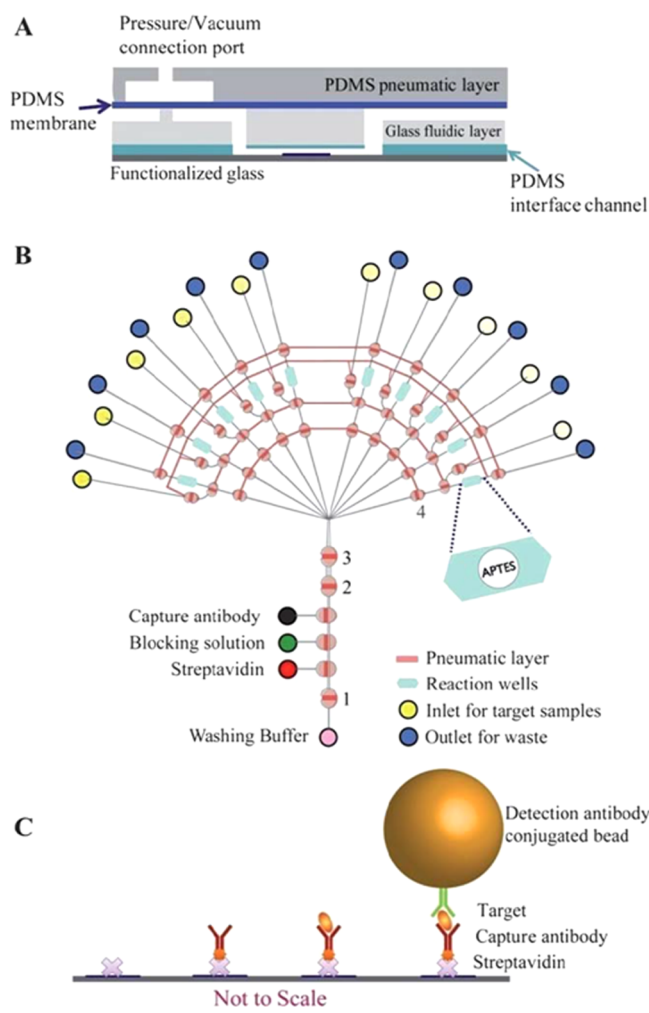


Figure 7. Integrated microfluidic bioprocessor for solid phase capture IAs: (A) cross section of the reaction chamber where PDMS is polydimethylsiloxane; (B) integrated microfluidic system that uses monolithic membrane valves to transport reagents and washing buffer to the reaction chambers; and (C) schematic of the IA consisting of streptavidin, biotinylated capture Ab, target molecules, and detection beads that are pumped to the reaction chamber to form a total immune-complex on patterned APTES. Reproduced with permission from ref 198. Copyright 2011 Royal Society of Chemistry.

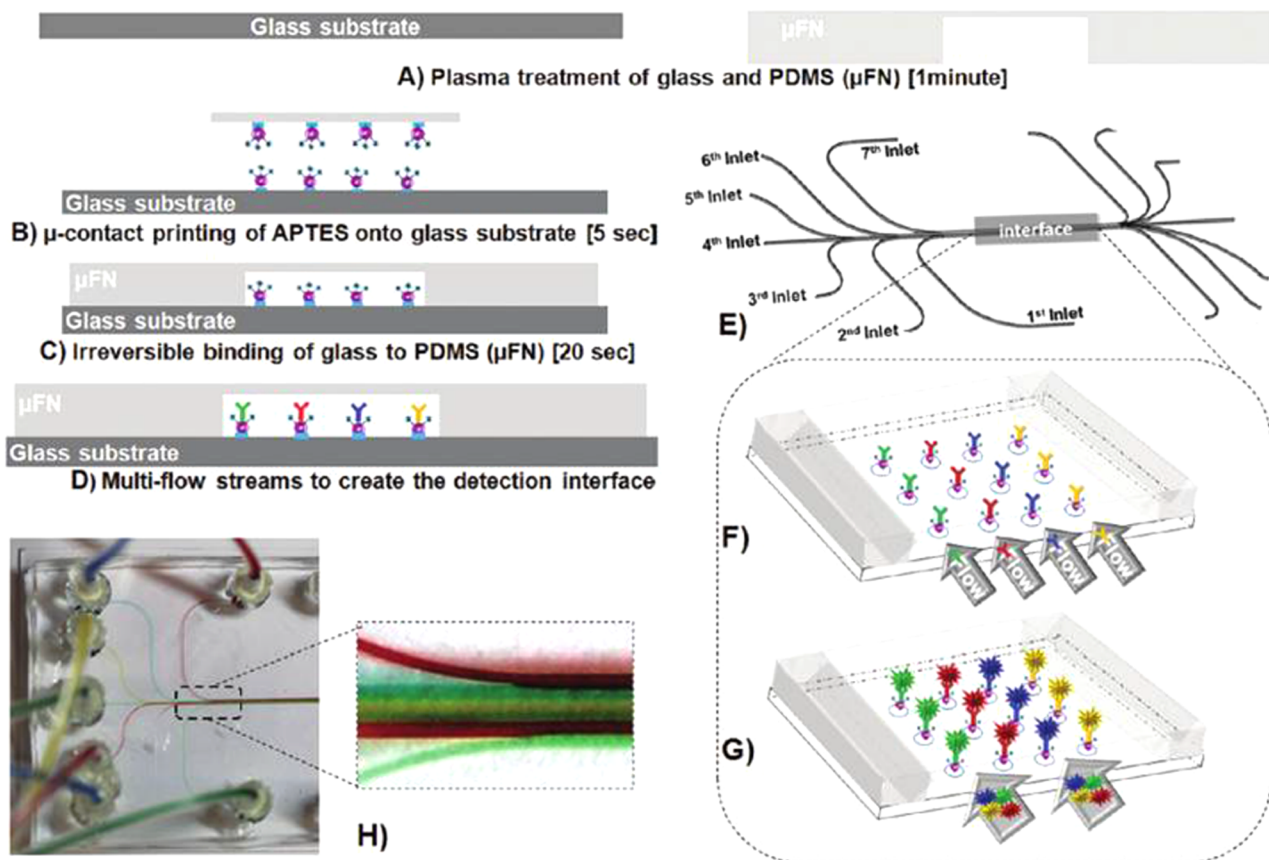


Figure 8. Patterning multiplex protein microarrays in a single microfluidic channel. (A) Plasma treatment of the glass and PDMS substrates. (B) Microcontact printing of APTES onto glass substrate. (C) Forming the irreversibly sealed microfluidic device. (D) Covalent binding of biomolecules using EDC-NHS chemistry. (E) Microfluidic design. (F) Multiple laminar flow streams carrying individual specific biomarkers to create multiplex protein patterns along the main channel. (G) Schematic of a mixture of secondary Abs specific to the primary Abs for a high throughput biomarker assay. (H) Magnified multiple laminar flows in the main channel. Reprinted with permission from ref 201. Copyright 2011 American Chemical Society.

It employs programmable microvalve-control structures for fully automated sample processing. The APTES-patterned glass surface was sequentially bound to streptavidin, biotinylated capture Ab, analyte, and detection Ab-conjugated magnetic beads. The integrated microfluidic device was used for two sandwich IAs, that is, for mouse IgG and prostate-specific antigen (PSA), with LODs of 1.8 and 3 pM, respectively.

PDMS is a silicon-based organic polymer with widespread uses because of its low cost and ease of fabrication.¹⁹⁹ This rubber-like flexible polymer (i.e., elastomer) is also transparent to enable optical imaging. PDMS is hydrophobic in native form, so nonspecific protein is problematic and it lacks functional groups for covalent derivatization. Silanol groups can be introduced by oxygen plasma treatment, but these groups only have limited long-term stability.²⁰⁰ Nevertheless, the patterning of five different Ab arrays in a single microfluidic channel was demonstrated using microcontact printing for APTES-functionalization and Ab immobilization.²⁰¹ The Abs were activated by EDC-NHS and then immobilized on APTES-patterned glass substrate by microcontact printing using PDMS stamps (Figure 8). The multiplex Ab arrays maintained their functionality even at high flow rates and remained stable at shear stresses of up to 50 dyn cm^{-2} . The functionality was tested by employing a mixture of fluorescent-labeled secondary Abs that were specific to the primary Abs bound to the glass substrate.

Other plastic substrates such as PMMA, polystyrene (PS), and cyclic olefin copolymer (COC) exhibit optical transparency, high

chemical resistance, and low autofluorescence as compared to PDMS. Such materials have gained attention in microfluidics due to low cost of fabrication using injection molding or hot embossing. The surfaces of PS, COC, and PMMA lack ligands for covalent linkage; therefore, various methods have been attempted for surface modification. Besides common oxygen-plasma treatment, of interest is to coat the polymer surface with an intermediate polymer layer that has an attractive interaction with biomolecules.²⁰² Another important point is limited biomolecule density immobilized on the microchannel planar surface. Several strategies using 3D structures have been employed inside microfluidic channels for higher biomolecule capture capacity. They include patterning microstructures (e.g., microposts^{203,204} and micropits,²⁰⁵ insertion of porous membranes^{206,207}) before the assembly of microfluidic chips. Microbeads,^{208,209} sol–gels,²¹⁰ hydrogels,^{211,212} polymer monoliths,²¹³ or *in situ* polymerized membranes²¹⁴ can be packed into enclosed channels to create 3D structures. In general, for silica-based 3D structures such as silica beads and alkoxy silane-based sol–gels, a similar glass/silicon surface immobilization strategy with APTES can be used for biomolecule immobilization.

4.4. Microgravimetric Biosensors

The silanized platforms have been widely employed in microgravimetric biosensors, such as those employing microcantilevers and QCM, for the immobilization of Abs. A millimeter-sized lead zirconium titanate (PZT) glass cantilever was employed for the detection of *E. coli* O157:H7.²¹⁵ The

monoclonal anti-*E. coli* O157:H7 Ab was covalently bound to the APTES-functionalized cantilever glass tip by EDC-SNHS. *E. coli* O157:H7 was detected on the basis of the reduction in the resonant frequency of cantilever after the formation of immune complex. The LOD of the developed cantilever biosensor was 700 cells mL⁻¹.

The label-free detection of femtogram levels of biologics was demonstrated in flowing liquid samples using a PZT microcantilever-based IMS.²¹⁶ The cantilevers were functionalized with APTES, with Abs immobilized by the EDC-SNHS cross-linking strategy. It detected very low concentrations of pathogen (*E. coli* O157:H7, 10 cells mL⁻¹) and protein (BSA, 100 fg mL⁻¹) in about 10 min. The developed IMS was highly selective for *E. coli* as it detected 15–60 cells mL⁻¹ in a background of 10⁴ mL⁻¹ naturally occurring bacteria. The mass sensitivities of the sensor for BSA and *E. coli* were 0.8 ± 0.2 ag Hz⁻¹ and 1.5 ± 0.3 fg Hz⁻¹. Similarly, a PZT-anchored piezoelectric excited millimeter-sized cantilever (PAEPEMC) IMS was employed for the measurement of *Bacillus anthracis* (BA) spores (333 spores mL⁻¹).²¹⁷ The results showed that anti-BA Ab functionalized PAEPEMC IMS was highly selective to BA spores. The presence of other *Bacillus* species did not prevent the binding, but hindered the transport of BA to the sensor.

A Love-mode surface acoustic wave (SAW) IMS was employed for the real-time detection of hepatitis B surface Abs (HBsAbs) in whole blood samples.⁴⁴ The sensor was composed of a SiO₂ guiding layer deposited on a 36° YX LiTaO₃ piezoelectric single crystal substrate that protects the electrodes and traps acoustic energy near the surface. The hepatitis B surface antigen (HBsAg) was bound to the APTES-functionalized interdigitated transducer (IDT) electrodes by GLD cross-linking. The assay detects 10 pg mL⁻¹ to 10 ng mL⁻¹ of HBsAb with mass sensitivity of 0.74 Hz (pg μL⁻¹)⁻¹. It is applicable for the detection of HBsAb in whole blood samples from vaccinated patients, but not completely immune to hepatitis B virus (HBV), and fully vaccinated counterparts.

4.5. Electrochemical Biosensors

Different strategies using APTES have been applied for the detection of glucose,^{111,112,173–175,218–225} putrescine,^{226,227} xanthine,²²⁸ uric acid,²²⁹ amino acids,²³⁰ and cancer markers.^{231,232} Various electrode materials may influence critical factors for increased biosensor detection limits such as the efficiency of direct electron transfer, molecular recognition, enzyme matrix distribution, or stability. The application of APTES in layer-by-layer (LbL) and SAM,^{111,112,218–222,233} sol-gel,^{173,174} or electrodeposited systems^{223–225,234} resulted in different 2D and 3D structures that significantly improve the performance of electrochemical glucose biosensors. The most commonly used APTES-based electrochemical sensing techniques are steady-state amperometry at a fixed detecting potential in mediatorless sensing,^{112,174,175,219,220,224,226–230} DPV in redox detection of ferrocene-tagged Ab,²³² and electrochemical impedance spectroscopy.^{230,231}

4.5.1. Modification of Pristine Electrodes. Besides Au and Pt, graphite is commonly used due to its good electrochemical properties, ease-of-handling and low cost, and high surface area. All metals apart from the noble metals are covered by a native oxide layer with a thickness of only several nanometers under atmospheric conditions. These passive oxide layers are terminated by hydroxyl groups and covered with an adsorbed water layer to minimize the surface potential. The presence of oxides consisting of hydroxyl, phenolic, carbonyl, carboxylate,

etc., on electrode surfaces is well recognized. The distribution of oxide types is dependent upon the electrode material, its treatment, exposure to air or electrolytes, etc. Various procedures can be used to modify the oxide thickness, composition, and stability. The resulting structure of the obtained oxide layer is dependent on the method of production, such as thermal oxidation, plasma oxidation, physical and CVD, atomic layer deposition, magnetron sputtering, laser ablation, hydrothermal synthesis, and electrochemical anodization. Selective enrichment of surface hydroxyls is reported for KOH treatment of a vacuum heat-treated surface, while surface carboxyl groups can be selectively enriched by hot HNO₃.²³⁵ Freshly prepared boron-doped diamond (BDD) electrodes are hydrogen terminated,^{236–239} which are converted to oxygen-containing functional groups (i.e., carboxyl, carbonyl, and hydroxyl groups) upon anodic polarization.²⁴⁰ The immobilization of enzymes with APTES on bare electrodes has been performed on GCE and carbon surfaces,^{111,174} noble metals (Au and Pt),^{36,175,222–224} HOPG,¹⁷⁴ and indium tin oxide (ITO) surfaces.^{230–232,241}

A conductivity-based IMS detects methamphetamine (MA) in human urine in just 15 min with linearity of 1–10 μg mL⁻¹ and a minimum detectable concentration of 0.5 μg mL⁻¹.³⁶ The procedure involves the binding of anti-MA Ab on APTES-functionalized Pt electrodes using GLD. Therefore, it is applicable for detecting the critical concentration of MA (1 μg mL⁻¹) in human urine with high selectivity. The result obtained agrees well with that of gas chromatography–mass spectrometry, a time-consuming and complex analytical procedure.

Noteworthy is the detection of atrazine in the range of 50–700 μg mL⁻¹ using a niobium/nioibum oxide (Nb/NbOxHy) modified electrode.⁵⁰ The F_{ab} fragment k47 Ab against atrazine is covalently attached to the APTES-functionalized electrode via GLD. In this EIS scheme, a hexane-cyanoferrate(II)/(III) mixture serves as a redox probe with a cathodic polarization voltage of -1.2 V vs saturated calomel electrode (SCE). The mediatorless GOx-bound GCE is applicable for the detection of glucose over the entire pathophysiological glucose range in diabetics (1.3–28.2 mM) and eliminates any interactions between a mediator and electroactive interfering substances for precise blood glucose monitoring.

Optically transparent, extremely smooth, and electrically conducting ITO surfaces have found their application in optical, electroluminescence, and electrochemical biosensing. Despite low electrocatalytic activities, ITO electrodes have a very low and flat background current, which is favorable to noise reduction in an electrochemical biosensor. A SAM of APTES is used to modify the surface of an ITO microelectrode array for subsequent immobilization of uricase using the cross-linker bis(sulfosuccinimidyl)suberate.²²⁹ Figure 9 shows the AFM micrographs of ITO surfaces on glass and the change in roughness of the surface upon immobilization of uricase. The LOD for uric acid is excellent (8.4 μM); however, this approach is very vulnerable to endogenous electroactive interferences in biological samples.

For the first time, anti-HER-3 Ab was integrated in a disposable IMS using the ITO substrate for detecting HER-3, which is a transmembrane growth factor receptor of the human epidermal growth factor receptor that is associated with cancer cells.²³¹ Figure 10 shows the fabrication of the IMS as bare ITO surfaces are pretreated with a mixture of H₂O₂ and NH₄OH, prior to functionalization with APTES and anti-HER-3 immobilization and BSA blocking. HER-3 down to the fg mL⁻¹ level can be detected using an electrochemical impedance

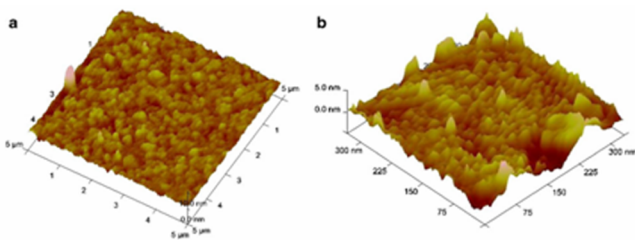


Figure 9. Contact-mode AFM images of (a) APTES/indium tin oxide microelectrode array (ITO- μ EA)/glass and (b) uricase/BS3/APTES/ITO- μ EA/glass. Reproduced with permission from ref 229. Copyright 2013 Springer.

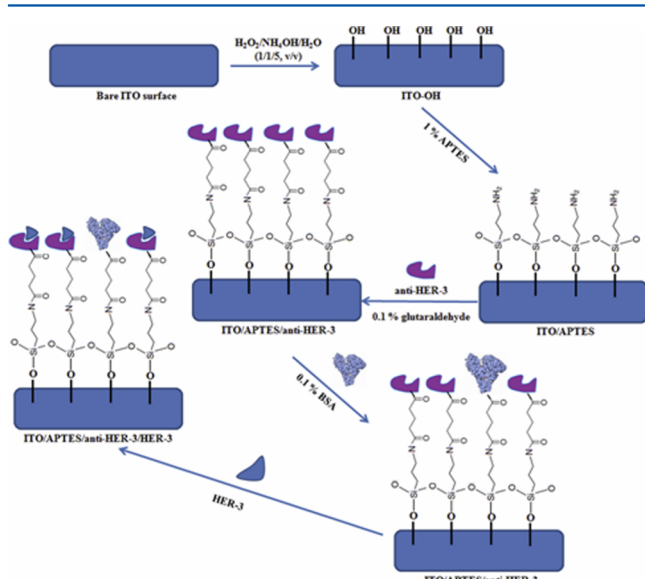


Figure 10. Schematic for IMS using anti-HER-3 Ab immobilized on an indium tin oxide (ITO) surface for HER-3, a type of transmembrane growth factor receptor of the human epidermal growth factor receptor associated with cancer cells. Reproduced with permission from ref 231. Copyright 2014 Elsevier B.V.

spectroscopy technique. However, attempts to monitor and reveal binding characteristics between HER-3 and anti-HER-3 using single frequency impedance are not conclusive due to interferences at a given single frequency.

Two tumor biomarkers, CEA and AFP, can be detected simultaneously using two ITO electrodes (1 mm diameter) patterned on a glass substrate at a spatial separation of 2.5 mm.⁴¹ Again, the electrode surface is functionalized with APTES for subsequent immobilization of their corresponding Abs via GLD cross-linking. The biomarkers are detected by electrochemical ELISA using streptavidin-labeled alkaline phosphatase. The response signal from electrochemical oxidation of alkaline phosphatase-generated hydroquinone provides a dynamic range of 25–150 and 10–200 ng mL⁻¹ for CEA and AFP detection with corresponding LODs of 1.2 and 1 ng mL⁻¹.

Electrochemical detection of goat IgG with a dynamic range of 118 fg mL⁻¹ to 1.18 ng mL⁻¹ is feasible using microchips with a dual-ring working and counter electrodes and a sensing cavity chamber fabricated on glass slides.⁴³ Goat IgG attached to APTES-functionalized glass using GLD binds to alkaline phosphatase (ALP)-conjugated antigoat IgG. Thereafter, goat IgG concentrations in samples can be determined by competitive ELISA using *p*-aminophenyl phosphate (PAPP) as an enzyme

substrate. The enzymatic conversion of PAPP to *p*-aminophenol (PAP) is analyzed by differential pulse voltammetry (DPV).

An electrochemical immunochip sensor involving the binding of antiaflatoxin M1 Abs to an APTES-functionalized Au microelectrode array (MEA) is useful for the detection of aflatoxin M₁ in milk.²⁴² The detection scheme is based on competitive ELISA using TMB/H₂O₂ and HRP as the enzyme label. The sensor exhibits a dynamic detection range of 10–100 ng mL⁻¹ and a LOD of 8 ng mL⁻¹, significantly lower than the legislative limit of 50 ng mL⁻¹. Similarly, anti-SEB Ab bound to the APTES-functionalized nanoporous aluminum surface via GLD activation has been described for detection of *Staphylococcus* enterotoxin B (SEB) as low as 10 pg mL⁻¹ in 15 min.²⁴³ The measurement is based on time-resolved electrochemical impedance spectroscopy (EIS).

SPR Au chips can be reused by treatment with 12 M HCl for 10 min and O₂-plasma scrapping for 5 min.²⁴⁴ In acidic milieu, hydroxyl (OH⁻), sulfate (SO₄²⁻), and chloride (Cl⁻) generated by the dissolution of siloxane bonds destabilize the siloxane framework in the presence of water.²⁴⁵ However, the acidic environment also favors the polymerization of silanes, resulting in incomplete regeneration. Therefore, a second treatment step involving O₂-plasma scrapping is mandatory for complete regeneration of the Au surface.

APTES has been used to modify a planar BDD electrode, pretreated with KOH to serve as a biosensing platform for biomolecule immobilization with GOx to achieve direct electron transfer (DET).²⁴⁶ The amino groups (mainly from lysine) of GOx and APTES were cross-linked by GLD to form a stable enzyme layer on the BDD surface. Cyclic voltammetry (CV) of GOx immobilized shows a pair of well-defined redox peaks in neutral phosphate buffer solution, corresponding to DET of FAD/FADH₂-GOx. This simple scheme for the achievement of DET is favorably compared to other complex sensing schemes involving the use of nanomaterials, redox polymers, and nanowires with respect to simplicity and reproducibility.

4.5.2. Film-Modified Electrodes. The benefits of using APTES in LbL deposition of a four-layered membrane are demonstrated in the development of an amperometric glucose biosensor consisting of APTES, Nafion, GOx, and perfluorocarbon polymer (PFCP) on a single-chip electrode set.²²¹ The PFCP layer acts as a glucose diffusion limiting membrane, while the Nafion layer prevents the diffusion of potential interference species. The biosensor exhibits a dynamic range of 2.8–167 mM, sensitivity of 2.21 nA mM⁻¹, and a response time of 15 s. Electroactive ascorbic acid, uric acid, and *p*-acetaminophen provoke no signal response, and the results obtained by the glucose biosensor agree well with those of the glucose DHD reference method-based analyzer, commonly used for the determination of diabetic urine glucose concentrations. Of interest also is the construction of a reference electrode in amperometric glucose sensing based on such PFCP properties.²²² A quasi-Ag/AgCl electrode coated with APTES and PFCP is invulnerable to interference species and provides adequate Nernst response under controlled ionic strength conditions. Unlike the standard Ag/AgCl reference electrode, this quasi-Ag/AgCl reference electrode can be easily integrated in miniaturized electrode arrays, each consisting of a working electrode, a reference electrode, and a counter electrode.

APTES-chitosan (CS) hybrid gel film was electrodeposited on Au or platinized Au (Pt-nano/Au) electrodes for the immobilization of GOx.²²⁴ The platinized Au electrode with an enhanced surface area displays broader linearity for glucose

detection. In such a study, an electrochemical QCM is used to monitor GOx–APTES–CS electrodeposition for optimized biosensor construction. A sensor based on the nonfaradic process, employing only deionized water as electrolyte, is useful for the detection of dengue infection.⁴⁸ The IMS, precoated with a sol–gel derived barium strontium titanate (BST) thin film, was functionalized with APTES and GLD for immobilization of preinactivated dengue virus. The detection of dengue Ab molecules in human serum is monitored by the impedance or current change. The same concept was extended for the detection of human IgG with a LOD of 40 ng mL⁻¹ using a sol–gel derived amorphous BST thin film and a highly diluted NaCl solution as electrolyte.²⁴⁷

4.5.3. Graphene and CNT Modification. The use of graphene and CNTs can enhance the electrochemical active surface area and electroconducting properties of the modifying layer.^{112,219–221,227–229,231} The graphene-functionalized GCE²¹⁸ and graphene/MWCNT-functionalized GCE¹¹² have been employed for mediatorless electrochemical glucose sensing. While both GCEs can detect the entire pathophysiological glucose range of blood glucose, the graphene/MWCNT-functionalized GCE exhibits a 4-fold higher current signal due to DET. GCEs and carbon-fiber microelectrodes with MWCNTs are fabricated into a high-performance electrochemical glucose microbiosensor with a detection limit of 25 μM, displaying a significant decrease in the diffusion current as compared to the bare electrode. The presence of APTES induces solubilization of MWCNTs and serves as an immobilization matrix for GOx.

Xanthine oxidase is immobilized on Fe₃O₄ NPs modified with APTES/CNTs for the determination of xanthine.²²⁸ This magnetic, disposable Au screen-printed electrode exhibits a remarkable LOD of 60 nM for xanthine. However, this sensor exhibits a narrow linear range (0.25–3.5 μM), which can be attributed to a relatively low enzyme loading and low reproducibility. More importantly, the electrode exhibits high reactivity toward electroactive uric and ascorbic acids. The inability to avoid detection of interfering molecules is a major challenge in developing any new electrode materials for biosensing applications.

Putrescine is associated with cancer markers,^{248,249} plant stress markers,²⁵⁰ bacterial vaginosis,²⁵¹ and food spoilage.²⁵² The GCE fabricated with MWCNTs, Nafion, putrescine oxidase (POx), and APTES offers a fast response time of 10 s and a detection limit of 500 nM.²²⁶ Again, APTES helps in the solubilization of MWCNTs in solution with EtOH and Nafion prior to casting on the GCE. MWCNTs can also be dispersed in poly(diallyldimethylammonium) chloride (PDDA) for the construction of an improved putrescine biosensor with greater sensitivity and selectivity.²²⁷ The level of putrescine in mouse plasma detected by the biosensor agrees well with the standard high performance liquid chromatography (HPLC) method.

The enantioselective discrimination of chiral, biologically active synthetic and natural compounds by APTES-modified ITO electrodes is an interesting research subject.²³⁰ Among the amino acids, tryptophan (Trp) as a precursor of melatonin and serotonin has a very important role in mental health. In this context, a modified ITO electrode (ITO/APTES/GO/HSA) using human serum albumin (HSA) differentiates D- and L-Trp enantiomers as exemplified by two well-defined irreversible oxidation peaks at +0.86 and +1.26 V. The modification of the ITO surface by subsequent addition of APTES and GO increases the polarization window, enabling the differentiation of the two tryptophan enantiomers. Besides its long-term stability of only

10 days, the interfering effect of other amino acids or endogenous compounds remains to be investigated, a subject of future endeavor. Nevertheless, this approach offers several advantages such as easiness of preparation, accuracy, and low material cost.

Ultrasensitive detection of AFP²⁵³ involves four sequential steps: (i) coating a graphene-CdS QDs-agarose composite on GCE, (ii) APTES-functionalization, (iii) activation with GLD, and (iv) binding of anti-AFP Ab (Figure 11). The detection of

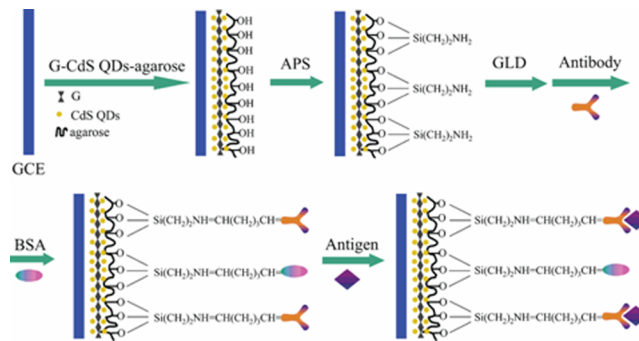


Figure 11. Fabrication of electrochemiluminescence (ECL) immunosensor for the ultrasensitive detection of alpha-fetoprotein; glassy carbon electrode (GCE), 3-aminopropyltriethoxysilane (APS), and GLD. Reproduced with permission from ref 253. Copyright 2012 Elsevier B.V.

AFP is followed by a decrease in ECL intensity after the immune complex formation with a linear range and a LOD of 0.0005–50 pg mL⁻¹ and 0.2 fg mL⁻¹, respectively. It is highly specific for AFP, as demonstrated by the detection of AFP in the presence of several nonspecific proteins. The assay is applicable for the detection of AFP in serum and saliva samples of patients with recoveries ranging from 89% to 100%. Of interest is the use of multilayer epitaxial graphene (MEG) for the detection of human chorionic gonadotropin (hCG).²⁵⁴ MEG was grown on silicon carbide substrates and modified by the Fenton reaction to yield a hydroxylated MEG layer. It was functionalized with APTES and then bound to anti-hCG Ab by EDC-NHS chemistry to provide a LOD of 0.62 ng mL⁻¹ and a linear range of 0.62–5.62 ng mL⁻¹.

4.6. Nanotechnology-Based Applications

Emerging nanomaterials play an important role in biosensors and diagnostics by offering a high surface area, functionalized platform for increased biomolecular loading, and resulting in low LOD for bioassays through signal amplification associated with their optical/electrical properties. Fe₃O₄ NPs with super paramagnetic properties can be easily separated from the reaction medium to facilitate product isolation/purification and the reuse of biocatalysts. Au,²⁵⁵ Fe,²⁵⁶ Si,²⁵⁷ and Zn NPs,²⁵⁸ which can be synthesized to precise dimensions and are fairly inexpensive to produce, are attached via APTES as part of covalent attachment systems for enzymes/proteins. Despite the numerous advantages of using nanomaterials for in vitro applications, their use in in vivo application is limited due to toxic effects in the human body. The incompatibility of NPs inside the body can lead to metal agglomeration that will significantly decrease diagnostic sensitivity.²⁵⁹

4.6.1. Gold. Au NPs with different nanoscale sizes can easily be dispersed in water and functionalized with enzymes with appropriate cross-linking agents. An ECL-based sensor for progastrin-releasing-peptide (ProGRP), a biomarker for small cell lung cancer, uses glucose oxidation as a means to detect other

biomolecules. Modifying the GCE with Nafion-cysteine-graphene sheets followed by Au NPs increases the surface area to enable higher loading density for anti-GRP.²⁶⁰ GOx and ferrocene-labeled secondary Abs are conjugated onto APTES-functionalized Au-TiO₂ NPs to produce a tracer (Figure 12). In

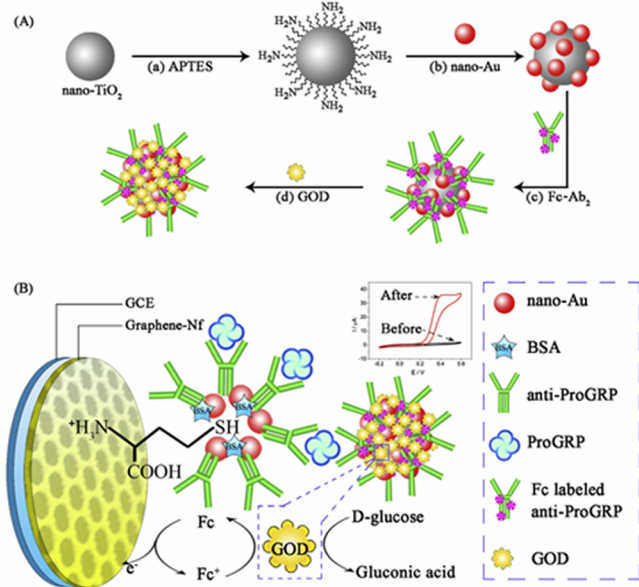


Figure 12. Schematic of an IMS using glucose oxidation for the detection of progastrin-releasing-peptide (ProGRP). The IMS consists of GCE with Nafion-cysteine-graphene sheets loaded with anti-GRP conjugated on Au NPs. GOx and ferrocene-labeled secondary antibodies (Fc-Ab₂) are conjugated onto APTES-functionalized Au-TiO₂ NPs to produce a tracer; bovine serum albumin (BSA) and Nafion (Nf). Reproduced with permission from ref 260. Copyright 2011 Elsevier B.V.

the presence of ProGRP, a sandwich complex is obtained between the GCE and the tracer. Exposure to glucose results in oxidation of glucose, which can be measured by CV, giving a quantitative measurement of ProGRP with a LOD of 3.0 pg mL⁻¹.

An Au/ITO electrode suited for the detection of vascular endothelial growth factors (VEGF) offers a LOD of 100 pg mL⁻¹.²³² The modified sandwich-type electrochemical IA platform takes advantage of the ITO electrodes low background

current with the high electrocatalytic activity of Au NPs. VEGF Abs are cleaved into two half-fragments by 2-mercaptoethylamine-HCl and immobilized onto the Au NPs. VEGF target molecules bind to the Ab fragments to form antigen-Ab complexes (Figure 13). Subsequently, ferrocene-tagged Abs react with these complexes and release electrons at an appropriate applied potential for detection by DPV.

The rapid detection of gibberellic acid (GA) in rice grain uses the coupling of electrochemical IMS with square wave anodic stripping voltammetry (SWASV) involving Cu ion-labeled antigen in a competitive immunoreaction.³⁷ The GCE is sequentially functionalized with APTES, Au NPs, anti-GA Ab, and milk. For the detection of GA, the IMS exhibits a linear range of 1–150 µg mL⁻¹ and provides reliable results as corroborated by HPLC and ELISA.

Signal enhancement with Au NPs is demonstrated in the design of evanescent field coupled waveguide mode sensors.²⁶¹ Au NP-conjugated streptavidin is immobilized onto silica-based sensor chips functionalized with different surface chemistries to investigate the effects of surface roughness induced by such functionalization. APTES/GLD-modified surfaces are suitable for small molecules with diameters ~5 nm due to the resulting surface roughness, whereas carbonyldiimidazole-modified surfaces are a better choice for the direct immobilization of biomolecular assemblies without any intermediate reactions.

An inexpensive and disposable impedimetric IMS uses stainless steel electrodes modified with APTES and electrodeposited Au NPs for the detection of doxorubicin.²⁶² Au NPs enhance the conductivity and sensitivity of the electrode and allow for the passive adsorption of doxorubicin-specific monoclonal Abs onto the electrode surface. The sensor detects doxorubicin concentrations in two ranges, that is, 2.5–30 pg mL⁻¹ and 30–1000 pg mL⁻¹, with a LOD of 1.7 pg mL⁻¹. The analysis of spiked human serum samples shows recoveries in the range of 88–122.2%.

4.6.2. Iron. Fe₃O₄ NPs are a popular substrate for immobilization of enzymes because enzymes can be separated and reused for subsequent analysis with the aid of a magnetic field. The abundance of oxide groups on the iron surface enables APTES to bind efficiently to the NP to effect cross-linking. Several studies use Fe₃O₄ NPs as means to study the binding properties of Abs in relation to particle size and reaction conditions. Fe₃O₄ NPs with different coating agents can be used to establish the optimal conditions for the binding of goat IgG to the NP surface in which complementary fluorescein isothiocyanate-

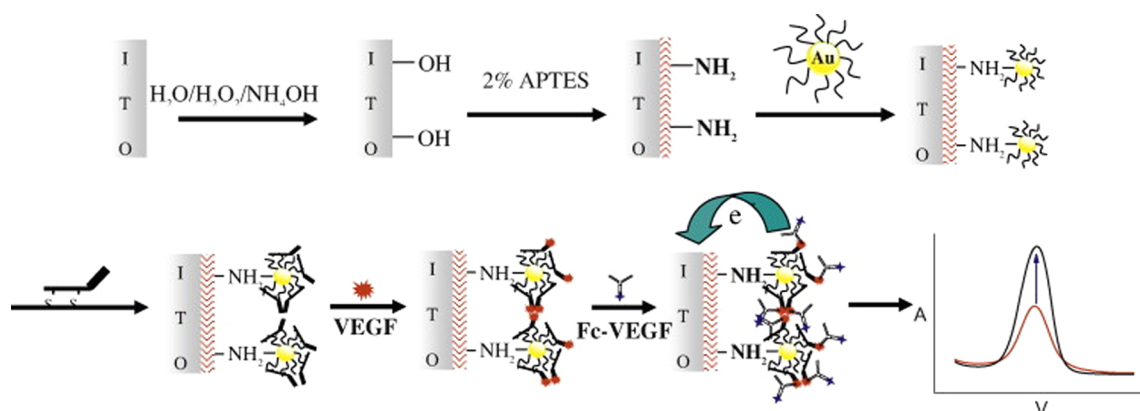


Figure 13. Schematic for the fabrication of an indium tin oxide (ITO) IMS for vascular endothelial growth factors (VEGF) in which ferrocene-tagged Abs release electrons under an applied voltage for detection by DPV. Reproduced with permission from ref 232. Copyright 2010 Elsevier B.V.

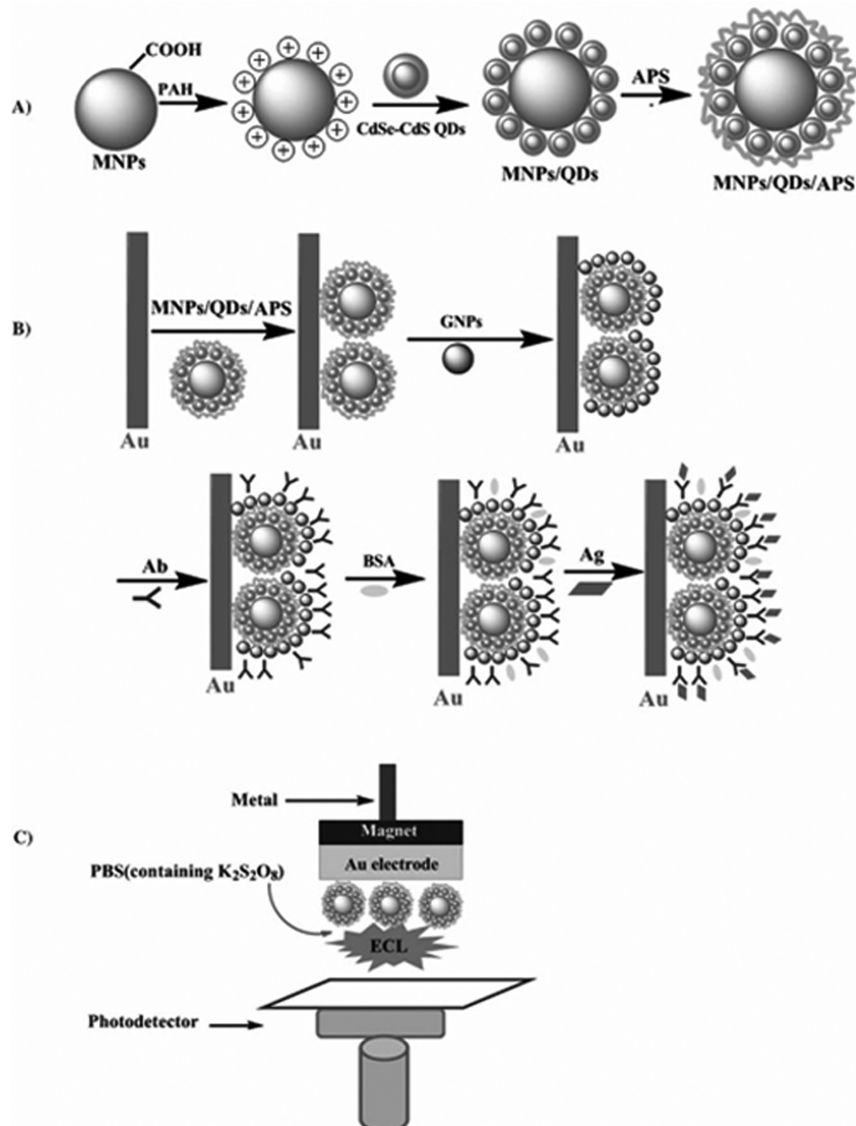


Figure 14. Schematic illustration of (A) preparation of the magnetic nanoparticle (MNP)/CdSe-CdS/APS hybrid nanostructure, (B) fabrication of the electrochemiluminescence (ECL) IMS, and (C) ECL detection by the IMS; poly(allylamine hydrochloride) (PAH), 3-aminopropyltriethoxysilane (APS), QD, gold nanoparticle (GPN), and phosphate buffered saline (PBS). Reproduced with permission from ref 268. Copyright 2011 Wiley-VCH Verlag GmbH & Co. KGaA.

nate (FITC) labeled anti-goat IgG is used to probe the presence of surface immobilized goat IgG by fluorescence microscopy.²⁶³ APTES functionalization is the most optimal immobilization technique for IgG on Fe₃O₄ NPs.

Two studies investigated the link between the number of Abs bound to Fe₃O₄ NPs and activity. The immobilization of IgG Abs on Fe₃O₄ NPs with an average size of 32 nm results in about 36% of the theoretical limit for surface coverage, corresponding to 34 bound Ab molecules, as determined by quantitative fluorescence assays.²⁶⁴ In the second study, 17 molecules of serratiopeptidase per Fe₃O₄ NPs (average size 13 nm) with 67% enzymatic activity is determined by mass measurement. The immobilized enzyme enhances the anti-inflammatory effect on carrageenan-induced paw edema in rats at much lower doses than the free enzyme.²⁶⁵ The decreased enzymatic activity could be attributed to covalent attachment of amino groups of APTES to the catalytic sites of the enzyme or changes in conformation of the native enzyme structure by overcrowding effects.²⁶⁶ A similar phenomenon is noted for GOx immobilized on different Fe₃O₄ NPs (5, 26, and

51 nm) with APTES and GLD.²⁶⁷ The immobilized enzyme retains only 15–23% of the free enzyme activity. Smaller NPs exhibit greater activity loss over repeated runs due to a poor recovery of the enzyme.

Highly sensitive detection of CEA is feasible using a magnetic electrochemiluminescent (ECL) Fe₃O₄/CdSe-CdS NP/polyelectrolyte nanocomposite.²⁶⁸ The nanocomposite (Fe₃O₄/QDs) is functionalized with APTES via ionic interactions to form Fe₃O₄/QDs/APTES, which was then bound to a gold electrode (Figure 14). Au NPs were bound to the surface of Fe₃O₄/QDs/APTES-functionalized electrodes, followed by anti-CEA Ab and BSA immobilization. As the CEA concentration increases, the ECL signal decreases. The detection of CEA occurs in a linear range of 0.064 pg mL⁻¹ to 10 ng mL⁻¹ with a LOD of 0.032 pg mL⁻¹. The determination of CEA spiked in normal serum shows a recovery of 93.1–107.5%, and its results correlate well with conventional ELISA.

A clever use of the magnetic separation property of Fe₃O₄ NPs is demonstrated when trypsin is immobilized on hairy non-cross-

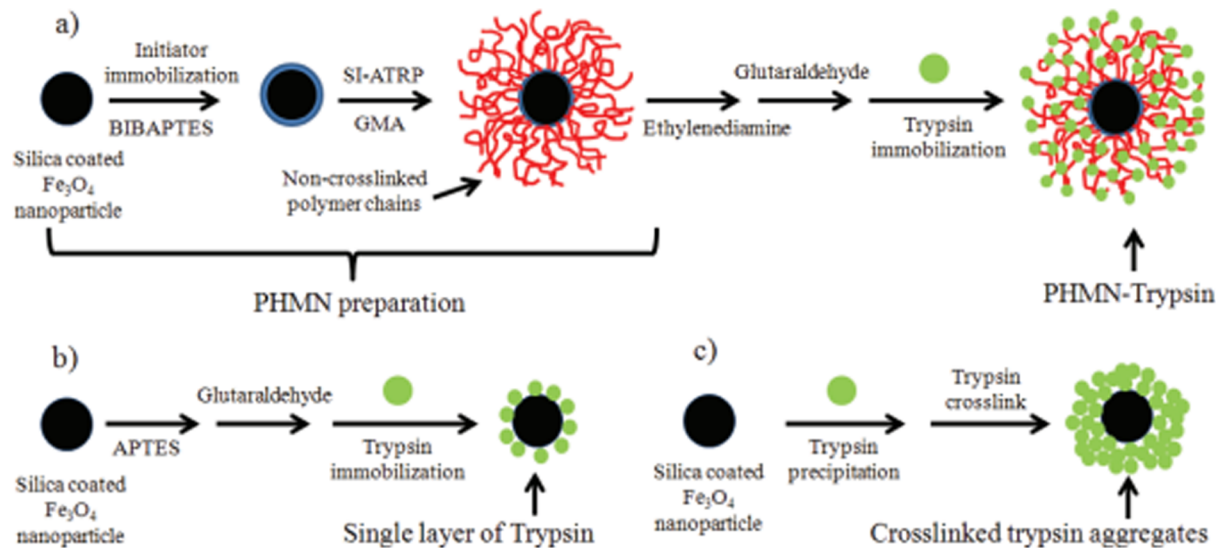


Figure 15. Schematic for the immobilization of trypsin on hairy non-cross-linked polymer chains attached to Fe_3O_4 NPs (PHMN); surface initiated atom transfer radical polymerization (SI-ATRP), 3-(2-bromoisobutyramido)propyl(triethoxy)-silane (BIBAPTES), and glycidyl methacrylate (GMA). Reprinted with permission from ref 269. Copyright 2012 American Chemical Society.

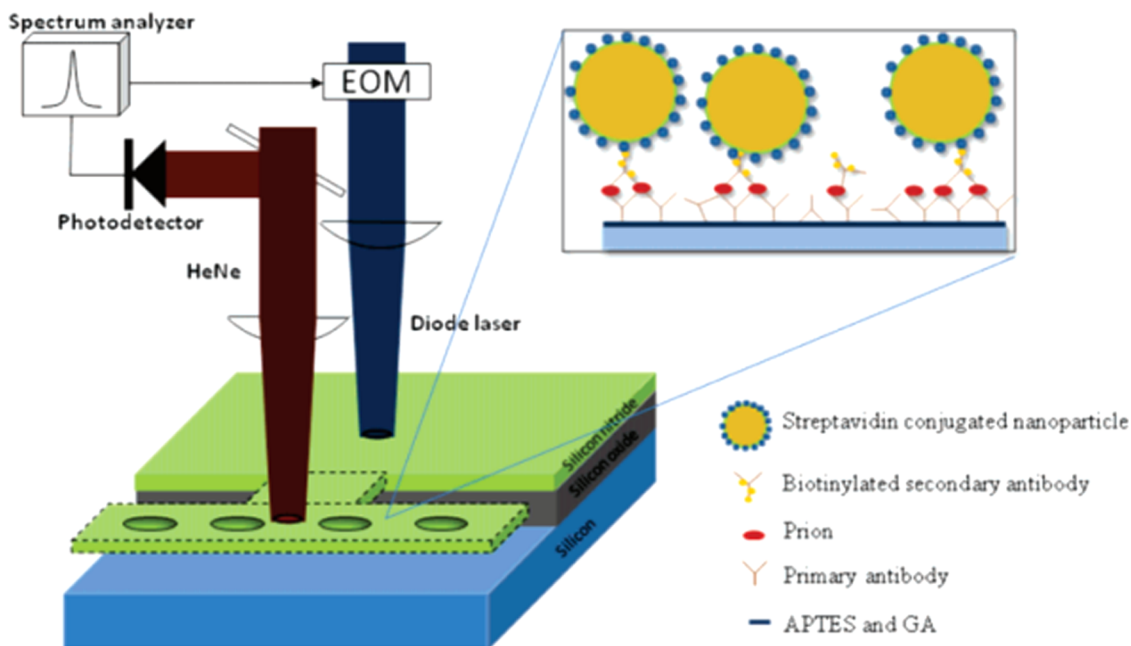


Figure 16. A dynamic resonance-based IA for the detection of protein prions (PrP). Streptavidin conjugated Fe_3O_4 NPs improved the detection of PrP to 2 ng mL^{-1} ; GLD (GA) and electro-optic modulator (EOM). Reprinted with permission from ref 18. Copyright 2008 American Chemical Society.

linked polymer chains with hybrid magnetic NPs (Figure 15).²⁶⁹ The materials facilitate ^{18}O labeling for protein quantification with H_2^{18}O , with the Fe_3O_4 NPs easily separated from the solution to prevent ^{18}O to ^{16}O back-exchange after labeling. The polymer chains provide a large number of binding sites and scaffolds to support 3D trypsin immobilization for increased enzyme density and accessibility over conventional free trypsin digestion in proteomic samples.

A facile and sensitive bioanalytical procedure is demonstrated for the detection of *Salmonella* as low as 10 cfu mL^{-1} in milk using a personal glucose meter (PGM).²⁷⁰ Magnetic NP clusters are functionalized with APTES and GLD followed by the immobilization of monoclonal anti-*Salmonella* Abs. These clusters then bind to *Salmonella* in milk and are magnetically

separated from solution using a magnet. Subsequently, the *Salmonella* complexes are detected by binding to polyclonal Ab-functionalized invertase and dispersing in a 0.5 M sucrose solution at 40°C . A PGM measures the amount of glucose produced from the hydrolysis of sucrose by invertase.

Fe_3O_4 NPs can improve the detection limits of IAs as well. A dynamic resonance-based technique is used to detect prion proteins (PrP) that cause neurodegenerative diseases when proteins undergo conformational changes.¹⁸ When PrP is immobilized onto a monoclonal Ab that is conjugated onto a resonator's surface via APTES/GLD, LOD increases from 20 to $2 \mu\text{g mL}^{-1}$. Binding streptavidin-functionalized Fe_3O_4 NPs further improves PrP detection to 2 ng mL^{-1} (Figure 16). In this case, the magnetic properties of the NPs do not play any role as a

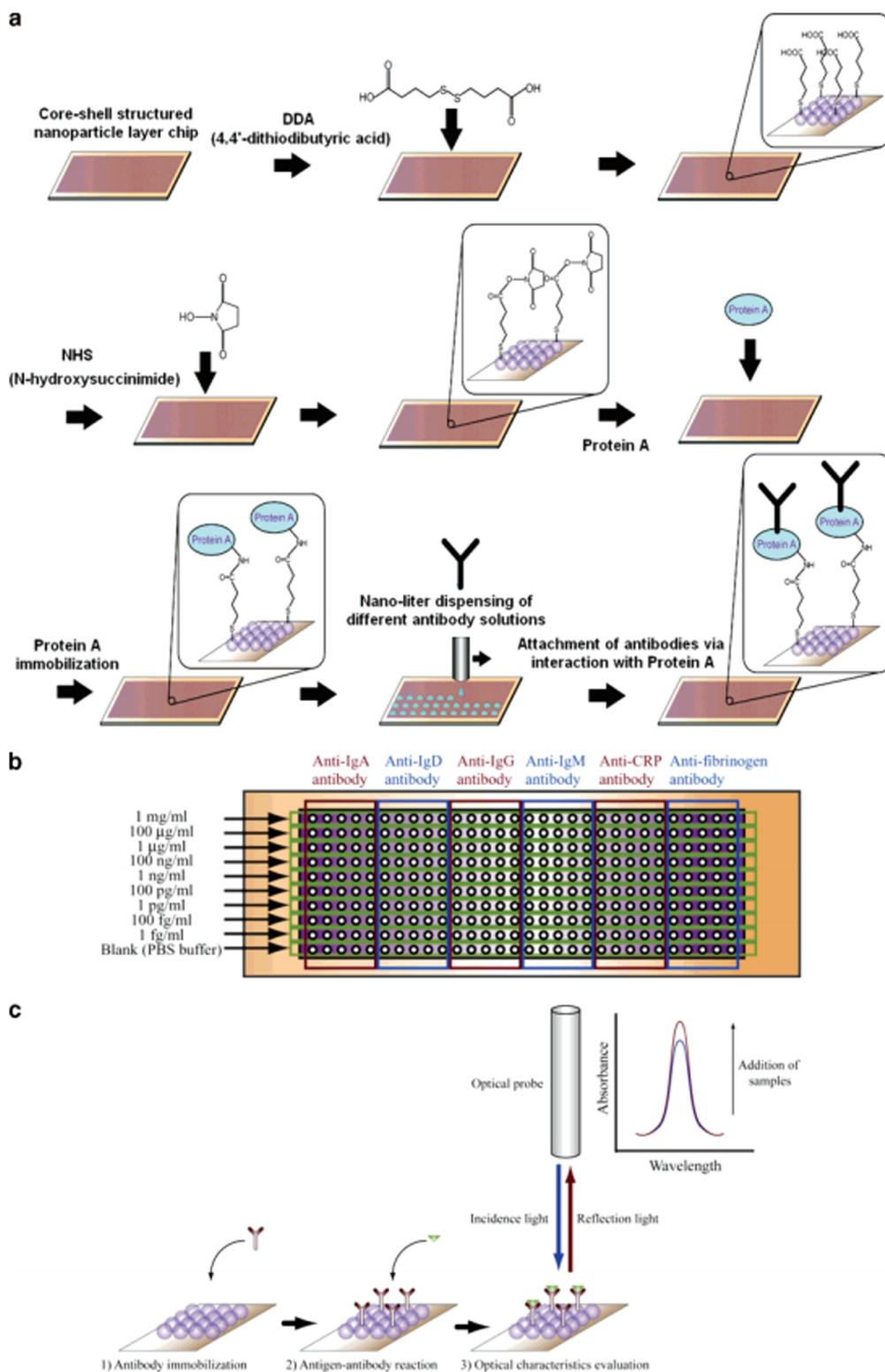


Figure 17. Schematic for the fabrication of a label free localized surface plasmon resonance (LSPR)-based bioanalysis method for developing multiarray optical nanochips: (a) Immobilization of Abs on the surface of the nanochip. (b) Six kinds of Abs and antigens were spotted onto the surface at different concentration. (c) Experimental setup for the multiarray LSPR-based nanochip. Immunoglobulin A (IgA), immunoglobulin D (IgD), immunoglobulin G (IgG), immunoglobulin M (IgM), C-reactive protein (CRP), and phosphate buffered saline (PBS). Reprinted with permission from ref 273. Copyright 2006 American Chemical Society.

separation technique, but amplify the signal given from optical frequency measurement. A magnetic ELISA to detect multi-residue organophosphorus pesticides uses Abs immobilized on Fe_3O_4 NPs coated with APTES.²⁷¹ The abundance of functional

groups on Fe_3O_4 NPs enables efficient binding of Abs on the surface of the NP to improve sensitivity and specificity over conventional ELISA.

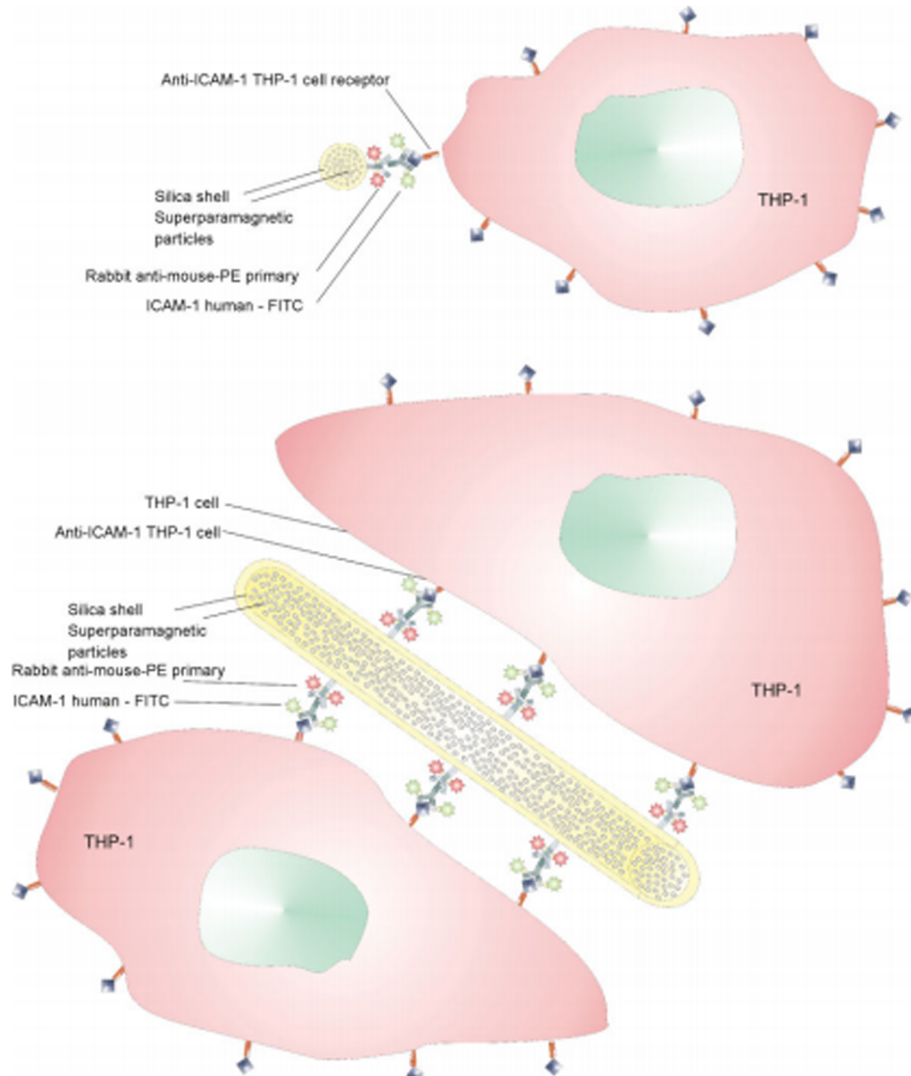


Figure 18. Increased number of binding sites for human acute monocytic leukemia THP-1 monocyte cells and intracellular adhesion molecule (ICAM-1) secondary Abs available along a Silica nanowire in comparison to Silica NPs; phycoerythrin (PE) and fluorescein isothiocyanate (FITC). Reproduced with permission from ref 275. Copyright 2011 Wiley-VCH Verlag GmbH & Co. KGaA.

4.6.3. Silicon. Silicon nanomaterials are functionalized with APTES to introduce amino functionalities for enzyme binding. The hydrolysis of silyl ether group forms reactive Si—OH groups that condense on the surface of silica to form a lateral siloxane network.⁹¹ The orientation of the amino groups points away from the silicon surface, a favorable orientation for binding enzymes. Nanostructured silicon NP/polycarbonate films can be prepared by immersing polycarbonate in alternating solutions PDDA and 40 nm colloidal silica.²⁷² After functionalization with APTES and GLD, Abs are covalently attached onto the film surface. The efficiency of binding IgG Abs to the APTES-functionalized silicon NP films is only 33% due to steric effects in binding the larger IgG structure over the smaller APTES molecule. However, the introduction of silicon NPs does increase the surface area of the film, which increases protein loading over native polycarbonate film. A sensitive and quantitative IA for human chorionic gonadotropin is demonstrated with the modified films. Similarly, improved sensitivity and signal amplification associated with increased surface area effects is noticed for a chemiluminescence IA with HRP on

APTES-functionalized mesoporous silicon NPs for the detection of CEA Ab.¹⁸⁰

The deposition layer of APTES on NPs can influence the activity of Abs. Dye-doped silicon NPs can be functionalized with APTES, in which the encapsulated cyanine-based near-infrared dye functions as a probe of the NP surface environment to identify the optimal deposition parameters for the APTES monolayer.⁷¹ An appropriate reaction time is required to form a stable amine layer, but higher reaction times results in disordered cross-linking. By using an IgG plate-based direct binding assay, the optimum APTES monolayer results in the binding of a maximum number of IgG-conjugated silicon NPs to the immobilized anti-IgG Abs.

Silicon nanomaterials have been used to fabricate highly sensitive diagnostic devices. One example is the fabrication of a label free LSPR-based bioanalysis method for developing multiarray optical nanochips (Figure 17).²⁷³ The multiarray LSPR nanochip is constructed with Abs immobilized on 300 nanospots of a sensing surface consisting of APTES-functionalized silicon NPs. The antigen concentration is determined from the peak absorption intensity of the LSPR spectra, providing a

detection limit of 100 pg mL^{-1} . In another example, SiNW field effect transistors (FETs) can be fabricated to be responsive to CRP, a marker of inflammation and possible indicator of future progression of cancer.²⁷⁴ The FETs are connected to an automated fluidic control system where the conjugation of CRP to the anti-CRP (immobilized on the SiNWs via APTES/GLD) results in a change in the detected current.

The effects of nanomaterial aspect ratio can significantly increase the sensitivity of detection. Specific binding between THP-1 monocyte cells and ICAM-1 secondary Ab is measured by flow cytometry for both silicon NPs and nanowires.²⁷⁵ Silica nanowires are better than silica NPs due to the aspect ratio, which can be easily distinguished from NPs when utilized as carriers for immunodetection. A NP forms a single bond to a cell/cell receptor, whereas a wire binds at several points to maximize the functional binding of the nanomaterials along their principal axis (Figure 18). Similarly, GOx is immobilized on SiO_2 nanowires deposited on an Au electrode (Figure 19),²²³ where the SiO_2 nanowires increase the effective surface area resulting in higher enzyme loading, better sensitivity, and lower glucose detection limit (0.6 mM).

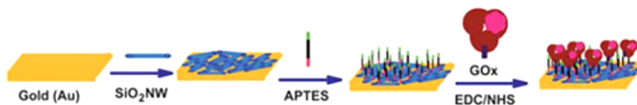


Figure 19. Schematic for the immobilization of GOx on SiO_2 nanowires (SiO_2NW) deposited on an Au surface. Reproduced with permission from ref 223. Copyright 2011 Royal Society of Chemistry.

4.6.4. Quantum Dots. QD materials in various morphologies and sizes are applicable for the evaluation of enzyme activity with respect to structural and spectroscopic characteristic of the substrate to which the enzyme is immobilized.^{276–278} Although organic fluorophores such as fluorescein and rhodamine are used extensively for Ab labeling, QDs are beginning to gain greater use in biosensing applications. A major advantage of QDs is its sharply defined emission spectra, which enable a single light source to excite multiple QDs simultaneously without the signal overlap in multiarray applications.²⁷⁹ Strategies to conjugate QDs to biomolecules can range from functionalization of the biomolecule with thiol groups that can bind to the QD surfaces, and electrostatic interactions between negatively charged QDs and positively charged biomolecules.²⁸⁰ Covalent attachment of biomolecules is achieved by functionalizing the QD surface with surfactant molecules to give COOH, NH₂, or SH groups. APTES is one such cross-linking agent used in this process.²⁸¹

ZnO nanocrystals with different morphologies can be prepared by varying the ratio of MeOH to water in the hydrothermal synthesis reaction system. Subsequently, these nanocrystals are functionalized with amino groups using APTES and tetraethyl orthosilicate, and then with HRP immobilized via GLD cross-linking.²⁸² 3D ZnO nanomultipods are more appropriate for the enzyme immobilization in comparison to NPs and nanodisks. The increase in activity of the enzymes on multipods could be attributed to less conformation changes in the HRP.

The detection of proteins has been achieved by an Ab-based sandwich assay with ZnO/Au NPs probes.²⁸³ ZnO NPs are considered nontoxic and biosafe materials with distinct Raman signatures. The addition of small amounts of Au NPs to ZnO enhances the ZnO Raman scattering intensity. Initially, an Ab specific for the target protein is bound to the silicon surface. An

antigen then binds to the first Ab followed by the addition of a secondary Ab (attached with a ZnO/Au NPs probe), which specifically recognizes and binds to the immune complex formed between the first Ab and the target protein. Good selectivity and sensitivity for the quantitative detection of proteins are facilitated by the amplified Raman scattering signal of the ZnO substrate.

QD-labeled secondary Ab can detect human IgG in human serum using immunoaffinity monolithic capillary microextraction coupled with microcentric nebulizer inductively coupled plasma mass spectrometry (MCN-ICP-MS).⁴⁷ Goat antihuman IgG is immobilized on APTES–silica hybrid monolithic capillary and binds to human IgG in a sample. Subsequently, goat antihuman IgG labeled with CdSe@ZnS QDs is added to bind to the human IgG. The linear detection range is $0.2\text{--}10 \mu\text{g L}^{-1}$ (LOD $0.058 \mu\text{g L}^{-1}$) and $0.5\text{--}10 \mu\text{g L}^{-1}$ (LOD $0.097 \mu\text{g L}^{-1}$) based on Cd and Se signals.

A simple CdSe/ZnS QD-based optical IMS has been described for the detection of HSA in the range of 2×10^{-1} to $2 \times 10^{-4} \text{ mg mL}^{-1}$ with a LOD of $3.2 \times 10^{-5} \text{ mg mL}^{-1}$.²⁸⁴ The optical system is comprised of a 405 nm diode laser, an optical lens, a Si-photodiode, and a 515 nm long pass filter. The monoclonal anti-HSA Ab is immobilized on APTES-functionalized glass by adsorption followed by blocking with BSA, binding of HSA, and detection using biotinylated polyclonal anti-HSA Ab bound to streptavidin-conjugated CdSe/ZnS QD (Figure 20).

An ECL IMS uses several different nanomaterials previously discussed in this Review to produce an efficient sensor for carbohydrate antigen 125 (CA125) in clinical serum samples.²⁸⁵ Fe₃O₄ NPs are functionalized with APTES followed by reduction of HAuCl₄ to form a core–shell carrier for the Ab of CA125, while graphene loaded with QDs serves as the site of immobilization for secondary Abs. Using microfluidic strategies, the synergistic effects of high surface area and conductivity greatly enhance the ECL signal for a low detection limit (1.2 mU mL^{-1}), with the Fe₃O₄ NPs facilitating the recovery of the IMS. Similar strategies are employed for another ECL immunosensor for the detection of prostate specific antigen (PSA).²⁸⁶ A sandwich-type IMS uses CdTe QDs on silicon NPs, in conjunction with high surface Fe₃O₄ NPs-coated graphene sheets on ITO, to enhance the ECL signal for the detection of PSA down to 0.72 pg mL^{-1} .

CdTe QDs were cross-linked on ZnO using APTES and mercaptopropionic acid as part of a biosensor for the detection of DNA.²⁸⁷ This ZnO composite, showing enhanced photoelectric activity attributed to appropriate band alignment between ZnO and the QDs, is immobilized on an ITO surface with biotin-labeled DNA (Figure 21). When the target DNA and assistant DNA interact with the biotin-labeled DNA, a so-called Y-junction structure is produced, which induces a restriction endonuclease-aided target recycling that results in the release of biotin. As the number of binding sites for HRP-labeled streptavidin decreases due to the loss of biotin, the amount of H₂O₂ consumed by a concurrent HRP-mediated electrochemical reduction will also decrease. With less H₂O₂ consumed, an enhanced photoelectrical response for DNA (LOD = $9.3 \times 10^{-16} \text{ M}$) can be achieved using the available H₂O₂ as an electron acceptor.

4.7. Other Detection Methods and Biomolecule Patterning

A fiber-optic-based evanescent wave IMS was developed for the detection of Newcastle disease virus (NDV) based on a sandwich IA.³³ The capture anti-NDV polyclonal Ab was covalently bound to APTES-functionalized quartz fibers using carbonyldiimidazole

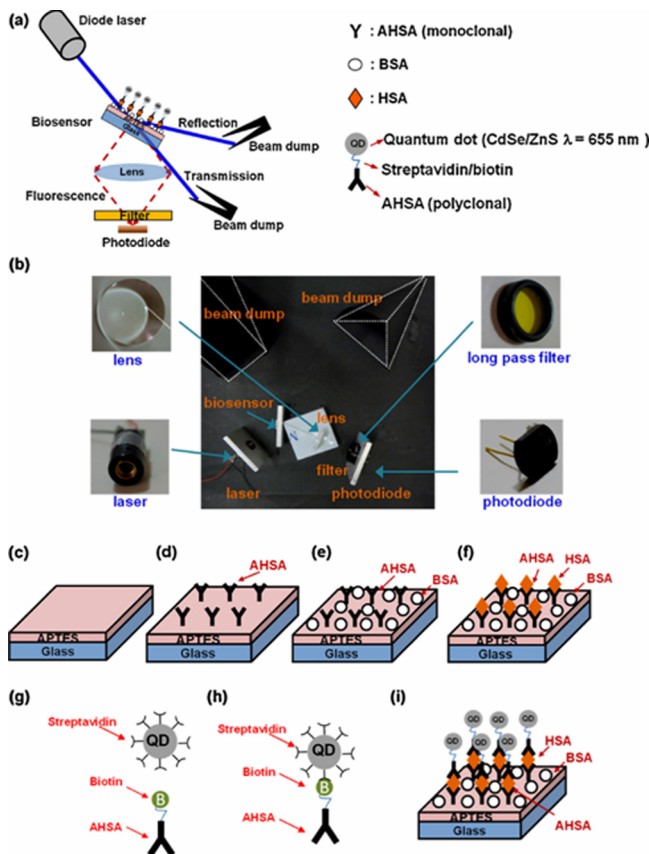


Figure 20. (a) Schematic and (b) real picture of a QD-based optical biosensing system. Schematics of the glass surface modification including (c) APTES deposition; (d) antihuman serum albumin (AHSA) Ab immobilization on APTES; (e) bovine serum albumin (BSA) blocking; and (f) human serum albumin (HAS) immobilization. Schematics of (g) before and (h) after the bonding between QD-streptavidin and biotin-AHSA to form the AHSA-QD complex, and (i) the conjugation of the AHSA-QD complex with the HAS precaptured on the biosensors. Reproduced with permission from ref 284. Copyright 2012 Elsevier B.V.

in dimethyl sulfoxide as the cross-linking agent. The binding of NDV was detected using the fluorescein-labeled anti-NDV as the detection Ab. The developed IMS detected NDV in the dynamic range of 2–250 ng NDV in just 15 min with a LOD of 0.5 ng (5 ng mL^{-1} for 0.1 mL sample).

The fabrication of rigid Ab-modified FETs and their use for the detection of alpha-fetoprotein (AFP), a tumor cancer biomarker, were also reported.¹⁹ The anti-AFP Abs were immobilized on an APTES-functionalized surface by homobifunctional cross-linking through GLD. The Ab-modified FETs attained increased sensitivity, high reproducibility, and selective analyte detection. The quantitative detection of AFP in the range of 10 ng mL^{-1} to $1 \mu\text{g mL}^{-1}$ was attained in the presence of other nonspecific proteins.

The biomolecule patterning on analytical devices has also been demonstrated, maintaining their 3D biological functionalization on silicon-based analytical devices.²⁸⁸ It involves the generation of a scaffold on a silicon substrate by the polycondensation of APTES followed by the binding of proteins and nucleic acid sequences, as demonstrated by IA and nucleic acid assays. Similarly, epoxy-functionalized magnetic poly(divinylbenzene-*co*-glycidyl methacrylate) colloidal particles (mPDGs) were prepared by microcontact printing and employed for the

detection of recombinant human interleukin (IL)-10 protein.²⁸⁹ APTES and octadecyltrichlorosilane were patterned on a glass surface by microcontact printing and subsequently bound to prepared mPDGs. The monoclonal antihuman IL-10 Ab was conjugated to the functionalized mPDGs and used for the capture of human IL-10, with the detection performed using fluorescent-labeled antihuman IL-10 Ab.

5. CRITIQUES AND OUTLOOK

Various conditions have been reported for the deposition of APTES on different solid materials, electrode materials, and nanomaterials toward the development of biosensors and diagnostic platforms. Regardless of the choice of the solid substrate, its surface must be conditioned to have sufficient hydroxyl groups and improve the silane grafting density and reproducibility of silanization. Surface treatment steps involving oxidation (such as treatment by piranha, UV light, ozone, and oxygen-plasma) and treatments in KOH/NaOH or even hot water lead to higher silane grafting density as they increase the density of hydroxyl groups on the surface. The cleaning of the surface makes it hydrophilic and hydroxylated as it is covered by water molecules. Therefore, the freshly cleaned surface must be dried to ensure reproducible results. Besides APTES, *N*-(2-aminoethyl)-3-aminopropyltrimethoxysilane is also widely used to modify hydroxylated supports such as silica and glass. Deposition of APTES in water often results in thin layers that initially bind to a negative surface via electrostatic interaction. However, lengthy incubation of a substrate like silicon for several hours results in a thick multilayer. The presence and absence of surface oxide groups changes the reactivity of the APTES. A mixture of neutral amine and protonated and hydrogen-bonded amine coexists on the solid surface; however, the former orients away from the surface and is available for biomolecule immobilization, while the latter is close to the surface. The mechanisms of silanization on surface oxide have not been fully understood because there is no direct analysis (*in situ*).

Immobilization of a sensing molecule also deserves a brief comment here because several techniques can be used for biomolecule immobilization. Although protonated amine can display electrostatic interaction with the negative moiety of the biomolecule, the immobilized biomolecule is not stable and easily escapes from the APTES bound-surface. GLD activation of amine is popular, followed by NHS ester and carbodiimide. A downside of amine cross-linking is that multiple bonds can be formed due to numerous lysine residues on a protein surface, which leads to conformational changes and/or blocking of the biomolecule's active sites. APTES can be conjugated with a spacer molecule like polyethylene glycol (PEG) or a hydrophilic polymer to reduce steric hindrance and the possibility of biomolecule denaturation.²²⁸ In addition, when the sensing platform involves an Ab molecule or a specific enzyme, affinity immobilization using avidin–biotin interaction might be a better choice to preserve the functional group of the Ab. A typical example is the control of a well-defined 3D nanostructure of HRP via a LbL assembly of avidin and biotin-HRP.²⁹⁰

Both electrostatic and covalent immobilization procedures do not effectively control the orientation of the biomolecule; therefore, many active sites of the immobile biomolecule become inaccessible after immobilization. In contrast, the immobilization of biomolecules using Ab–Protein A/G interaction or DNA hybridization can preserve the biomolecule functionality by the orientated immobilization and increased stability. Protein A or G specifically binds the F_c region of the Ab, and this procedure

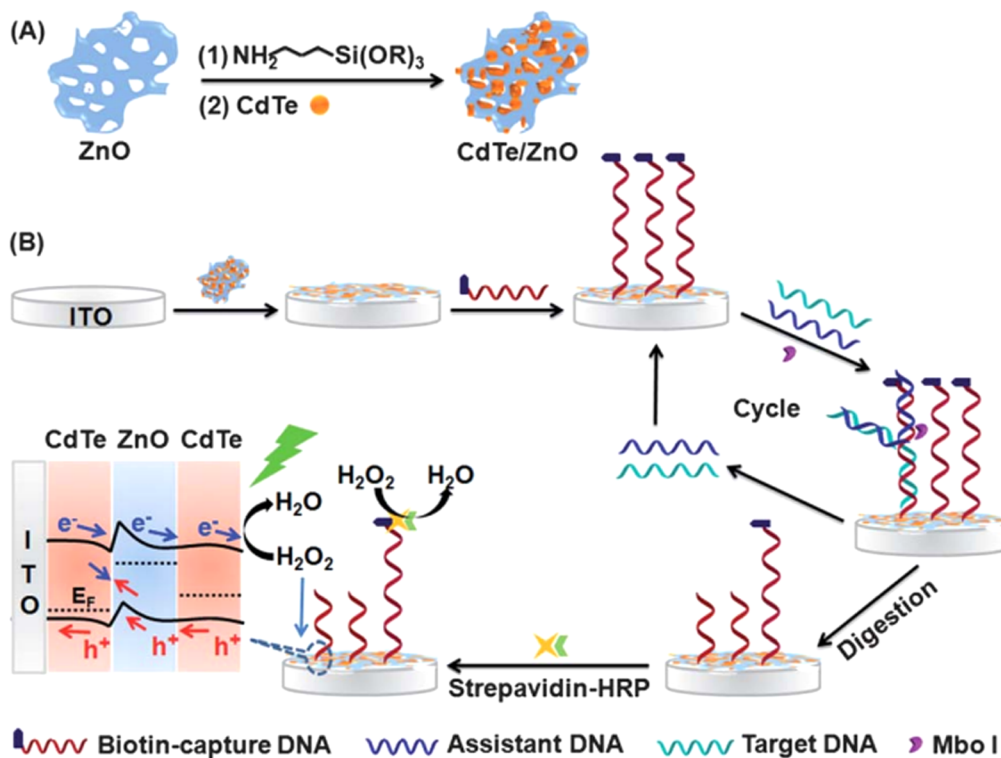


Figure 21. Schematic of a biosensor for the detection of DNA assisted by concurrent horseradish peroxidase (HRP)-mediated electrochemical reduction reaction of H_2O_2 . Reproduced with permission from ref 287. Copyright 2014 Royal Society of Chemistry.

provides highly improved antigen detection of *Salmonella* over GLD cross-linking.²⁹¹ Nevertheless, GLD or carbodiimide activation has been proven applicable for the immobilization of GOx and other enzymes. This Review focuses on enzymes and Abs in biosensing and diagnostic platforms; however, aptamers can be potential molecular recognition elements because they are relatively inexpensive and more stable than Abs.²⁹² Aptamers are oligonucleotides, which selectively bind to the targeted proteins with high affinity. Nevertheless, Ab still remains as the bioanalytical workhorses due to its exceptional specificity toward its binding partner regardless of the high cost and short shelf life.

The incorporation of nanomaterials into biosensing interfaces offers improved stability, minimal surface fouling, higher sensitivity, cost-effectiveness, and capability for multiplex analysis. Popular examples include Au NPs, CNTs, nanowires, and graphene due to their beneficial contribution in biosensors and diagnostic platforms. Electrodes modified with metal NPs with ultrahigh surface areas can be used to enhance the amount of immobilized biomolecules in the construction of sensors to ultimately lower the detection limit for target analytes. All oxide surfaces can be functionalized with APTES for subsequent bioconjugation. APTES is also useful for the preparation of CNT and graphene suspensions, which can be drop-casted on any surface. Another elegant approach is the preparation of uniform thin coatings of MWCNTs by electrophoretic deposition of MWCNT suspension on APTES-functionalized silicon.²⁹³ It is of importance to design an affinity tag for the reversible binding of biomolecules with high density on carbon-based substrates such as graphene or CNTs. Therefore, such biosensors can be effectively regenerated and reused after the loss of enzyme activity by washing the electrode with a pertinent buffer and providing the activated enzyme. New nanomaterials and nanostructures have been explored for a plethora of analytical

applications. However, more attention must focus on the quantum size effect, surface effect, macro-quantum tunnel effect, and small size effect that are apparent in case of nanomaterials.

Although specific binding between streptavidin has been exploited in various analytical platforms, the binding event is irreversible. Therefore, the biomolecular immobilized platform based on streptavidin–biotin interactions cannot be reused, which leads to higher analysis cost. Of interest is desthiobiotin,²⁹⁴ a biotin analogue with a lower binding constant for streptavidin as compared to biotin. The biomolecular multilayer formed on the surface can be washed away by using biotin solution to pave the way for repeated uses of the APTES-avidin modified surface.

6. CONCLUSIONS

In brief, APTES offers several advantages in analytical applications: (a) easy-to-prepare, (b) stable monolayers, and (c) uniform immobilization surface. APTES also protects the biomolecules from the sensor surface, preventing possible denaturation and nonspecific adsorption. Various surface coatings including Au NPs, polymers (poly(vinyl alcohol), PEG, polyacrylamide, etc.), and biopolymers (dextran, CS, and protein aggregates) help to reduce nonspecific adsorption. Moreover, it is desirable to incorporate multiple functions, that is, a functional group for biomolecule immobilization and an antibiofouling layer for reduced nonspecific protein adsorption in a single copolymer. APTES can be modified for its incorporation in such smart materials, and this is a subject of future endeavors. Improvement of detection limits and the ability to regenerate the sensor are two key prerequisites for the successful deployment of biosensors and diagnostic platforms for diversified applications in analytical, bioanalytical, and clinical chemistry. There is a wide variety of cross-linkers available commercially, which can bind the free amino groups on APTES-

functionalized substrates to the various functional groups, such as carboxyl, amino, sulfhydryl, hydroxyl, and carbonyl, present on the biomolecule. Therefore, in the coming years, we will witness more rapid, efficient, robust, and highly simplified Ab immobilization chemistries, which will significantly improve the bioanalytical performance of biosensors and diagnostics apart from decreasing the cost of analysis.

The APTES immobilization technology is anticipated to be widely applied in electrochemical, SPR-based and electrochemical-QCM-based sensors, and various IA formats, such as those based on smartphone-based detection. Last, it would have potential utility in the development of a highly integrated multiparameter assay, where biomolecules such as Abs, proteins, and aptamers could be coimmobilized into the microfluidic channel for more sophisticated multianalyte assays using multiple detectors, for example, SPR, fluorescence, and electrochemical detectors. We anticipate substantial innovation in this area in the “not-too-long distant” future. Last, the biomolecule-bound APTES-functionalized surfaces would be appropriate for in vivo applications based on their high stability, less biofouling, and leach-proof binding of biomolecules. However, this needs to be investigated in more depth in animal models before they can be used for in vivo applications.

AUTHOR INFORMATION

Corresponding Author

*Tel.: +49 761 2037252. Fax: +49 761 20373299. E-mail: sandeep.kumar.vashist@hsg-imit.de.

Notes

The authors declare no competing financial interest.

Biographies



Sandeep K. Vashist is the Head of Immunodiagnostics at HSG-IMIT, Freiburg, and Laboratory for MEMS applications, Department of Microsystems Engineering (IMTEK), University of Freiburg, Germany. He was the Bioanalytical Scientist at Bristol-Myers Squibb Co., Dublin, Ireland (2006–2009), and the Team Leader at NUS Nanoscience and Nanotechnology Institute, Singapore (2009–2012), after completing his Ph.D. from Central Scientific Instruments Organization, India, in 2006. His research outputs include many successful technology transfers, several in vitro diagnostic products and smart point-of-care devices, six patents, over 80 journal publications, and numerous conference publications and book chapters. He has constantly received highly prestigious fellowships and awards for scientific research excellence and innovation. He is the Executive Editor and Editorial Board member for several reputed journals. His research interests include in vitro diagnostics, smartphone-based POC devices and mobile healthcare, and nanotechnology.



Edmond Lam received a B.S. degree in chemistry from the University of British Columbia (2001) and a Ph.D. degree in inorganic chemistry from the University of Toronto (2007) under the supervision of David H. Farrar. His research interests include catalysis, nanotechnology, and biomass conversion technologies. He is currently a Research Officer with the National Research Council Canada in Montreal, Quebec, Canada.



Sabahudin Hrapovic received a B.Eng. in chemical engineering from the University of Sarajevo (1988) and a M.Sc. degree in surface electrochemistry from the University of Sherbrooke (1999) under the supervision of Gregory Jerkiewicz. His research interests include electrochemistry and surface microscopy. He is currently a Technical Officer with the National Research Council Canada in Montreal, Quebec, Canada.



Keith B. Male received a B.Sc. in biochemistry from Carleton University (1980) and a M.Sc. degree in biology (enzymology) from Carleton University (1982) under the supervision of Kenneth Storey. His research interests include enzymology, nanotechnology, and biosensors.

He is currently a Technical Officer and Team Leader with the National Research Council Canada in Montreal, Quebec, Canada.



John H. T. Luong received his Ph.D. in Chemical Engineering at McGill in Montreal, Canada, in 1979. He is a Walton Fellow (Science Foundation of Ireland, SFI), associated with the Department of Chemistry at University College Cork (UCC) and Innovative Chromatography Group, Irish Separation Science Cluster (ISSC), Ireland. He was professor and head of the Biomedical Engineering Division of Nanyang Technological University, Singapore, and visiting professor of National University of Singapore. He is also a visiting professor at Zhengzhou University of Henan, China (high end foreign expert, Chinese recruitment program). With over 290 research papers and 10 patents, he has received several awards for his contribution to various research areas such as nanobiotechnology, biosensor technology, separation science, and biochemical engineering. He has served as an Editorial Member and Guest Editor of several journals.

ACKNOWLEDGMENTS

We acknowledge the financial support received from Bristol-Myers Squibb (BMS), Syracuse, NY, and Industrial Development Agency, Ireland, under the Centre for Bioanalytical Sciences (CBAS) project code 116294.

ABBREVIATIONS

Abs	antibodies	CNT	carbon nanotubes
AFOB	all-fiber optofluidics-based platform	COC	cyclic olefin copolymer
AFM	atomic force microscopy	CPG	controlled pore glass
AFP	α -fetoprotein	CRP	C-reactive protein
ALP	alkaline phosphatase	CS	chitosan
APTES	3-aminopropyltriethoxysilane	CV	cyclic voltammetry
ARXPS	angle-resolved X-ray photoelectron spectroscopy	CVD	chemical vapor deposition
BA	<i>Bacillus anthracis</i>	cTNT	cardiac troponin-T
BDD	boron-doped diamond	DCC	<i>N,N'</i> -dicyclohexylcarbodiimide
BMP2	bone morphogenetic protein 2	DET	direct electron transfer
BPA	bisphenol A	DHD	D-fructose dehydrogenase
BSA	bovine serum albumin	DMSO	dimethyl sulfoxide
BST	barium strontium titanate	DNA	deoxyribonucleic acid
BVA	4,4-bis(4-hydroxyphenyl) valeric acid	DPV	differential pulse voltammetry
CA125	carbohydrate antigen 125	EDC	1-ethyl-3-[3-(dimethylamino)propyl]-carbodiimide
CBP	choline binding protein	EIS	electrochemical impedance spectroscopy
CEA	carcinoembryonic antigen	ELISA	enzyme-linked immunosorbent assays
CiELISA	competitive enzyme-linked immunosorbent assay	FABP	fatty acid binding protein
CK-MB	creatinine kinase MB	FBP	Fc-binding protein
CMOS	complementary metal–oxide semiconductor	FETs	field effect transistors
CNBr	cyanogen bromide	FITC	fluorescein isothiocyanate
		FTIR	Fourier transform infrared spectroscopy
		GA	gibberellic acid
		GCE	glassy carbon electrode
		GLD	glutaraldehyde
		GMA	glycidyl methacrylate
		GMR	guided-mode resonance
		GNPs	graphene nanoplatelets
		GOPTS	(3-glycidopropyl)-triethoxysilane
		GOx	glucose oxidase
		HA	human albumin
		HbsAbs	hepatitis B surface antibodies
		HBsAg	hepatitis B surface antigen
		HBV	hepatitis B virus
		hCG	human chorionic gonadotropin
		HEPES	4-(2-hydroxyethyl)-1-piperazineethanesulfonic acid
		HFA	human fetuin A
		HOPG	highly oriented pyrolytic graphite
		H-PDLC	holographic polymer-dispersed liquid crystal
		HPLC	high performance liquid chromatography
		HRP	horseradish peroxidase
		HSA	human serum albumin
		IA	immunoassay
		ICAM	intracellular adhesion molecule
		IDT	interdigitated transducer
		IgG	immunoglobulin G
		IL	interleukin
		IMS	immunosensors
		ITO	indium tin oxide
		JEV	Japanese encephalitis virus
		LBL	layer-by-layer
		LCN2	human lipocalin-2
		LOD	limit of detection
		LSPR	localized surface plasmon resonance
		MA	methamphetamine
		MCN-ICP-MS	microcentric nebulizer inductively coupled plasma mass spectrometry
		MEA	microelectrode array
		MEG	multilayer epitaxial graphene
		MWCNT	multiwalled carbon nanotubes

mPDGs	magnetic poly(divinylbenzene- <i>co</i> -glycidyl methacrylate)
MTMOS	methyltrimethoxysilane
MSN	mesoporous silica nanoparticles
MTP	microtiter plate
MYO	myoglobin
NDV	Newcastle disease virus
NHS	<i>N</i> -hydroxysuccinimide
NMR	nuclear magnetic resonance
NPs	nanoparticles
OGC	optical grating coupler
PAEPEMC	piezoelectric excited millimeter-sized cantilever
PAP	<i>p</i> -aminophenol
PAPP	<i>p</i> -aminophenyl phosphate
PDDA	poly(diallyldimethylammonium) chloride
PDMS	polydimethylsiloxane
PDITC	1,4-phenylene diisothiocyanate
PECVD	plasma enhanced-chemical vapor deposition
PEG	polyethylene glycol
PFCP	perfluorocarbon polymer
PGM	personal glucose meter
PMMA	poly(methyl methacrylate)
PNA	peptide nucleic acid
POC	point-of-care
POx	putrescine oxidase
ProGRP	progastrin releasing peptide
PrP	prion proteins
PS	polystyrene
PSA	prostate specific antigen
PZT	lead zirconium titanate
QCM	quartz crystal microbalance
QD	quantum dot
RI	refractive index
S-4FB	succinimidyl 4-formylbenzoate
SAM	self-assembled monolayers
SAW	surface acoustic wave
SCE	saturated calomel electrode
SEB	<i>Staphylococcus</i> enterotoxin B
SELS	surface enhanced light scattering
S-HyNic	succinimidyl 6-hydrazinonicotinamide acetone hydrazine
SiNW	silicon nanowire
SOI	silicon-on-insulator
SPR	surface plasmon resonance
SulfoNHS	sulfo- <i>N</i> -hydroxysuccinimide
SWASV	square wave anodic stripping voltammetry
TEOS	tetraethoxysilane (or tetraethyl orthosilicate)
TMB	3,3',5,5'-tetramethylbenzidine
ToF-SIMS	time-of-flight secondary ion mass spectrometry
Trp	tryptophan
TrI	troponin I
VEGF	vascular endothelial growth factors
XPS	X-ray photoelectron spectroscopy

REFERENCES

- (1) Sagiv, J. *J. Am. Chem. Soc.* **1980**, *102*, 92.
- (2) Vansant, E. F.; Van Der Voort, P.; Vrancken, K. C. *Characterization and Chemical Modification of the Silica Surface*; Elsevier Science B.V.: Amsterdam, 1995.
- (3) White, L. D.; Tripp, C. P. *J. Colloid Interface Sci.* **2000**, *227*, 237.
- (4) Blitz, J. P.; Murthy, R. S. S.; Leyden, D. E. *J. Am. Chem. Soc.* **1987**, *109*, 7141.
- (5) Weetall, H. H. *Appl. Biochem. Biotechnol.* **1993**, *41*, 157.
- (6) Howarter, J. A.; Youngblood, J. P. *Langmuir* **2006**, *22*, 11142.
- (7) Landoulsi, J.; Genet, M. J.; Karat, K. E.; Richard, C.; Pulvin, S.; Rouxhet, P. G. *Silanization with APTES for Controlling the Interactions Between Stainless Steel and Biocomponents: Reality vs Expectation*. In *Biomaterials-Physics and Chemistry*; Pignatello, R., Ed.; InTech: Rijeka, 2011; pp 99–126.
- (8) Weng, Y. J.; Hou, R.; Xie, D.; Wang, J.; Huang, N. *Key Eng. Mater.* **2007**, *330*, 865.
- (9) Yamaura, M.; Camilo, R.; Sampaio, L.; Macedo, M.; Nakamura, M.; Toma, H. *J. Magn. Magn. Mater.* **2004**, *279*, 210.
- (10) Asenath Smith, E.; Chen, W. *Langmuir* **2008**, *24*, 12405.
- (11) Gandhiraman, R. P.; Volcke, C.; Gubala, V.; Doyle, C.; Basabe-Desmonts, L.; Dotzler, C.; Toney, M. F.; Iacono, M.; Nooney, R. I.; Daniels, S. *J. Mater. Chem.* **2010**, *20*, 4116.
- (12) Rozlosnik, N.; Gerstenberg, M. C.; Larsen, N. B. *Langmuir* **2003**, *19*, 1182.
- (13) Fadeev, A. Y.; Helmy, R.; Marcinko, S. *Langmuir* **2002**, *18*, 7521.
- (14) Mateo, C.; Fernández-Lorente, G.; Abian, O.; Fernández-Lafuente, R.; Guisán, J. M. *Biomacromolecules* **2000**, *1*, 739.
- (15) Vandenberg, E. T.; Bertilsson, L.; Liedberg, B.; Uvdal, K.; Erlandsson, R.; Elwing, H.; Lundström, I. *J. Colloid Interface Sci.* **1991**, *147*, 103.
- (16) Torabi, F.; Mobini Far, H. R.; Danielsson, B.; Khayyami, M. *Biosens. Bioelectron.* **2007**, *22*, 1218.
- (17) Blagoi, G.; Keller, S.; Johansson, A.; Boisen, A.; Dufva, M. *Appl. Surf. Sci.* **2008**, *255*, 2896.
- (18) Varshney, M.; Waggoner, P. S.; Tan, C. P.; Aubin, K.; Montagna, R. A.; Craighead, H. G. *Anal. Chem.* **2008**, *80*, 2141.
- (19) Hidemitsu, S.; Sato, R.; Kuroiwa, S.; Osaka, T. *Biosens. Bioelectron.* **2011**, *26*, 2419.
- (20) Gupta, S.; Huda, S.; Kilpatrick, P. K.; Velev, O. D. *Anal. Chem.* **2007**, *79*, 3810.
- (21) Ma, L.; Wang, C.; Hong, Y.; Zhang, M.; Su, M. *Anal. Chem.* **2010**, *82*, 1186.
- (22) Killian, M. S.; Krebs, H. M.; Schmuki, P. *Langmuir* **2011**, *27*, 7510.
- (23) Huang, Y. F.; Wang, Y. F.; Yan, X. P. *Environ. Sci. Technol.* **2010**, *44*, 7908.
- (24) van der Maaden, K.; Sliedregt, K.; Kros, A.; Jiskoot, W.; Bouwstra, J. *Langmuir* **2012**, *28*, 3403.
- (25) Li, W.; Yuan, R.; Chai, Y. *J. Phys. Chem. C* **2010**, *114*, 21397.
- (26) Yuan, L.; Hua, X.; Wu, Y.; Pan, X.; Liu, S. *Anal. Chem.* **2011**, *83*, 6800.
- (27) Yuan, P.; Southon, P. D.; Liu, Z.; Green, M. E. R.; Hook, J. M.; Antill, S. J.; Kepert, C. J. *J. Phys. Chem. C* **2008**, *112*, 15742.
- (28) Yang, Y. J.; Tao, X.; Hou, Q.; Chen, J. F. *Acta Biomater.* **2009**, *5*, 3488.
- (29) Xue, A.; Zhou, S.; Zhao, Y.; Lu, X.; Han, P. *J. Hazard. Mater.* **2011**, *194*, 7.
- (30) Sanchez-Vaquero, V.; Satriano, C.; Tejera-Sanchez, N.; Gonzalez Mendez, L.; Garcia Ruiz, J. P.; Manso Silvan, M. *Biointerphases* **2010**, *5*, 23.
- (31) Luo, K.; Zhou, S.; Wu, L.; Gu, G. *Langmuir* **2008**, *24*, 11497.
- (32) Su, F.; Lu, C.; Chen, H. S. *Langmuir* **2011**, *27*, 8090.
- (33) Lee, W. L.; Thompson, H. G. *Can. J. Chem.* **1996**, *74*, 707.
- (34) Hu, P.; Huang, C. Z.; Li, Y. F.; Ling, J.; Liu, Y. L.; Fei, L. R.; Xie, J. P. *Anal. Chem.* **2008**, *80*, 1819.
- (35) Skottrup, P. D.; Hansen, M. F.; Lange, J. M.; Deryabina, M.; Svendsen, W. E.; Jakobsen, M. H.; Dufva, M. *Acta Biomater.* **2010**, *6*, 3936.
- (36) Yagiuda, K.; Hemmi, A.; Ito, S.; Asano, Y.; Fushinuki, Y.; Chen, C.-Y.; Karube, I. *Biosens. Bioelectron.* **1996**, *11*, 703.
- (37) Li, J.; Xiao, L. T.; Zeng, G. M.; Huang, G. H.; Shen, G. L.; Yu, R. Q. *J. Agric. Food Chem.* **2005**, *53*, 1348.
- (38) Kim, N.; Park, I. S.; Kim, W. Y. *Sens. Actuators, B: Chem.* **2007**, *121*, 606.
- (39) Shiku, H.; Uchida, I.; Matsue, T. *Langmuir* **1997**, *13*, 7239.
- (40) Balasundaram, G.; Sato, M.; Webster, T. J. *Biomaterials* **2006**, *27*, 2798.
- (41) Wilson, M. S. *Anal. Chem.* **2005**, *77*, 1496.

- (42) Faure, A. C.; Hoffmann, C.; Bazzi, R.; Goubard, F.; Pauthe, E.; Marquette, C. A.; Blum, L. J.; Perriat, P.; Roux, S.; Tillement, O. *ACS Nano* **2008**, *2*, 2273.
- (43) Dong, H.; Li, C. M.; Zhou, Q.; Sun, J. B.; Miao, J. M. *Biosens. Bioelectron.* **2006**, *22*, 621.
- (44) Lee, H. J.; Namkoong, K.; Cho, E. C.; Ko, C.; Park, J. C.; Lee, S. S. *Biosens. Bioelectron.* **2009**, *24*, 3120.
- (45) Qi, C.; Feng, J.; Wang, Z.-H.; Meng, Y.-H.; Yan, X.-Y.; Jin, G. *Chin. J. Biotechnol.* **2006**, *22*, 856.
- (46) Chua, J. H.; Chee, R.-E.; Agarwal, A.; Wong, S. M.; Zhang, G.-J. *Anal. Chem.* **2009**, *81*, 6266.
- (47) Chen, B.; Peng, H.; Zheng, F.; Hu, B.; He, M.; Zhao, W.; Pang, D. *J. Anal. At. Spectrom.* **2010**, *25*, 1674.
- (48) Fang, X.; Tan, O. K.; Tse, M. S.; Ooi, E. E. *Biosens. Bioelectron.* **2010**, *25*, 1137.
- (49) Gan, S.; Yang, P.; Yang, W. *Biomacromolecules* **2009**, *10*, 1238.
- (50) Helali, S.; Abdelghani, A.; Hafnia, I.; Martelet, C.; Prodromidis, M. I.; Albanis, T.; Jaffrezic-Renault, N. *Mater. Sci. Eng., C* **2008**, *28*, 826.
- (51) Raj, J.; Herzog, G.; Manning, M.; Volcke, C.; MacCraith, B. D.; Ballantyne, S.; Thompson, M.; Arrigan, D. W. *Biosens. Bioelectron.* **2009**, *24*, 2654.
- (52) Charles, P. T.; Rangasammy, J. G.; Andersona, G. P.; Romanoskib, T. C.; Kusterbecka, A. W. *Anal. Chim. Acta* **2004**, *525*, 199.
- (53) Behringer, K. D.; Blümel, J. *J. Liq. Chromatogr. Relat. Technol.* **1996**, *19*, 2753.
- (54) Liu, Y.; Li, Y.; Li, X. M.; He, T. *Langmuir* **2013**, *29*, 15275.
- (55) Song, Y.-Y.; Hildebrand, H.; Schmuki, P. *Surf. Sci.* **2010**, *604*, 346.
- (56) Hernandez, O. *3-Aminopropyltriethoxysilane (APTES)*; UNEP Publications: Arona, Italy, 2003.
- (57) Herder, P.; Vägberg, L.; Stenius, P. *Colloids Surf.* **1989**, *34*, 117.
- (58) Iler, R. K. *The Chemistry of Silica: Solubility, Polymerization, Colloid and Surface Properties, and Biochemistry*; Wiley Interscience: New York, 1979.
- (59) Ishida, H. *Polym. Compos.* **1984**, *5*, 101.
- (60) Dixit, C. K.; Vashist, S. K.; MacCraith, B. D.; O'Kennedy, R. *Nat. Protoc.* **2011**, *6*, 439.
- (61) Vashist, S. K. *Biosens. Bioelectron.* **2013**, *40*, 297.
- (62) Dixit, C. K.; Vashist, S. K.; MacCraith, B. D.; O'Kennedy, R. *Analyst* **2011**, *136*, 1406.
- (63) Vashist, S. K.; Dixit, C. K.; MacCraith, B. D.; O'Kennedy, R. *Analyst* **2011**, *136*, 4431.
- (64) Avseenko, N. V.; Morozova, T. Y.; Ataullakhanov, F. I.; Morozov, V. N. *Anal. Chem.* **2002**, *74*, 927.
- (65) Aran, K.; Sasso, L. A.; Kamdar, N.; Zahn, J. D. *Lab Chip* **2010**, *10*, 548.
- (66) Cheng, Y.; Xiong, P.; Yun, C. S.; Strouse, G. F.; Zheng, J. P.; Yang, R. S.; Wang, Z. L. *Nano Lett.* **2008**, *8*, 4179.
- (67) Park, J. H.; Sun, Y.; Goldman, Y. E.; Composto, R. J. *Langmuir* **2010**, *26*, 10961.
- (68) Chaijareenont, P.; Takahashi, H.; Nishiyama, N.; Arksornnukit, M. *Dent. Mater. J.* **2012**, *31*, 610.
- (69) Bruce, I. J.; Sen, T. *Langmuir* **2005**, *21*, 7029.
- (70) Roque, A. C.; Bicho, A.; Batalha, I. L.; Cardoso, A. S.; Hussain, A. J. *Biotechnol.* **2009**, *144*, 313.
- (71) Roy, S.; Dixit, C. K.; Woolley, R.; MacCraith, B. D.; O'Kennedy, R.; McDonagh, C. *Langmuir* **2010**, *26*, 18125.
- (72) Roy, S.; Dixit, C. K.; Woolley, R.; O'Kennedy, R.; McDonagh, C. *Langmuir* **2011**, *27*, 10421.
- (73) Nguyen, Q. X.; Belgard, T. G.; Taylor, J. J.; Murthy, V. S.; Halas, N. J.; Wong, M. S. *Chem. Mater.* **2012**, *24*, 1426.
- (74) Engelhardt, H.; Orth, P. *J. Liq. Chromatogr.* **1987**, *10*, 1999.
- (75) Zhu, M.; Lerum, M. Z.; Chen, W. *Langmuir* **2011**, *28*, 416.
- (76) Wang, W.; Vaughn, M. W. *Scanning* **2008**, *30*, 65.
- (77) Jönsson, U.; Olofsson, G.; Malmqvist, M.; Rönnberg, I. *Thin Solid Films* **1985**, *124*, 117.
- (78) Singh, S.; Sharma, S. N.; Govind; Shivaprasad, S. M.; Lal, M.; Khan, M. A. *J. Mater. Sci.: Mater. Med.* **2009**, *20*, S181.
- (79) Lyubchenko, Y.; Shlyakhtenko, L.; Harrington, R.; Oden, P.; Lindsay, S. *Proc. Natl. Acad. Sci. U.S.A.* **1993**, *90*, 2137.
- (80) Hong, Z.; Chasan, B.; Bansil, R.; Turner, B. S.; Bhaskar, K. R.; Afshal, N. H. *Biomacromolecules* **2005**, *6*, 3458.
- (81) Krumdieck, S. P.; Raj, R. *Chem. Vap. Deposition* **2001**, *7*, 85.
- (82) Krumdieck, S. P.; Sbaizer, O.; Bullert, A.; Raj, R. *Surf. Coat. Technol.* **2003**, *167*, 226.
- (83) Krumdieck, S. *J. Aust. Ceram. Soc.* **2012**, *48*, 69.
- (84) Metwalli, E.; Haines, D.; Becker, O.; Conzone, S.; Pantano, C. G. *J. Colloid Interface Sci.* **2006**, *298*, 825.
- (85) Price, J.; Wu, S.-Y. *Plasma enhanced CVD*. US 4692343, September 8, 1987.
- (86) Gandhiraman, R. P.; Gubala, V.; O'Mahony, C. C.; Cummins, T.; Raj, J.; Eltayeb, A.; Doyle, C.; James, B.; Daniels, S.; Williams, D. E. *Vacuum* **2012**, *86*, 547.
- (87) Culler, S.; Ishida, H.; Koenig, J. *J. Colloid Interface Sci.* **1986**, *109*, 1.
- (88) Naviroj, S.; Culler, S. R.; Koenig, J. L.; Ishida, H. *J. Colloid Interface Sci.* **1984**, *97*, 308.
- (89) Chiang, C.-H.; Liu, N.-I.; Koenig, J. L. *J. Colloid Interface Sci.* **1982**, *86*, 26.
- (90) Luzinov, I.; Julthongpiput, D.; Liebmann-Vinson, A.; Cregger, T.; Foster, M. D.; Tsukruk, V. V. *Langmuir* **2000**, *16*, 504.
- (91) Kim, J.; Seidler, P.; Wan, L. S.; Fill, C. *J. Colloid Interface Sci.* **2009**, *329*, 114.
- (92) Jeyachandran, Y. L.; Mielczarski, J. A.; Mielczarski, E.; Rai, B. J. *Colloid Interface Sci.* **2010**, *341*, 136.
- (93) Ouerghi, O.; Touhami, A.; Othmane, A.; Ouada, H. B.; Martelet, C.; Fretigny, C.; Jaffrezic-Renault, N. *Biomol. Eng.* **2002**, *19*, 183.
- (94) Lu, B.; Smyth, M. R.; O'Kennedy, R. *Analyst* **1996**, *121*, 29R.
- (95) Chen, S.; Liu, L.; Zhou, J.; Jiang, S. *Langmuir* **2003**, *19*, 2859.
- (96) Paynter, R.; Ratner, B.; Horbett, T.; Thomas, H. *J. Colloid Interface Sci.* **1984**, *101*, 233.
- (97) Scofield, J. *J. Electron Spectrosc.* **1976**, *8*, 129.
- (98) Raiteri, R.; Grattarola, M.; Butt, H.-J.; Skládal, P. *Sens. Actuators, B: Chem.* **2001**, *79*, 115.
- (99) Dubey, M.; Emoto, K.; Takahashi, H.; Castner, D. G.; Grainger, D. W. *Adv. Funct. Mater.* **2009**, *19*, 3046.
- (100) Samuel, N. T.; Wagner, M.; Dornfeld, K.; Castner, D. G. *Surf. Sci. Spectra* **2001**, *8*, 163.
- (101) Wang, Z. H.; Jin, G. *J. Immunol. Methods* **2004**, *285*, 237.
- (102) Sandoval, J. E.; Pesek, J. J. *Anal. Chem.* **1989**, *61*, 2067.
- (103) Ashu-Arrah, B. A.; Glennon, J. D.; Albert, K. *J. Chromatogr., A* **2012**, *1236*, 42.
- (104) Betancor, L.; López-Gallego, F.; Hidalgo, A.; Alonso-Morales, N.; Mateo, G. D.-O. C.; Fernández-Lafuente, R.; Guisán, J. M. *Enzyme Microb. Technol.* **2006**, *39*, 877.
- (105) Vashist, S. K. *Diagnostics* **2012**, *2*, 23.
- (106) Wagner, P.; Hegner, M.; Kernen, P.; Zaugg, F.; Semenza, G. *Biophys. J.* **1996**, *70*, 2052.
- (107) Byeon, J. Y.; Limpoco, F. T.; Bailey, R. C. *Langmuir* **2010**, *26*, 15430.
- (108) Zaitsev, V. N.; Colomiets, L. I.; Elskaya, A. V.; Skopenko, V. V.; Evans, J. *J. Anal. Chim. Acta* **1991**, *252*, 1.
- (109) Yoshioka, M.; Mukai, Y.; Matsui, T.; Udagawa, A.; Funakubo, H. *J. Chromatogr.* **1991**, *566*, 361.
- (110) Tatsuma, T.; Okawa, Y.; Watanabe, T. *Anal. Chem.* **1989**, *61*, 2352.
- (111) Zheng, D.; Vashist, S. K.; Al-Rubeaan, K.; Luong, J. H. T.; Sheu, F. S. *Analyst* **2012**, *137*, 3800.
- (112) Zheng, D.; Vashist, S.; Dykas, M.; Saha, S.; Al-Rubeaan, K.; Lam, E.; Luong, J. H. T.; Sheu, F.-S. *Materials* **2013**, *6*, 1011.
- (113) Björck, I.; Petersson, B. Å.; Sjöquist, J. *Eur. J. Biochem.* **1972**, *29*, 579.
- (114) Sjöquist, J.; Meloun, B.; Hjelm, H. *Eur. J. Biochem.* **1972**, *29*, 572.
- (115) Akerström, B.; Björck, I. *J. Biol. Chem.* **1986**, *261*, 10240.
- (116) Akerström, B.; Brodin, T.; Reis, K.; Björk, L. *J. Immunol.* **1985**, *135*, 2589.
- (117) Sikkema, W. D. *Am. Biotechnol. Lab.* **1989**, *7*, 42.
- (118) Yang, L.; Biswas, M.; Chen, P. *Biophys. J.* **2003**, *84*, 509.
- (119) Kastern, W.; Sjöbring, U.; Björck, I. *J. Biol. Chem.* **1992**, *267*, 12820.

- (120) Nilson, B. H.; Lögdberg, L.; Kastern, W.; Björck, L.; Åkerström, B. *J. Immunol. Methods* **1993**, *164*, 33.
- (121) Arnau, J.; Lauritzen, C.; Petersen, G. E.; Pedersen, J. *Protein Expression Purif.* **2006**, *48*, 1.
- (122) Nogi, T.; Sangawa, T.; Tabata, S.; Nagae, M.; Tamura-Kawakami, K.; Beppu, A.; Hattori, M.; Yasui, N.; Takagi, J. *Protein Sci.* **2008**, *17*, 2120.
- (123) Darain, F.; Ban, C.; Shim, Y. B. *Biosens. Bioelectron.* **2004**, *20*, 857.
- (124) Jones, C. J.; Stoddart, R. W. *Histochem. J.* **1986**, *18*, 371.
- (125) Hopp, T. P.; Prickett, K. S.; Price, V. L.; Libby, R. T.; March, C. J.; Pat Cerretti, D.; Urdal, D. L.; Conlon, P. J. *Nat. Biotechnol.* **1988**, *6*, 1204.
- (126) Nakajima, H.; Brindle, P. K.; Handa, M.; Ihle, J. N. *EMBO J.* **2001**, *20*, 6836.
- (127) Zhang, L.; Liu, Y.; Chen, T. *Microchim. Acta* **2009**, *164*, 161.
- (128) Bain, C. D.; Troughton, E. B.; Tao, Y. T.; Evall, J.; Whitesides, G. M.; Nuzzo, R. G. *J. Am. Chem. Soc.* **1989**, *111*, 321.
- (129) Bhatia, S. K.; Shriver-Lake, L. C.; Prior, K. J.; Georger, J. H.; Calvert, J. M.; Bredehorst, R.; Ligler, F. S. *Anal. Biochem.* **1989**, *178*, 408.
- (130) Rao, S. V.; Anderson, K. W.; Bachas, L. G. *Microchim. Acta* **1998**, *128*, 127.
- (131) Brogan, K. L.; Wolfe, K. N.; Jones, P. A.; Schoenfisch, M. H. *Anal. Chim. Acta* **2003**, *496*, 73.
- (132) Morfill, J.; Blank, K.; Zahnd, C.; Luginbuhl, B.; Kuhner, F.; Gottschalk, K. E.; Pluckthun, A.; Gaub, H. E. *Biophys. J.* **2007**, *93*, 3583.
- (133) Kipriyanov, S. M.; Little, M. *Anal. Biochem.* **1997**, *244*, 189.
- (134) Saerens, D.; Huang, L.; Bonroy, K.; Muyldermans, S. *Sensors* **2008**, *8*, 4669.
- (135) Nielsen, P. E.; Egholm, M.; Berg, R. H.; Buchardt, O. *Science* **1991**, *254*, 1497.
- (136) Egholm, M.; Buchardt, O.; Christensen, L.; Behrens, C.; Freier, S. M.; Driver, D. A.; Berg, R. H.; Kim, S. K.; Norden, B.; Nielsen, P. E. *Nature* **1993**, *365*, 566.
- (137) Sheng, H.; Ye, B. C. *Appl. Biochem. Biotechnol.* **2009**, *152*, 54.
- (138) Silva, T. A.; Ferreira, L. F.; Souza, L. M.; Goulart, L. R.; Madurro, J. M.; Brito-Madurro, A. G. *Mater. Sci. Eng., C* **2009**, *29*, 539.
- (139) Ray, A.; Norden, B. *FASEB J.* **2000**, *14*, 1041.
- (140) Höök, F.; Ray, A.; Nordén, B.; Kasemo, B. *Langmuir* **2001**, *17*, 8305.
- (141) Masuko, M. *Nucleic Acids Symp. Ser.* **2003**, *3*, 145.
- (142) Zhong, M.; Fang, J.; Wei, Y. *Bioconjugate Chem.* **2010**, *21*, 1177.
- (143) Rabe, M.; Verdes, D.; Seeger, S. *Adv. Colloid Interface Sci.* **2011**, *162*, 87.
- (144) Vogler, E. A. *Biomaterials* **2012**, *33*, 1201.
- (145) Tsapikouni, T. S.; Missirlis, Y. F. *Mater. Sci. Eng., B* **2008**, *152*, 2.
- (146) Bremer, M. G.; Duval, J.; Norde, W.; Lyklema, J. *Colloids Surf., A* **2004**, *250*, 29.
- (147) van der Veen, M.; Stuart, M. C.; Norde, W. *Colloids Surf., B* **2007**, *54*, 136.
- (148) Norde, W.; Lyklema, J. *Adv. Colloid Interface Sci.* **2012**, *179–182*, 5.
- (149) Denis, F. A.; Hanarp, P.; Sutherland, D. S.; Gold, J.; Mustin, C.; Rouxhet, P. G.; Dufrêne, Y. F. *Langmuir* **2002**, *18*, 819.
- (150) Zhou, T.; Llizo, A.; Wang, C.; Xu, G.; Yang, Y. *Nanoscale* **2013**, *5*, 8288.
- (151) Kim, T. H.; Kim, M.; Eltohamy, M.; Yun, Y. R.; Jang, J. H.; Kim, H. W. *J. Biomed. Mater. Res., Part A* **2013**, *101*, 1651.
- (152) Weiss, S. A.; Jeuken, L. J. *Biochem. Soc.* **2009**, *37*, 707.
- (153) Lee, K. B.; Park, S. J.; Mirkin, C. A.; Smith, J. C.; Mrksich, M. *Science* **2002**, *295*, 1702.
- (154) Awsiuk, K.; Bernasik, A.; Kitsara, M.; Budkowski, A.; Rysz, J.; Haberko, J.; Petrou, P.; Beltsios, K.; Raczkowska, J. *Colloids Surf., B* **2010**, *80*, 63.
- (155) Barat, B.; Wu, A. M. *Biomol. Eng.* **2007**, *24*, 283.
- (156) Emerman, A. B.; Zhang, Z. R.; Chakrabarti, O.; Hegde, R. S. *Mol. Biol. Cell* **2010**, *21*, 4325.
- (157) Hermanson, G. T. *Bioconjugate Techniques*; Academic Press: San Diego, CA, 1996.
- (158) Hofmann, K.; Wood, S. W.; Brinton, C. C.; Montibeller, J. A.; Finn, F. M. *Proc. Natl. Acad. Sci. U.S.A.* **1980**, *77*, 4666.
- (159) Hirsch, J. D.; Eslamizar, L.; Filanowski, B. J.; Malekzadeh, N.; Haugland, R. P.; Beechem, J. M.; Haugland, R. P. *Anal. Biochem.* **2002**, *308*, 343.
- (160) Hofmann, K.; Titus, G.; Montibeller, J. A.; Finn, F. M. *Biochemistry* **1982**, *21*, 978.
- (161) Zhang, K.; Diehl, M. R.; Tirrell, D. A. *J. Am. Chem. Soc.* **2005**, *127*, 10136.
- (162) Kwon, Y.; Coleman, M. A.; Camarero, J. A. *Angew. Chem., Int. Ed.* **2006**, *45*, 1726.
- (163) Camarero, J. A.; Kwon, Y.; Coleman, M. A. *J. Am. Chem. Soc.* **2004**, *126*, 14730.
- (164) Helms, B.; van Baal, I.; Merkx, M.; Meijer, E. W. *ChemBioChem* **2007**, *8*, 1790.
- (165) Nakanishi, K.; Sakiyama, T.; Kumada, Y.; Imamura, K.; Imanaka, H. *Curr. Proteomics* **2008**, *5*, 161.
- (166) Waugh, D. S. *Trends Biotechnol.* **2005**, *23*, 316.
- (167) Schröper, F.; Baumann, A.; Offenhäusser, A.; Mayer, D. *Biosens. Bioelectron.* **2012**, *34*, 171.
- (168) Schröper, F.; Baumann, A.; Offenhäusser, A.; Mayer, D. *Chem. Commun.* **2010**, *46*, 5295.
- (169) Ley, C.; Holtmann, D.; Mangold, K. M.; Schrader, J. *Colloids Surf., B* **2011**, *88*, 539.
- (170) Millner, P.; Hays, H.; Vakurov, A.; Pchelintsev, N.; Billah, M.; Rodgers, M. *Semin. Cell. Dev. Biol.* **2009**, *20*, 34.
- (171) Bello-Gil, D.; Maestro, B.; Fonseca, J.; Feliu, J. M.; Climent, V.; Sanz, J. M. *PLoS One* **2014**, *9*, e87995.
- (172) Lopez, R.; Garcia, E. *FEMS Microbiol. Rev.* **2004**, *28*, 553.
- (173) Pandey, P.; Upadhyay, S.; Pathak, H. *Sens. Actuators, B: Chem.* **1999**, *60*, 83.
- (174) Chioreia-Paquim, A. M.; Pauliuikaite, R.; Brett, C. M.; Oliveira-Brett, A. M. *Biosens. Bioelectron.* **2008**, *24*, 297.
- (175) Matsuhisa, H.; Tsuchiya, M.; Hasebe, Y. *Colloids Surf., B* **2013**, *111*, 523.
- (176) Vashist, S. K. *Anal. Biochem.* **2014**, *446*, 96.
- (177) North, S. H.; Lock, E. H.; Cooper, C. J.; Franek, J. B.; Taitt, C. R.; Walton, S. G. *ACS Appl. Mater. Interfaces* **2010**, *2*, 2884.
- (178) Vashist, S. K.; Marion Schneider, E.; Lam, E.; Hrapovic, S.; Luong, J. H. T. *Sci. Rep.* **2014**, *4*, 4407.
- (179) Vashist, S. K.; Schneider, E. M.; Luong, J. H. T. *Biosens. Bioelectron.* **2014**, DOI: 10.1016/j.bios.2014.06.058.
- (180) Chen, L.; Zhang, Z.; Zhang, P.; Zhang, X.; Fu, A. *Sens. Actuators, B: Chem.* **2011**, *155*, 557.
- (181) Feng, Y.; Ning, B.; Su, P.; Wang, H.; Wang, C.; Chen, F.; Gao, Z. *Talanta* **2009**, *80*, 803.
- (182) Lirtsman, V.; Ziblat, R.; Golosovsky, M.; Davidov, D.; Pogreb, R.; Sacks-Granek, V.; Rishpon, J. *J. Appl. Phys.* **2005**, *98*, 093506.
- (183) Palasantzas, G.; Svetovoy, V.; Van Zwol, P. *Phys. Rev. B* **2009**, *79*, 235434.
- (184) Pan, L.; Jung, S.; Yoon, R. H. *J. Colloid Interface Sci.* **2011**, *361*, 321.
- (185) Siqueira Petri, D. F.; Wenz, G.; Schunk, P.; Schimmel, T. *Langmuir* **1999**, *15*, 4520.
- (186) Endo, T.; Yamamura, S.; Nagatani, N.; Morita, Y.; Takamura, Y.; Tamiya, E. *Sci. Technol. Adv. Mater.* **2005**, *6*, 491.
- (187) Vashist, S. K.; Schneider, E. M.; Luong, J. H. T. *Analyst* **2014**, *139*, 2237.
- (188) Zhao, H. W.; Huang, C. Z.; Li, Y. F. *Anal. Chim. Acta* **2006**, *564*, 166.
- (189) De Vos, K. M.; Bartolozzi, I.; Bienstman, P.; Baets, R.; Schacht, E. K. Optical biosensor based on silicon-on-insulator microring cavities for specific protein binding detection. In *Proc. SPIE 6447, Nanoscale Imaging, Spectroscopy, Sensing, and Actuation for Biomedical Applications IV*, San Jose, CA, February 12, 2007; Cartwright, A. N., Nicolau, D. V., Eds.; SPIE: San Jose, CA, 2007; p 64470K.
- (190) Park, M. K.; Kee, J. S.; Quah, J. Y.; Netto, V.; Song, J.; Fang, Q.; La Fosse, E. M.; Lo, G.-Q. *Sens. Actuators, B: Chem.* **2013**, *176*, 552.

- (191) Washburn, A. L.; Gunn, L. C.; Bailey, R. C. *Anal. Chem.* **2009**, *81*, 9499.
- (192) Hsiao, V. K.; Waldeisen, J. R.; Zheng, Y.; Lloyd, P. F.; Bunning, T. J.; Huang, T. J. *J. Mater. Chem.* **2007**, *17*, 4896.
- (193) Kim, W. J.; Kim, B. K.; Kim, A.; Huh, C.; Ah, C. S.; Kim, K. H.; Hong, J.; Park, S. H.; Song, S.; Song, J.; Sung, G. Y. *Anal. Chem.* **2010**, *82*, 9686.
- (194) Long, F.; Zhu, A.; Zhou, X.; Wang, H.; Zhao, Z.; Liu, L.; Shi, H. *Biosens. Bioelectron.* **2014**, *55*, 19.
- (195) Liu, Y.; Li, Y. *Anal. Chem.* **2001**, *73*, 5180.
- (196) Acharya, G.; Chang, C. L.; Savran, C. *J. Am. Chem. Soc.* **2006**, *128*, 3862.
- (197) Mura, S.; Greppi, G.; Marongiu, M. L.; Roggero, P. P.; Ravindranath, S. P.; Mauer, L. J.; Schibeci, N.; Perria, F.; Piccinini, M.; Innocenzi, P.; Irudayraj, J. *Beilstein J. Nanotechnol.* **2012**, *3*, 485.
- (198) Kim, J.; Jensen, E. C.; Megens, M.; Boser, B.; Mathies, R. A. *Lab Chip* **2011**, *11*, 3106.
- (199) McDonald, J. C.; Whitesides, G. M. *Acc. Chem. Res.* **2002**, *35*, 491.
- (200) Wang, Y.; Lai, H.-H.; Bachman, M.; Sims, C. E.; Li, G.; Allbritton, N. L. *Anal. Chem.* **2005**, *77*, 7539.
- (201) Didar, T. F.; Foudeh, A. M.; Tabrizian, M. *Anal. Chem.* **2012**, *84*, 1012.
- (202) Bai, Y.; Koh, C. G.; Boreman, M.; Juang, Y. J.; Tang, I. C.; Lee, L. J.; Yang, S. T. *Langmuir* **2006**, *22*, 9458.
- (203) Lee, A. G.; Arena, C. P.; Beebe, D. J.; Palecek, S. P. *Biomacromolecules* **2010**, *11*, 3316.
- (204) Lee, A. G.; Beebe, D. J.; Palecek, S. P. *Biomed. Microdevices* **2012**, *14*, 247.
- (205) Ekstrom, S.; Onnerfjord, P.; Nilsson, J.; Bengtsson, M.; Laurell, T.; Marko-Varga, G. *Anal. Chem.* **2000**, *72*, 286.
- (206) de Jong, J.; Lammertink, R. G.; Wessling, M. *Lab Chip* **2006**, *6*, 1125.
- (207) Peterson, D. S. *Lab Chip* **2005**, *5*, 132.
- (208) Tennico, Y. H.; Hutana, D.; Koesdjojo, M. T.; Bartel, C. M.; Remcho, V. T. *Anal. Chem.* **2010**, *82*, 5591.
- (209) Sivagnanam, V.; Song, B.; Vandevyver, C.; Gijs, M. A. *Anal. Chem.* **2009**, *81*, 6509.
- (210) Ji, J.; Zhang, Y.; Zhou, X.; Kong, J.; Tang, Y.; Liu, B. *Anal. Chem.* **2008**, *80*, 2457.
- (211) He, M.; Herr, A. E. *Anal. Chem.* **2009**, *81*, 8177.
- (212) Sung, W. C.; Chen, H. H.; Makamba, H.; Chen, S. H. *Anal. Chem.* **2009**, *81*, 7967.
- (213) Peterson, D. S.; Rohr, T.; Svec, F.; Fréchet, J. M. *Anal. Chem.* **2002**, *74*, 4081.
- (214) Hisamoto, H.; Shimizu, Y.; Uchiyama, K.; Tokeshi, M.; Kikutani, Y.; Hibara, A.; Kitamori, T. *Anal. Chem.* **2003**, *75*, 350.
- (215) Campbell, G. A.; Mutharasan, R. *Anal. Sci.* **2005**, *21*, 355.
- (216) Maraldo, D.; Rijal, K.; Campbell, G.; Mutharasan, R. *Anal. Chem.* **2007**, *79*, 2762.
- (217) Campbell, G. A.; Mutharasan, R. *Anal. Chem.* **2007**, *79*, 1145.
- (218) Zheng, D.; Vashist, S. K.; Al-Rubeaan, K.; Luong, J. H. T.; Sheu, F. S. *Talanta* **2012**, *99*, 22.
- (219) Zheng, D.; Vashist, S. K.; Al-Rubeaan, K.; Lam, E.; Hrapovic, S.; Luong, J. H. T.; Sheu, F.-S. *Nanopharmaceutics Drug Del.* **2013**, *1*, 64.
- (220) Luong, J. H. T.; Hrapovic, S.; Wang, D.; Bensebaa, F.; Simard, B. *Electroanalysis* **2004**, *16*, 132.
- (221) Matsumoto, T.; Ohashi, A.; Ito, N.; Fujiwara, H.; Matsumoto, T. *Biosens. Bioelectron.* **2001**, *16*, 271.
- (222) Matsumoto, T.; Ohashi, A.; Ito, N. *Anal. Chim. Acta* **2002**, *462*, 253.
- (223) Murphy-Perez, E.; Arya, S. K.; Bhansali, S. *Analyst* **2011**, *136*, 1686.
- (224) Lei, L.; Cao, Z.; Xie, Q.; Fu, Y.; Tan, Y.; Ma, M.; Yao, S. *Sens. Actuators, B: Chem.* **2011**, *157*, 282.
- (225) Lin, J.-J.; Hsu, P.-Y.; Wu, Y.-L.; Jhuang, J.-J. *Sensors* **2011**, *11*, 2796.
- (226) Luong, J. H. T.; Hrapovic, S.; Wang, D. *Electroanalysis* **2005**, *17*, 47.
- (227) Rochette, J. F.; Sacher, E.; Meunier, M.; Luong, J. H. T. *Anal. Biochem.* **2005**, *336*, 305.
- (228) Villalonga, R.; Villalonga, M. L.; Díez, P.; Pingarrón, J. M. *J. Mater. Chem.* **2011**, *21*, 12858.
- (229) Puri, N.; Sharma, V.; Tanwar, V. K.; Singh, N.; Biradar, A. M. *Prog. Biomater.* **2013**, *2*, 1.
- (230) Zor, E.; Patir, I. H.; Bingol, H.; Ersoz, M. *Biosens. Bioelectron.* **2013**, *42*, 321.
- (231) Canbaz, M. C.; Sezginturk, M. K. *Anal. Biochem.* **2014**, *446*, 9.
- (232) Kim, G. I.; Kim, K. W.; Oh, M. K.; Sung, Y. M. *Biosens. Bioelectron.* **2010**, *25*, 1717.
- (233) Vashist, S. K.; Saraswat, M.; Holthšfer, H. *Procedia Chem.* **2012**, *6*, 184.
- (234) Jung, J.; Lim, S. *Appl. Surf. Sci.* **2013**, *265*, 24.
- (235) Ray, K. G., III; McCreery, R. L. *J. Electroanal. Chem.* **1999**, *469*, 150.
- (236) Girard, H.; Simon, N.; Ballutaud, D.; Herlem, M.; Etcheberry, A. *Diamond Relat. Mater.* **2007**, *16*, 316.
- (237) Martin, H. B.; Argoitia, A.; Landau, U.; Anderson, A. B.; Angus, J. C. *J. Electrochem. Soc.* **1996**, *143*, L133.
- (238) Xu, J.; Granger, M. C.; Chen, Q.; Strojek, J. W.; Lister, T. E.; Swain, G. M. *Anal. Chem.* **1997**, *69*, 591A.
- (239) Goeting, C. H.; Marken, F.; Gutiérrez-Sosa, A.; Compton, R. G.; Foord, J. S. *Diamond Relat. Mater.* **2000**, *9*, 390.
- (240) Notsu, H.; Fukazawa, T.; Tatsuma, T.; Tryk, D. A.; Fujishima, A. *Electrochim. Solid-State Lett.* **2001**, *4*, H1.
- (241) Haak, R. M.; Wezenberg, S. J.; Kleij, A. W. *Chem. Commun.* **2010**, *46*, 2713.
- (242) Parker, C. O.; Lanyon, Y. H.; Manning, M.; Arrigan, D. W. M.; Tothill, I. E. *Anal. Chem.* **2009**, *81*, 5291.
- (243) Chai, C.; Takhistov, P. *Sensors* **2010**, *10*, 655.
- (244) Leu, G.; Brockhaus, A.; Engemann, J. *Surf. Coat. Technol.* **2003**, *174*, 928.
- (245) Bai, S.; Urabe, S.; Okabe, Y.; Yokoyama, T. *J. Colloid Interface Sci.* **2009**, *331*, 551.
- (246) Bai, Y.-F.; Xu, T.-B.; Luong, J. H. T.; Cui, H.-F. *Anal. Chem.* **2014**, *86*, 4910.
- (247) Fang, X.; Tan, O. K.; Gan, Y. Y.; Tse, M. S. *Sens. Actuators, B: Chem.* **2010**, *149*, 381.
- (248) Teti, D.; Visalli, M.; McNair, H. J. *Chromatogr., B* **2002**, *781*, 107.
- (249) Harik, S. I.; Sutton, C. H. *Cancer Res.* **1979**, *39*, 5010.
- (250) Flores, H. E.; Galston, A. W. *Science* **1982**, *217*, 1259.
- (251) Wolrath, H.; Forsum, U.; Larsson, P. G.; Boren, H. *J. Clin. Microbiol.* **2001**, *39*, 4026.
- (252) Nagy, L.; Nagy, G.; Gyurcsányi, R. E.; Neuman, M. R.; Lindner, E. *J. Biochem. Biophys. Methods* **2002**, *53*, 165.
- (253) Guo, Z.; Hao, T.; Duan, J.; Wang, S.; Wei, D. *Talanta* **2012**, *89*, 27.
- (254) Teixeira, S.; Burwell, G.; Castaing, A.; Gonzalez, D.; Conlan, R.; Guy, O. *Sens. Actuators, B: Chem.* **2014**, *190*, 723.
- (255) Zhong, Z.; Patskovskyy, S.; Bourette, P.; Luong, J. H. T.; Gedanken, A. *J. Phys. Chem. B* **2004**, *108*, 4046.
- (256) Huang, K. C.; Ehrman, S. H. *Langmuir* **2007**, *23*, 1419.
- (257) Menz, W. J.; Shekar, S.; Brownbridge, G. P.; Mosbach, S.; Körmer, R.; Peukert, W.; Kraft, M. *J. Aerosol Sci.* **2012**, *44*, 46.
- (258) Wang, L.; Muhammed, M. *J. Mater. Chem.* **1999**, *9*, 2871.
- (259) Ladj, R.; Bitar, A.; Eissa, M.; Mugnier, Y.; Le Dantec, R.; Fessi, H.; Elaissari, A. *J. Mater. Chem. B* **2013**, *1*, 1381.
- (260) Zhuo, Y.; Chai, Y.-Q.; Yuan, R.; Mao, L.; Yuan, Y.-L.; Han, J. *Biosens. Bioelectron.* **2011**, *26*, 3838.
- (261) Gopinath, S. C.; Awazu, K.; Fujimaki, M.; Shimizu, K.; Mizutani, W.; Tsukagoshi, K. *Analyst* **2012**, *137*, 3520.
- (262) Rezaei, B.; Havakeshian, E.; Ensafi, A. A. *Biosens. Bioelectron.* **2013**, *48*, 61.
- (263) Roque, A. C.; Bispo, S.; Pinheiro, A. R.; Antunes, J. M.; Goncalves, D.; Ferreira, H. A. *J. Mol. Recognit.* **2009**, *22*, 77.
- (264) Koh, I.; Wang, X.; Varughese, B.; Isaacs, L.; Ehrman, S. H.; English, D. S. *J. Phys. Chem. B* **2006**, *110*, 1553.

- (265) Kumar, S.; Jana, A. K.; Dhamija, I.; Singla, Y.; Maiti, M. *Eur. J. Pharm. Biopharm.* **2013**, *85*, 413.
- (266) Branco, R. V.; Estrada Gutarra, M. L.; Freire, D. M.; Almeida, R. V. *Enzyme Res.* **2010**, *2010*, 180418.
- (267) Park, H. J.; McConnell, J. T.; Boddohi, S.; Kipper, M. J.; Johnson, P. A. *Colloids Surf., B* **2011**, *83*, 198.
- (268) Jie, G.; Wang, L.; Zhang, S. *Chem.—Eur. J.* **2011**, *17*, 641.
- (269) Qin, W.; Song, Z.; Fan, C.; Zhang, W.; Cai, Y.; Zhang, Y.; Qian, X. *Anal. Chem.* **2012**, *84*, 3138.
- (270) Joo, J.; Kwon, D.; Shin, H. H.; Park, K.-H.; Cha, H. J.; Jeon, S. *Sens. Actuators, B: Chem.* **2013**, *188*, 1250.
- (271) Hu, Y.; Shen, G.; Zhu, H.; Jiang, G. *J. Agric. Food Chem.* **2010**, *58*, 2801.
- (272) Cunningham, E.; Campbell, C. *J. Langmuir* **2003**, *19*, 4509.
- (273) Endo, T.; Kerman, K.; Nagatani, N.; Hiepa, H. M.; Kim, D. K.; Yonezawa, Y.; Nakano, K.; Tamiya, E. *Anal. Chem.* **2006**, *78*, 6465.
- (274) Lee, M. H.; Lee, D. H.; Jung, S. W.; Lee, K. N.; Park, Y. S.; Seong, W. K. *J. Nanomed. Nanotechnol.* **2010**, *6*, 78.
- (275) Prina-Mello, A.; Whelan, A. M.; Atzberger, A.; McCarthy, J. E.; Byrne, F.; Davies, G. L.; Coey, J. M.; Volkov, Y.; Gun'ko, Y. K. *Small* **2010**, *6*, 247.
- (276) Alivisatos, A. P. *Science* **1996**, *271*, 933.
- (277) Burda, C.; Chen, X.; Narayanan, R.; El-Sayed, M. A. *Chem. Rev.* **2005**, *105*, 1025.
- (278) Algar, W. R.; Tavares, A. J.; Krull, U. *J. Anal. Chim. Acta* **2010**, *673*, 1.
- (279) Alivisatos, A. P.; Gu, W.; Larabell, C. *Annu. Rev. Biomed. Eng.* **2005**, *7*, 55.
- (280) Parak, W. J.; Pellegrino, T.; Plank, C. *Nanotechnology* **2005**, *16*, R9.
- (281) Zhang, B.; Gong, X.; Hao, L.; Cheng, J.; Han, Y.; Chang, J. *Nanotechnology* **2008**, *19*, 465604.
- (282) Zhang, Y.; Wu, H.; Huang, X.; Zhang, J.; Guo, S. *Nanoscale Res. Lett.* **2011**, *6*, 450.
- (283) Shan, G.; Wang, S.; Fei, X.; Liu, Y.; Yang, G. *J. Phys. Chem. B* **2009**, *113*, 1468.
- (284) Tu, M. C.; Chang, Y. T.; Kang, Y. T.; Chang, H. Y.; Chang, P.; Yew, T. R. *Biosens. Bioelectron.* **2012**, *34*, 286.
- (285) Liu, W.; Zhang, Y.; Ge, S.; Song, X.; Huang, J.; Yan, M.; Yu, J. *Anal. Chim. Acta* **2013**, *770*, 132.
- (286) Liu, F.; Zhang, Y.; Ge, S.; Lu, J.; Yu, J.; Song, X.; Liu, S. *Talanta* **2012**, *99*, 512.
- (287) Wang, W.; Hao, Q.; Wang, W.; Bao, L.; Lei, J.; Wang, Q.; Ju, H. *Nanoscale* **2014**, *6*, 2710.
- (288) Suarez, G.; Keegan, N.; Spoores, J. A.; Ortiz, P.; Jackson, R. J.; Hedley, J.; Borrise, X.; McNeil, C. *J. Langmuir* **2010**, *26*, 6071.
- (289) Eissa, M. M.; Rahman, M. M.; Zine, N.; Jaffrezic, N.; Errachid, A.; Fessi, H.; Elaissari, A. *Acta Biomater.* **2013**, *9*, 5573.
- (290) Rauf, S.; Zhou, D.; Abell, C.; Klenerman, D.; Kang, D. *J. Chem. Commun.* **2006**, *1721*.
- (291) Babacan, S.; Pivarnik, P.; Letcher, S.; Rand, A. G. *Biosens. Bioelectron.* **2000**, *15*, 615.
- (292) Maehashi, K.; Katsura, T.; Kerman, K.; Takamura, Y.; Matsumoto, K.; Tamiya, E. *Anal. Chem.* **2007**, *79*, 782.
- (293) Sarkar, A.; Daniels-Race, T. *Nanomaterials* **2013**, *3*, 272.
- (294) Chen, A.; Kozak, D.; Battersby, B. J.; Forrest, R. M.; Scholler, N.; Urban, N.; Trau, M. *Langmuir* **2009**, *25*, 13510.
- (295) Williamson, M. L.; Atha, D. H.; Reeder, D. J.; Sundaram, P. V. *Anal. Lett.* **1989**, *22*, 803.
- (296) Berney, H.; Roseingrave, P.; Alderman, J.; Lane, W.; Collins, J. K. *Sens. Actuators, B: Chem.* **1997**, *44*, 341.
- (297) Yuan, S.; Szakalas-Gratzl, G.; Ziats, N. P.; Jacobsen, D. W.; Kottke-Marchant, K.; Marchant, R. E. *J. Biomed. Mater. Res.* **1993**, *27*, 81.
- (298) Skládal, P.; Minunni, M.; Mascini, M.; Kolář, V.; Fránek, M. J. *Immunol. Methods* **1994**, *176*, 117.
- (299) Suri, C. R.; Raje, M.; Mishra, G. C. *Biosens. Bioelectron.* **1994**, *9*, 325.
- (300) Suri, C. R.; Mishra, G. C. *Biosens. Bioelectron.* **1996**, *11*, 1199.
- (301) Sasaki, S.; Nagata, R.; Hock, B.; Karube, I. *Anal. Chim. Acta* **1998**, *368*, 71.
- (302) Qian, W.; Yao, D.; Xu, B.; Yu, F.; Lu, Z.; Knoll, W. *Chem. Mater.* **1999**, *11*, 1399.
- (303) Weiping, Q.; Bin, X.; Danfeng, Y.; Yihua, L.; Lei, W.; Chunxiao, W.; Fang, Y.; Zhuhong, L.; Yu, W. *Mater. Sci. Eng., C* **1999**, *8*, 475.
- (304) Gao, Z.; Chao, F.; Chao, Z.; Li, G. *Sens. Actuators, B: Chem.* **2000**, *66*, 193.
- (305) Nisnevitch, M.; Kolog-Gulco, M.; Trombka, D.; Green, B. S.; Firer, M. A. *J. Chromatogr., B* **2000**, *738*, 217.
- (306) Yuan, H.; Mullett, W. M.; Pawliszyn, J. *Analyst* **2001**, *126*, 1456.
- (307) Claudon, P.; Donner, M.; Stoltz, J. F. *J. Mater. Sci.: Mater. Med.* **1991**, *2*, 197.
- (308) Herzog, G.; Raj, J.; Arrigan, D. W. M. *Microchim. Acta* **2009**, *166*, 349.
- (309) Eun, A. J.-C.; Huang, L.; Chew, F.-T.; Li, S. F.-Y.; Wong, S.-M. *J. Virol. Methods* **2002**, *99*, 71.
- (310) Benesch, J.; Tengvall, P. *Biomaterials* **2002**, *23*, 2561.
- (311) Yakovleva, J.; Davidsson, R.; Lobanova, A.; Bengtsson, M.; Eremin, S.; Laurell, T.; Emnéus, J. *Anal. Chem.* **2002**, *74*, 2994.
- (312) Kusnezow, W.; Jacob, A.; Walijew, A.; Diehl, F.; Hoheisel, J. D. *Proteomics* **2003**, *3*, 254.
- (313) Wang, Z. H.; Jin, G. *Colloids Surf., B* **2004**, *34*, 173.
- (314) Kim, J.-K.; Shin, D.-S.; Chung, W.-J.; Jang, K.-H.; Lee, K.-N.; Kim, Y.-K.; Lee, Y.-S. *Colloids Surf., B* **2004**, *33*, 67.
- (315) Wei, Y.; Ning, G.; Hai-Qian, Z.; Jian-Guo, W.; Yi-Hong, W.; Wesche, K.-D. *Sens. Actuators, B: Chem.* **2004**, *98*, 83.
- (316) Kandimalla, V. B.; Neeta, N. S.; Karanth, N. G.; Thakur, M. S.; Roshini, K. R.; Rani, B. E.; Pasha, A.; Karanth, N. G. *Biosens. Bioelectron.* **2004**, *20*, 903.
- (317) Diao, J.; Ren, D.; Engstrom, J. R.; Lee, K. H. *Anal. Biochem.* **2005**, *343*, 322.
- (318) Liu, M.; Liu, Z. Y.; Lu, Q.; Yuan, H.; Ma, L.; Li, J. H.; Bai, Y. B.; Li, T. *J. Chin. J. Chem.* **2005**, *23*, 875.
- (319) Vashist, S. K.; Raiteri, R.; Tewari, R.; Bajpai, R. P.; Bharadwaj, L. M. *J. Phys.: Conf. Ser.* **2006**, *34*, 806.
- (320) Chu, X.; Zhao, Z.-L.; Shen, G.-L.; Yu, R.-Q. *Sens. Actuators, B: Chem.* **2006**, *114*, 696.
- (321) Qian, W.; Xu, B.; Song, Z.; Wu, L.; Yao, D.; Yu, F.; Lu, Z.; Wei, Y. *Mol. Cryst. Liq. Cryst.* **1999**, *337*, 277.
- (322) Qin, M.; Hou, S.; Wang, L.; Feng, X.; Wang, R.; Yang, Y.; Wang, C.; Yu, L.; Shao, B.; Qiao, M. *Colloids Surf., B* **2007**, *60*, 243.
- (323) Liu, Y.; Li, C. M.; Yu, L.; Chen, P. *Front. Biosci.* **2007**, *12*, 3768.
- (324) Goyal, D. K.; Pribil, G. K.; Woollam, J. A.; Subramanian, A. *Mater. Sci. Eng., B* **2008**, *149*, 26.
- (325) Stanford, C.; Dagenais, M.; Park, J.-H.; DeShong, P. *Curr. Anal. Chem.* **2008**, *4*, 356.
- (326) Mace, C. R.; Yadav, A. R.; Miller, B. L. *Langmuir* **2008**, *24*, 12754.
- (327) Jang, L. S.; Liu, H. J. *Biomed. Microdevices* **2009**, *11*, 331.
- (328) Sabella, S.; Brunetti, V.; Vecchio, G.; Torre, A. D.; Rinaldi, R.; Cingolani, R.; Pompa, P. P. *Nanoscale Res. Lett.* **2009**, *4*, 1222.
- (329) Niotis, A. E.; Mastichiadis, C.; Petrou, P. S.; Christofidis, I.; Siafaka-Kapadai, A.; Misiakos, K.; Kakabakos, S. E. *Anal. Bioanal. Chem.* **2009**, *393*, 1081.
- (330) Jayagopal, A.; Stone, G. P.; Haselton, F. R. *Bioconjugate Chem.* **2008**, *19*, 792.
- (331) Sandison, M. E.; Cumming, S. A.; Kolch, W.; Pitt, A. R. *Lab Chip* **2010**, *10*, 2805.
- (332) Briand, E.; Humblot, V.; Landoulsi, J.; Petronis, S.; Pradier, C. M.; Kasemo, B.; Svedhem, S. *Langmuir* **2011**, *27*, 678.
- (333) Wildeboer, D.; Jiang, P.; Price, R. G.; Yu, S.; Jeganathan, F.; Abuknesha, R. A. *Talanta* **2010**, *81*, 68.
- (334) Blinka, E.; Loeffler, K.; Hu, Y.; Gopal, A.; Hoshino, K.; Lin, K.; Liu, X.; Ferrari, M.; Zhang, J. X. *Nanotechnology* **2010**, *21*, 415302.
- (335) Huy, T. Q.; Hanh, N. T. H.; Chung, P. V.; Anh, D. D.; Nga, P. T.; Tuan, M. A. *Appl. Surf. Sci.* **2011**, *257*, 7090.
- (336) Wu, X.; Tang, Q.; Liu, C.; Li, Q.; Guo, Y.; Yang, Y.; Lv, X.; Geng, L.; Deng, Y. *Appl. Surf. Sci.* **2011**, *257*, 7415.

- (337) Vacic, A.; Criscione, J. M.; Rajan, N. K.; Stern, E.; Fahmy, T. M.; Reed, M. A. *J. Am. Chem. Soc.* **2011**, *133*, 13886.
- (338) Oliver, M. J.; Hernando-Garcia, J.; Pobedinskas, P.; Haenen, K.; Rios, A.; Sanchez-Rojas, J. L. *Colloids Surf, B* **2011**, *88*, 191.
- (339) Son, K. J.; Ahn, S. H.; Kim, J. H.; Koh, W. G. *ACS Appl. Mater. Interfaces* **2011**, *3*, 573.
- (340) Lim, T. S.; Vedula, S. R.; Kausalya, P. J.; Hunziker, W.; Lim, C. T. *Langmuir* **2008**, *24*, 490.
- (341) Lee, H. U.; Shin, H. Y.; Lee, J. Y.; Song, Y. S.; Park, C.; Kim, S. W. *J. Agric. Food Chem.* **2010**, *58*, 12096.
- (342) Zimnitsky, D.; Jiang, C.; Xu, J.; Lin, Z.; Zhang, L.; Tsukruk, V. V. *Langmuir* **2007**, *23*, 10176.
- (343) Huy, T. Q.; Hanh, N. T.; Thuy, N. T.; Chung, P. V.; Nga, P. T.; Tuan, M. A. *Talanta* **2011**, *86*, 271.
- (344) Veerapandian, M.; Subbiah, R.; Lim, G. S.; Park, S. H.; Yun, K.; Lee, M. H. *Langmuir* **2011**, *27*, 8934.
- (345) Kim, J.-Y.; Ahn, J.-H.; Moon, D.-I.; Kim, S.; Park, T. J.; Lee, S. Y.; Choi, Y.-K. *BioNanoScience* **2012**, *2*, 35.
- (346) Kim, W. J.; Kim, S.; Lee, B. S.; Kim, A.; Ah, C. S.; Huh, C.; Sung, G. Y.; Yun, W. S. *Langmuir* **2009**, *25*, 11692.
- (347) Jonsson, C.; Aronsson, M.; Rundstrom, G.; Pettersson, C.; Mendel-Hartwig, I.; Bakker, J.; MacCraith, B.; Ohman, O.; Melin, J. *Eur. Cells Mater.* **2007**, *14*, 64.
- (348) Vashist, S. K. *Protocol Exchange* **2012**, DOI: 10.1028/protex.2012.051.
- (349) Gubala, V.; Siegrist, J.; Monaghan, R.; O'Reilly, B.; Gandhiraman, R. P.; Daniels, S.; Williams, D. E.; Ducree, J. *Anal. Chim. Acta* **2013**, *760*, 75.
- (350) Brothier, F.; Pichon, V. *Anal. Chim. Acta* **2013**, *792*, 52.
- (351) Chepyala, R.; Panda, S. *Appl. Surf. Sci.* **2013**, *271*, 77.
- (352) Choi, E.; Choi, Y.; Nejad, Y. H. P.; Shin, K.; Park, J. *Sens. Actuators, B: Chem.* **2013**, *180*, 107.
- (353) Matatagui, D.; Fontecha, J.; Fernández, M. J.; Oliver, M. J.; Hernando-García, J.; Sánchez-Rojas, J. L.; Gracia, I.; Cané, C.; Santos, J. P.; Horrillo, M. C. *Sens. Actuators, B: Chem.* **2013**, *189*, 123.
- (354) Gao, Z. D.; Guan, F. F.; Li, C. Y.; Liu, H. F.; Song, Y. Y. *Biosens. Bioelectron.* **2013**, *41*, 771.
- (355) Chang, A. Y.; Lu, M. S. *Biosens. Bioelectron.* **2013**, *45*, 6.
- (356) Zhang, B.; Morales, A. W.; Peterson, R.; Tang, L.; Ye, J. Y. *Biosens. Bioelectron.* **2014**, *58*, 107.
- (357) Sharma, V.; Kumar, A.; Ganguly, P.; Biradar, A. *Appl. Phys. Lett.* **2014**, *104*, 043705.
- (358) Şimşek, C. S.; Teke, M.; Sezgintürk, M. K. *Electroanalysis* **2014**, *26*, 328.
- (359) Wang, L.; Wang, F.; Shang, L.; Zhu, C.; Ren, W.; Dong, S. *Talanta* **2010**, *82*, 113.
- (360) Torabi, S. F.; Khajeh, K.; Ghasempur, S.; Ghaemi, N.; Siadat, S. O. *J. Biotechnol.* **2007**, *131*, 111.
- (361) Tien, C. J.; Chiang, B. H. *Process Biochem.* **1999**, *35*, 377.
- (362) Vinoba, M.; Bhagiyalakshmi, M.; Jeong, S. K.; Yoon, Y. I.; Nam, S. C. *Colloids Surf, B* **2012**, *90*, 91.
- (363) Alptekin, Ö.; Tükel, S. S.; Yıldırım, D.; Alagöz, D. *J. Mol. Catal. B: Enzym.* **2009**, *58*, 124.
- (364) Hartono, S. B.; Qiao, S. Z.; Liu, J.; Jack, K.; Ladewig, B. P.; Hao, Z.; Lu, G. Q. *M. J. Phys. Chem. C* **2010**, *114*, 8353.
- (365) Yadav, R.; Wanjari, S.; Prabhu, C.; Kumar, V.; Labhsetwar, N.; Satyanarayanan, T.; Kotwal, S.; Rayalu, S. *Energy Fuels* **2010**, *24*, 6198.
- (366) Lomako, O. V.; Menyailova, I. I.; Nakhapetyan, L. A.; Nikitin, Y.; Kiselev, A. V. *Enzyme Microb. Technol.* **1982**, *4*, 89.
- (367) Rogalski, J.; Szczodrak, J.; Dawidowicz, A.; Ilczuk, Z.; Leonowicz, A. *Enzyme Microb. Technol.* **1985**, *7*, 395.
- (368) Wojtas-Wasilewska, M.; Luterek, J.; Rogalski, J. *Phytochemistry* **1988**, *27*, 2731.
- (369) Sarkar, J. M.; Leonowicz, A.; Bollag, J.-M. *Soil Biol. Biochem.* **1989**, *21*, 223.
- (370) Janowski, F.; Fischer, G.; Urbaniak, W.; Foltynowicz, Z.; Marciniec, B. *J. Chem. Technol. Biotechnol.* **1991**, *51*, 263.
- (371) Emneus, J.; Gorton, L. *Anal. Chim. Acta* **1993**, *276*, 303.
- (372) Jen, J.-F.; Zen, J.-H.; Cheng, F.-C.; Yang, G.-Y. *Anal. Chim. Acta* **1994**, *292*, 23.
- (373) Rogalski, J.; Joźwik, E.; Hattaka, A.; Leonowicz, A. *J. Mol. Catal. A: Chem.* **1995**, *95*, 99.
- (374) Rogalski, J.; Szczodrak, J.; Pleszczyńska, M.; Fiedurek, J. *J. Mol. Catal. B: Enzym.* **1997**, *3*, 271.
- (375) Licklider, L.; Kuhr, W. G. *Anal. Chem.* **1998**, *70*, 1902.
- (376) Rogalski, J.; Dawidowicz, A.; Jóźwik, E.; Leonowicz, A. *J. Mol. Catal. B: Enzym.* **1999**, *6*, 29.
- (377) Kharitonov, A. B.; Zayats, M.; Lichtenstein, A.; Katz, E.; Willner, I. *Sens. Actuators, B: Chem.* **2000**, *70*, 222.
- (378) Ida, J.; Matsuyama, T.; Yamamoto, H. *J. Electrost.* **2000**, *49*, 71.
- (379) Ferreira, L.; Ramos, M. A.; Dordick, J. S.; Gil, M. H. *J. Mol. Catal. B: Enzym.* **2003**, *21*, 189.
- (380) Shioji, S.; Hanada, M.; Hayashi, Y.; Tokami, K.; Yamamoto, H. *Adv. Powder Technol.* **2003**, *14*, 231.
- (381) Chong, A. S. M.; Zhao, X. S. *Catal. Today* **2004**, *93–95*, 293.
- (382) Chong, A. S. M.; Zhao, X. S. *Appl. Surf. Sci.* **2004**, *237*, 398.
- (383) de Lathouder, K. M.; Bakker, J.; Kreutzer, M. T.; Kapteijn, F.; Moulijn, J. A.; Wallin, S. A. *Chem. Eng. Sci.* **2004**, *59*, 5027.
- (384) Tukel, S. S.; Alptekin, O. *Process Biochem.* **2004**, *39*, 2149.
- (385) Phadtare, S.; Vinod, V. P.; Mukhopadhyay, K.; Kumar, A.; Rao, M.; Chaudhari, R. V.; Sastry, M. *Biotechnol. Bioeng.* **2004**, *85*, 629.
- (386) Minier, M.; Salmain, M.; Yacoubi, N.; Barbes, L.; Methivier, C.; Zanna, S.; Pradier, C. M. *Langmuir* **2005**, *21*, 5957.
- (387) Longo, L.; Vasapollo, G.; Guascito, M. R.; Malitesta, C. *Anal. Bioanal. Chem.* **2006**, *385*, 146.
- (388) Bai, Y. X.; Li, Y. F.; Yang, Y.; Yi, L. X. *J. Biotechnol.* **2006**, *125*, 574.
- (389) Brandi, P.; D'Annibale, A.; Galli, C.; Gentili, P.; Pontes, A. S. N. *J. Mol. Catal. B: Enzym.* **2006**, *41*, 61.
- (390) Bai, Y.-X.; Li, Y.-F.; Yang, Y.; Yi, L.-X. *Process Biochem.* **2006**, *41*, 770.
- (391) David, A. E.; Wang, N. S.; Yang, V. C.; Yang, A. *J. J. Biotechnol.* **2006**, *125*, 395.
- (392) Kim, J.; Jia, H.; Lee, C.-W.; Chung, S.-W.; Kwak, J. H.; Shin, Y.; Dohnalkova, A.; Kim, B.-G.; Wang, P.; Grate, J. W. *Enzyme Microb. Technol.* **2006**, *39*, 474.
- (393) Gómez, J. L.; Bódalo, A.; Gómez, E.; Bastida, J.; Hidalgo, A. M.; Gómez, M. *Enzyme Microb. Technol.* **2006**, *39*, 1016.
- (394) Oliveira, E. M.; Beyer, S.; Heinze, J. *Bioelectrochemistry* **2007**, *71*, 186.
- (395) Libertino, S.; Fichera, M.; Aiello, V.; Statello, G.; Fiorenza, P.; Sinatra, F. *Microelectron. Eng.* **2007**, *84*, 468.
- (396) Libertino, S.; Scandurra, A.; Aiello, V.; Giannazzo, F.; Sinatra, F.; Renis, M.; Fichera, M. *Appl. Surf. Sci.* **2007**, *253*, 9116.
- (397) Wang, A.; Zhou, C.; Wang, H.; Shen, S.; Xue, J.; Ouyang, P. *Chin. J. Chem. Eng.* **2007**, *15*, 788.
- (398) Kahraman, M.; Bayramoglu, G.; Kayamanapohan, N.; Gungor, A. *Food Chem.* **2007**, *104*, 1385.
- (399) Shah, P.; Sridevi, N.; Prabhune, A.; Ramaswamy, V. *Microporous Mesoporous Mater.* **2008**, *116*, 157.
- (400) de Lathouder, K. M.; van Benthem, D. T. J.; Wallin, S. A.; Mateo, C.; Lafuente, R. F.; Guisan, J. M.; Kapteijn, F.; Moulijn, J. A. *J. Mol. Catal. B: Enzym.* **2008**, *50*, 20.
- (401) Kim, M. I.; Kim, J.; Lee, J.; Shin, S.; Na, H. B.; Hyeon, T.; Park, H. G.; Chang, H. N. *Microporous Mesoporous Mater.* **2008**, *111*, 18.
- (402) Fernandez, R. E.; Bhattacharya, E.; Chadha, A. *Appl. Surf. Sci.* **2008**, *254*, 4512.
- (403) Ma, J.; Liang, Z.; Qiao, X.; Deng, Q.; Tao, D.; Zhang, L.; Zhang, Y. *Anal. Chem.* **2008**, *80*, 2949.
- (404) Manyar, H. G.; Gianotti, E.; Sakamoto, Y.; Terasaki, O.; Coluccia, S.; Tumbiolo, S. *J. Phys. Chem. C* **2008**, *112*, 18110.
- (405) Zimmermann, J.; Rabe, M.; Verdes, D.; Seeger, S. *Langmuir* **2008**, *24*, 1053.
- (406) Libertino, S.; Giannazzo, F.; Aiello, V.; Scandurra, A.; Sinatra, F.; Renis, M.; Fichera, M. *Langmuir* **2008**, *24*, 1965.
- (407) Pita, M.; Kramer, M.; Zhou, J.; Poghossian, A.; Schoning, M. J.; Fernandez, V. M.; Katz, E. *ACS Nano* **2008**, *2*, 2160.

- (408) Lee, C. C.; Chiang, H. P.; Li, K. L.; Ko, F. H.; Su, C. Y.; Yang, Y. *S. Anal. Chem.* **2009**, *81*, 2737.
- (409) Kannan, K.; Jasra, R. V. *J. Mol. Catal. B: Enzym.* **2009**, *56*, 34.
- (410) Tanvir, S.; Pantigny, J.; Boulnois, P.; Pulvin, S. *J. Membr. Sci.* **2009**, *329*, 85.
- (411) Wang, A.; Zhou, C.; Du, Z.; Liu, M.; Zhu, S.; Shen, S.; Ouyang, P. *J. Biosci. Bioeng.* **2009**, *107*, 219.
- (412) Wang, Y.; Hasebe, Y. *Talanta* **2009**, *79*, 1135.
- (413) Upadhyay, S.; Rao, G. R.; Sharma, M. K.; Bhattacharya, B. K.; Rao, V. K.; Vijayaraghavan, R. *Biosens. Bioelectron.* **2009**, *25*, 832.
- (414) Shi, B.; Wang, Y.; Guo, Y.; Wang, Y.; Wang, Y.; Guo, Y.; Zhang, Z.; Liu, X.; Lu, G. *Catal. Today* **2009**, *148*, 184.
- (415) Lee, Y.; Kim, J.; Kim, S.; Jang, W.-D.; Park, S.; Koh, W.-G. *J. Mater. Chem.* **2009**, *19*, 5643.
- (416) Arrabito, G.; Musumeci, C.; Aiello, V.; Libertino, S.; Compagnini, G.; Pignataro, B. *Langmuir* **2009**, *25*, 6312.
- (417) Goykhman, I.; Korbakov, N.; Bartic, C.; Borghs, G.; Spira, M. E.; Shappir, J.; Yitzchaik, S. *J. Am. Chem. Soc.* **2009**, *131*, 4788.
- (418) Song, Y. S.; Lee, J. H.; Kang, S. W.; Kim, S. W. *Food Chem.* **2010**, *123*, 1.
- (419) Park, S. W.; Kim, Y. I.; Chung, K. H.; Hong, S. I.; Kim, S. W. *React. Funct. Polym.* **2002**, *51*, 79.
- (420) Kroll, S.; Treccani, L.; Rezwan, K.; Grathwohl, G. *J. Membr. Sci.* **2010**, *365*, 447.
- (421) Bautista, L. F.; Morales, G.; Sanz, R. *Bioresour. Technol.* **2010**, *101*, 8541.
- (422) Pedrosa, V. A.; Paliwal, S.; Balasubramanian, S.; Nepal, D.; Davis, V.; Wild, J.; Ramanculov, E.; Simonian, A. *Colloids Surf., B* **2010**, *77*, 69.
- (423) Wang, M.; Qi, W.; Yu, Q.; Su, R.; He, Z. *Biochem. Eng. J.* **2010**, *52*, 168.
- (424) Shi, B.; Wang, Y.; Ren, J.; Liu, X.; Zhang, Y.; Guo, Y.; Guo, Y.; Lu, G. *J. Mol. Catal. B: Enzym.* **2010**, *63*, 50.
- (425) Zheng, X. T.; Yang, H. B.; Li, C. M. *Anal. Chem.* **2010**, *82*, 5082.
- (426) Sun, L.; Ma, J.; Qiao, X.; Liang, Y.; Zhu, G.; Shan, Y.; Liang, Z.; Zhang, L.; Zhang, Y. *Anal. Chem.* **2010**, *82*, 2574.
- (427) Arrabito, G.; Pignataro, B. *Anal. Chem.* **2010**, *82*, 3104.
- (428) Areskogh, D.; Henriksson, G. *Process Biochem.* **2011**, *46*, 1071.
- (429) Alptekin, O.; Tukel, S. S.; Yildirim, D.; Alagoz, D. *Enzyme Microb. Technol.* **2011**, *49*, 547.
- (430) Wang, A.; Wang, M.; Wang, Q.; Chen, F.; Zhang, F.; Li, H.; Zeng, Z.; Xie, T. *Bioresour. Technol.* **2011**, *102*, 469.
- (431) Yilmaz, E.; Can, K.; Sezgin, M.; Yilmaz, M. *Bioresour. Technol.* **2011**, *102*, 499.
- (432) Meizler, A.; Roddick, F.; Porter, N. *Chem. Eng. J.* **2011**, *172*, 792.
- (433) Song, Y. S.; Lee, H. U.; Lee, J. H.; Park, C.; Kim, S. W. *Process Biochem.* **2011**, *46*, 817.
- (434) Xu, Y.-Q.; Zhou, G.-W.; Wu, C.-C.; Li, T.-D.; Song, H.-B. *Solid State Sci.* **2011**, *13*, 867.
- (435) Wang, Y.; Hasebe, Y. *J. Environ. Sci. (Beijing, China)* **2011**, *23*, 1038.
- (436) Vinoba, M.; Lim, K. S.; Lee, S. H.; Jeong, S. K.; Alagar, M. *Langmuir* **2011**, *27*, 6227.
- (437) Wang, C.; Zhou, G.; Xu, Y.; Chen, J. *J. Phys. Chem. C* **2011**, *115*, 22191.
- (438) Guyomard-Lack, A.; Delorme, N.; Moreau, C.; Bardeau, J. F.; Cathala, B. *Langmuir* **2011**, *27*, 7629.
- (439) Zhao, G.; Wang, J.; Li, Y.; Huang, H.; Chen, X. *Biochem. Eng. J.* **2012**, *68*, 159.
- (440) Lee, H. U.; Park, C.; Kim, S. W. *Process Biochem.* **2012**, *47*, 1282.
- (441) Albertini, A. V. P.; Cadena, P. G.; Silva, J. L.; Nascimento, G. A.; Reis, A. L. S.; Freire, V. N.; Santos, R. P.; Martins, J. L.; Cavada, B. S.; Neto, P. J. R.; Pimentel, M. C. B.; Martínez, C. R.; Porto, A. L. F.; Lima Filho, J. L. *Chem. Eng. J.* **2012**, *187*, 341.
- (442) Deep, A.; Tiwari, U.; Kumar, P.; Mishra, V.; Jain, S. C.; Singh, N.; Kapur, P.; Bharadwaj, L. M. *Biosens. Bioelectron.* **2012**, *33*, 190.
- (443) Ma, Y.-X.; Li, Y.-F.; Zhao, G.-H.; Yang, L.-Q.; Wang, J.-Z.; Shan, X.; Yan, X. *Carbon* **2012**, *50*, 2976.
- (444) Song, Y. S.; Shin, H. Y.; Lee, J. Y.; Park, C.; Kim, S. W. *Food Chem.* **2012**, *133*, 611.
- (445) Ida, J.; Matsuyama, T.; Yamamoto, H. *Biochem. Eng. J.* **2000**, *5*, 179.
- (446) You, Q.; Yin, X.; Gu, X.; Xu, H.; Sang, L. *Bioprocess Biosyst. Eng.* **2011**, *34*, 757.
- (447) Wang, X. R.; Zhang, S. P.; Wang, P. *Biotechnol. Lett.* **2011**, *33*, 1831.
- (448) Yokoyama, K.; Tamiya, E.; Karube, I. *Electroanalysis* **1991**, *3*, 469.
- (449) Murakami, Y.; Suda, M.; Yokoyama, K.; Takeuchi, T.; Tamiya, E.; Karube, I. *Microchem. J.* **1994**, *49*, 319.
- (450) Wilson, N. G.; McCready, T.; Greenway, G. M. *Analyst* **2000**, *125*, 237.
- (451) Huang, J.; Zhao, R.; Wang, H.; Zhao, W.; Ding, L. *Biotechnol. Lett.* **2010**, *32*, 817.
- (452) Li, W.; Yuan, R.; Chai, Y.; Zhou, L.; Chen, S.; Li, N. *J. Biochem. Biophys. Methods* **2008**, *70*, 830.
- (453) Kim, D. N.; Lee, Y.; Koh, W.-G. *Sens. Actuators, B: Chem.* **2009**, *137*, 305.
- (454) Cho, S.-H.; Shim, J.; Yun, S.-H.; Moon, S.-H. *Appl. Catal., A* **2008**, *337*, 66.
- (455) Cabana, H.; Alexandre, C.; Agathos, S. N.; Jones, J. P. *Bioresour. Technol.* **2009**, *100*, 3447.
- (456) Rekuc, A.; Bryjak, J.; Szymanska, K.; Jarzebski, A. B. *Bioresour. Technol.* **2010**, *101*, 2076.
- (457) Zeng, L.; Luo, K.; Gong, Y. *J. Mol. Catal. B: Enzym.* **2006**, *38*, 24.
- (458) Huang, J.; Liu, Y.; Wang, X. *J. Mol. Catal. B: Enzym.* **2008**, *55*, 49.
- (459) Abdullah, A. Z.; Sulaiman, N. S.; Kamaruddin, A. H. *Biochem. Eng. J.* **2009**, *44*, 263.
- (460) Huang, J.; Liu, Y.; Wang, X. *J. Mol. Catal. B: Enzym.* **2009**, *57*, 10.
- (461) Chaubey, A.; Parshad, R.; Taneja, S. C.; Qazi, G. N. *Process Biochem.* **2009**, *44*, 154.
- (462) Hu, B.; Pan, J.; Yu, H.-L.; Liu, J.-W.; Xu, J.-H. *Process Biochem.* **2009**, *44*, 1019.
- (463) Mitchell, S.; Bonilla, A.; Pérez-Ramírez, J. *Mater. Chem. Phys.* **2011**, *127*, 278.
- (464) Ranjbakhsh, E.; Bordbar, A. K.; Abbasi, M.; Khosropour, A. R.; Shams, E. *Chem. Eng. J.* **2012**, *179*, 272.
- (465) Malpass, C. A.; Millsap, K. W.; Sidhu, H.; Gower, L. B. *J. Biomed. Mater. Res.* **2002**, *63*, 822.
- (466) Baur, B.; Howgate, J.; von Ribbeck, H. G.; Gawlina, Y.; Bandalo, V.; Steinhoff, G.; Stutzmann, M.; Eickhoff, M. *Appl. Phys. Lett.* **2006**, *89*, 183901.
- (467) Li, B.; Zhang, J.; Dai, F.; Xia, W. *Carbohydr. Polym.* **2012**, *88*, 206.
- (468) Park, S.; Lee, Y.; Kim, D. N.; Park, S.; Jang, E.; Koh, W.-G. *React. Funct. Polym.* **2009**, *69*, 293.
- (469) Cordeiro, A. L.; Lenk, T.; Werner, C. *J. Biotechnol.* **2011**, *154*, 216.
- (470) Miyazaki, M.; Kaneno, J.; Uehara, M.; Fujii, M.; Shimizu, H.; Maeda, H. *Chem. Commun.* **2003**, 648.
- (471) Puleo, D. A. *J. Biomed. Mater. Res.* **1995**, *29*, 951.
- (472) Li, Y.; Yan, B.; Deng, C.; Yu, W.; Xu, X.; Yang, P.; Zhang, X. *Proteomics* **2007**, *7*, 2330.
- (473) Zhao, J.; Wu, D.; Zhi, J. *Bioelectrochemistry* **2009**, *75*, 44.
- (474) Liu, T.; Wang, S.; Chen, G. *Talanta* **2009**, *77*, 1767.
- (475) Vashist, S. K.; Zheng, D.; Sheu, F. S.; Al-Rubeaan, K. A. A mediator-less electrochemical glucose sensing procedure employing the leach-proof covalent binding of an enzyme(s) to electrodes and products thereof. WO 2013165318 A1, November 7, 2013.
- (476) Kjellander, M.; Mazari, A. M.; Boman, M.; Mannervik, B.; Johansson, G. *Anal. Biochem.* **2014**, *446*, 59.
- (477) Yu, D.; Ma, Y.; Xue, S. J.; Jiang, L.; Shi, J. *LWT-Food Sci. Technol.* **2013**, *50*, 519.
- (478) Kopp, W.; da Costa, T. P.; Pereira, S. C.; Jafelicci, M., Jr.; Giordano, R. C.; Marques, R. F. C.; Araújo-Moreira, F. M.; Giordano, R. L. C. *Process Biochem.* **2014**, *49*, 38.
- (479) Aissaoui, N.; Landoulsi, J.; Bergaoui, L.; Boujday, S.; Lambert, J. F. *Enzyme Microb. Technol.* **2013**, *52*, 336.
- (480) Anuar, S. T.; Zhao, Y.-Y.; Mug, S. M.; Curtis, J. M. *J. Mol. Catal. B: Enzym.* **2013**, *92*, 62.

- (481) Bayramoglu, G.; Akbulut, A.; Arica, M. Y. *J. Hazard. Mater.* **2013**, 244, S28.
- (482) Chauhan, N.; Narang, J.; Sunny; Pundir, C. S. *Enzyme Microb. Technol.* **2013**, 52, 265.
- (483) Gupta, K.; Jana, A. K.; Kumar, S.; Maiti, M. *J. Mol. Catal. B: Enzym.* **2013**, 98, 30.
- (484) Liu, T.; Zhao, Y.; Wang, X.; Li, X.; Yan, Y. *Bioresour. Technol.* **2013**, 132, 99.
- (485) Min, W.; Cui, S.; Wang, W.; Chen, J.; Hu, Z. *Anal. Biochem.* **2013**, 438, 32.
- (486) Raghavendra, T.; Basak, A.; Manocha, L. M.; Shah, A. R.; Madamwar, D. *Bioresour. Technol.* **2013**, 140, 103.
- (487) Bhange, P.; Sridevi, N.; Bhange, D. S.; Prabhune, A.; Ramaswamy, V. *Int. J. Biol. Macromol.* **2014**, 63, 218.
- (488) Hou, J.; Dong, G.; Ye, Y.; Chen, V. *J. Membr. Sci.* **2014**, 452, 229.